

DEVELOPMENT AND VERIFICATION OF A TWO PHASE REACTOR MODEL FOR
INDUSTRIAL LIGHT NAPHTHA ISOMERIZATION REACTORS

by

Hilal Fidan Acar

B.S., Chemical Engineering, Middle East Technical University, 2011

Submitted to the Institute for Graduate Studies in
Science and Engineering in partial fulfillment of
the requirements for the degree of
Master of Science

Graduate Program in Chemical Engineering
Boğaziçi University
2015

Dedicated to

My cousin's soul

Rest in Peace...

ACKNOWLEDGEMENTS

First of all, I would like to thank my supervisor Assoc. Prof. Ahmet Kerim Avcı, and Prof. Zeynep İlsen Önsan for their support, guidance and encouragement in this valuable project. They always helped me to be able to handle this valuable project and I usually felt comforted because of feeling a strong support behind me. I am very proud of being supported by such valuable people and have the opportunity to work with them.

I would also like to thank my committee members Prof. Ramazan Yıldırım, Assoc. Prof. Abdullah Kerem Uğuz, and Assoc. Prof. Hasan Bedir for devoting their valuable time to read, listen and comment on my thesis.

In addition, I would like to thank R&D department director of Tüpraş, Dr. Ahmet Murat Yıldırım for enabling my participation in this important project and for his continuing technical support.

I want to thank specially my team leader Mustafa Karakaya for his invaluable technical and moral support in this project. Without his encouragement, I would not have been successful on this work.

My special thanks go to my husband, Mehmet Acar, for supporting me whenever I needed. Without his presence, it would be so hard to deal with the challenges that I have been through. I am very happy for sharing my life with him and hope to be together till the end of my life.

Additionally, I want to thank my mother Nuriye, my father Mehmet, my brother Teoman and his wife Feyza for their endless love and support in my life. I would not be part of one of Turkey's best universities and graduate from there without their encouragement. I will always feel their love in my heart.

I also want to thank my team mates Sadık Ödemiş, Fatih Demir, Emre Can Bilir, Selin Gündür and specially Akın Paksoy for their support and friendship. Also I would like to thank Fırat Uzman for his endless technical support. Without them, I would not be able to learn modelling, be successful, and also have so much fun working on this project.

ABSTRACT

DEVELOPMENT AND VERIFICATION OF A TWO PHASE REACTOR MODEL FOR INDUSTRIAL LIGHT NAPHTHA ISOMERIZATION REACTORS

Isomerization process is one of the most important chemical processes used in the petroleum industry. Its product is named as the “isomerate” which is the major element of the gasoline pool that compensates for the octane rating and volume loss upon reduction of benzene and butane derivatives. In addition, environmental regulations limit the sulfur and benzene levels in gasoline, which are expected to become even more stringent with future restrictions on maximum vapor pressure and olefins content. UOP PenexTM process is one of the most preferred applications for isomerization. It converts low-octane light naphtha to higher-octane, branched isomers. In addition to isomerization reactions, benzene reduction, ring opening and cracking reactions also occur in reaction mixtures. A typical Penex reactor involves catalytic cracking and conversion on a fixed bed of chlorinated Pt/Al₂O₃ catalyst and increases the octane number from 60-70 to 85-87. The reactions take place in the presence of hydrogen with low partial pressure, at operating pressures around 32 bars and in a temperature range of 130-160°C. Isomerization involves moderately exothermic reversible reactions; hence, it is controlled by thermodynamic equilibrium that is more favorable at low temperatures. This implies that the reaction temperature has to be maintained in an optimal range between the thermodynamic and kinetic limits. A descriptive reactor model with sufficient complexity is essential in order to optimize the process by maximizing the isomerate up to a given octane number and quantity and related process improvement. In this work, the Penex reactors at Tüpras Izmir Refinery are handled rigorously, using a steady-state, co-current, down-flow, two-phase reactor model where chemical reaction rates are described by power law kinetics. Kinetic parameters are estimated by nonlinear regression that uses an objective function based on the minimization of the sum of square errors between plant data and calculated values. The results show that, i-C₅ product ratio is typically maximized at ca. 160°C, slightly above the required ca. 130°C for obtaining maximum 2,2-dimethylbutane product ratio. It is also seen that C₅ paraffins isomerize more readily than C₆ paraffins. Moreover, the benzene in the feed is found to be completely converted in the 100-200°C range studied.

ÖZET

ENDÜSTRİYEL HAFİF NAFTA İZOMERİZASYON REAKTÖRLERİ İÇİN İKİ FAZLI REAKTÖR MODELİ GELİŞTİRİLMESİ VE DOĞRULANMASI

İzomerizasyon prosesleri, petrol endüstrisinde en çok kullanılan kimyasal süreçlerden biridir. İzomerat olarak adlandırılan ürünü, benzen ve bütan türevlerinin giderilmesi sonucu meydana gelen hacim kaybını karşılamak için benzin havuzunda kullanılan ana maddedir. Ek olarak, çevre mevzuatı benzin içerisindeki sülfür ve benzen oranını belirli sınırlarda tutmakta ve gelecekte bu düzenlemelerin daha fazla kısıtlama yaratacağı öngörülmektedir. İzomerizasyon teknolojisinde, UOP PenexTM uygulaması en fazla tercih edilen proses türüdür. İşlem olarak düşük oktanlı hafif naftayı yüksek oktanlı, dallanmış izomerlerine dönüştürür ve aynı zamanda benzen azaltımı, halka açılması, ve kırılma reaksiyonlarının da olmasını sağlar. Tipik Penex reaktörü, klorlanmış Pt/Al₂O₃ katalizi üzerinde kırılma ve dönüşümle ürünün 60-70 oktandan 85-87 oktan aralığına çıkmasını sağlar. Reaksiyonlar düşük kısmi basınç altında hidrojen varlığında 32 bar ve 130-160 °C aralığında gerçekleşir. Reaksiyonlar yüksek egzotermik geri dönüşümlü olduğundan düşük sıcaklıkta daha etkili olan termodinamik denge ile kontrol edilir. Bu da sıcaklığın termodinamik ve kinetik limitler arasında optimum bir noktada olması gerektiğinin önemini gösterir. Süreci optimize edebilmek için gerekli düzeyde karmaşıklık içeren reaktor modeli kurulması önemlidir. Bu çalışmada, Tüpraş İzmir Rafinerisinde bulunan Penex reaktörlerinin, yatışkın halde, aşağı yönde akışla çift fazda ve reaksiyon hızlarının üs kuralı kinetiğiyle modellenmesi yapılmıştır. Kinetik parametreler, ünite verisi ve model çıktısı arasındaki hatanın kareleri toplamının minimize edilmesine dayanan hedef fonksiyonunun lineer olmayan regresyon yöntemi ile çözülmesinden elde edilmiştir. Sonuçlar izopentan ve 2,2-dimetilbütanın ürün oranının normalde olması gereken 130 °C'nin çok üzerinde, 160 °C'de maksimize edilebildiğini göstermiştir. Aynı zamanda beş karbonlu parafinlerin altı karbonlu parafinlere oranla daha kolay izomerleşmekte olduğu da görülmüştür. Ek olarak, ünite beslemesinin içerisinde bulunan benzen 100-200 °C aralığında neredeyse tamamen dönüşüme uğramıştır.

TABLE OF CONTENTS

ACKNOWLEDGEMENTS	iv
ABSTRACT.....	v
ÖZET	vi
LIST OF FIGURES	x
LIST OF TABLES	xiv
LIST OF SYMBOLS	xvi
LIST OF ACRONYMS/ABBREVIATIONS.....	xix
1. INTRODUCTION.....	1
2. LITERATURE SURVEY	4
2.1. Light Paraffin Isomerization.....	4
2.1.1. Isomerization Catalysts	4
2.1.1.1. PT–NI/H-Beta Zeolite Catalysts	5
2.1.1.2. Heteropoly Acid Catalysts	5
2.1.1.3. Molybdenum Oxide Based Catalysts	6
2.1.1.4. Chlorinated Platinum Alumina Catalysts	6
2.1.1.5. Zeolite Based Bifunctional Catalysts	7
2.1.1.6. Sulfated Zirconia.....	7
2.1.1.7. Benzene Saturation Catalysts.....	8
2.1.2. Reactions and Mechanisms	8
2.1.3. Kinetics.....	11
2.1.4. Coke Formation and Deactivation.....	14
2.1.5. Unit Performance	15
2.2. Industrial Isomerization Processes.....	17

2.3. Packed Bed Reactors	21
2.3.1. Trickle Bed Reactors	23
2.3.2. Plug Flow Reactor Model.....	24
3. REACTOR MODELING.....	26
3.1. Thermodynamic Analysis	26
3.2. Vapor Liquid Equilibrium	29
3.3. Plug Flow Reactor Model	36
3.3.1. Mass Balance.....	36
3.3.2. Energy Balance.....	37
3.3.3. Reactor Model	38
3.3.3.1. Data Files	42
3.3.3.2. Model.M.....	42
3.3.3.3. Simulation.M.....	43
3.3.3.4. Plant Model.M.....	43
3.3.3.5. Srk_Eos.M.....	43
3.3.3.6. Flash.M.....	43
3.3.3.7. Reactor Model.M	44
3.3.3.8. Rxn Rates.M.....	44
3.3.3.9. Heat of Reaction.M	44
3.3.4. Parameter Estimation	45
3.3.4.1. Par Est.M.....	46
3.3.4.2. Objective Function.M	47
4. RESULTS AND DISCUSSION	48
4.1. Simulation of Isomerization Reactor	48
4.2. Effect of Reactor Inlet Temperature	54
4.3. Effect of Reactor Inlet Pressure	58

4.4. Effect of Reactor Inlet Flow Rate	62
5. CONCLUSIONS AND RECOMMENDATIONS.....	67
5.1. Conclusions.....	67
5.2. Recommendations.....	67
APPENDIX A. DETAILED SIMULATION RESULTS.....	69
APPENDIX B. DETAILED MODEL FLOW CHARTS.....	90
REFERENCES	96

LIST OF FIGURES

Figure 2.1. Isomerization activity comparison of several different catalysts.	4
Figure 2.2. Classical bifunctional mechanism for hydroisomerization of n-alkanes.	10
Figure 2.3. Reaction pathways of hydrocarbons and benzene.	11
Figure 2.4. Dependence of n-paraffins conversion on reaction temperature.	12
Figure 2.5. Simplified mechanism of coke formation.	14
Figure 2.6. Selectivity to total isomers at different temperatures.	16
Figure 2.7. Process flow diagram of zeolite catalyst based isomerization.	17
Figure 2.8. Low-temperature isomerization process on chlorinated-alumina catalysts.	18
Figure 2.9. Process flow diagram of sulfated zirconia catalyst based isomerization.	18
Figure 2.10. Process flow diagram of Butamer process.	19
Figure 2.11. Process flow diagram of TIP process.	19
Figure 2.12. Basic types of catalytic packed bed reactors.	21
Figure 2.13. Transport resistances in trickle bed reactor catalyst.	24
Figure 3.1. Thermodynamic equilibrium for butane and its isomers.	27

Figure 3.2. Thermodynamic equilibrium for pentane and its isomers.....	28
Figure 3.3. Thermodynamic equilibrium for hexane and its isomers.....	28
Figure 3.4. A general flash process.....	29
Figure 3.5. Flow chart of flash calculation procedure.....	34
Figure 3.6. Comparison of flash calculations with ASPEN HYSYS.....	35
Figure 3.7. Control volume of a plug flow reactor system.....	36
Figure 3.8. Completed reaction scheme for isomerization reactions.....	41
Figure 4.1. Reactor simulation temperature profile for 57. Day.....	49
Figure 4.2. Comparison of outlet temperature or 58 days.....	50
Figure 4.3. Comparison of n-Pentane outlet compositions for 58 days.....	51
Figure 4.4. Comparison of n-Hexane outlet compositions for 58 days.....	51
Figure 4.5. Comparison of i-Pentane outlet compositions for 58 days.....	52
Figure 4.6. Comparison of 22DMB outlet compositions for 58 days.....	52
Figure 4.7. Comparison of 23DMB outlet compositions for 58 days.....	53
Figure 4.8. Comparison of 2MP outlet compositions for 58 days.....	53
Figure 4.9. Effect of reactor inlet temperature on hydrogen consumption.....	55

Figure 4.10. Effect of reactor inlet temperature on paraffin conversion.	55
Figure 4.11. Effect of reactor inlet temperature on isopentane production.	56
Figure 4.12. Effect of reactor inlet temperature on 22DMB and 23DMB production.	57
Figure 4.13. Effect of reactor inlet temperature on MCP and CYC-HEX production.	58
Figure 4.14. Effect of reactor inlet pressure on hydrogen consumption.....	59
Figure 4.15. Effect of reactor inlet pressure on paraffin conversion.	60
Figure 4.16. Effect of reactor inlet pressure on isopentane production.....	60
Figure 4.17. Effect of reactor inlet pressure on 22DMB and 23DMB production.....	61
Figure 4.18. Effect of reactor inlet pressure on MCP and CYC-HEX production.	62
Figure 4.19. Effect of reactor inlet flow rate on hydrogen consumption.....	63
Figure 4.20. Effect of reactor inlet flow rate on paraffin conversion.	63
Figure 4.21. Effect of reactor inlet flow rate on isopentane production.....	64
Figure 4.22. Effect of reactor inlet flow rate on 22DMB and 23DMB production.	65
Figure 4.23. Effect of reactor inlet flow rate on MCP and CYC-HEX production.	66
Figure A.1. Reactor simulation temperature profile for 28. Day.....	87
Figure A.2. Reactor simulation temperature profile for 35. Day.....	87

Figure A.3. Reactor simulation temperature profile for 36. Day.....	88
Figure A.4. Reactor simulation temperature profile for 40. Day.....	88
Figure A.5. Reactor simulation temperature profile for 54. Day.....	89
Figure B.1. Flow chart of main file.	90
Figure B.2. Flow chart of simulation file.....	90
Figure B.3. Flow chart of plant model file.	91
Figure B.4. Flow chart of SRK EOS calculation file.....	91
Figure B.5. Flow chart of flash calculation file.	92
Figure B.6. Flow chart of reactor model file.	92
Figure B.7. Flow chart of reaction rates calculation file.	93
Figure B.8. Flow chart of heat of reaction calculation file.....	93
Figure B.9. Flow chart of parameter estimation file.....	94
Figure B.10. Flow chart of objective function calculation file.....	94
Figure B.11. Whole code flow chart	95

LIST OF TABLES

Table 2.1. Comparison of industrially used isomerization catalysts.	5
Table 2.2. Isomerization reaction steps and required catalyst function.....	8
Table 2.3. Important isomerization reactions and their characteristics.	9
Table 2.4. Kinetic constants determined for binary mixtures.....	14
Table 2.5. Processes for light naphtha isomerization.	20
Table 2.6. Catalyst types used for different chemical reactions.	22
Table 3.1. Light naphtha blending components octane numbers.	26
Table 3.2. Isomerization reactions defined for reactor model.	39
Table 3.3. Benzene saturation and ring opening reactions.	39
Table 3.4. Cracking reactions defined for reactor model.	40
Table 4.1. Parameters studied in reactor model.....	48
Table A.1. Flash calculation results comparison with ASPEN HYSYS results.....	69
Table A.2. Reactor inlet data for 58 days*.	71
Table A.3. Plant data for reactor and reactor outlet for 58 days*.....	76

Table A.4. Heat of formation, specific heat and physical properties data of components. .	81
Table A.5. Reaction coefficients for 48 reactions.	82
Table A.6. Estimated reaction parameters for isomerization reactions.	84
Table A.7. Initial and final reaction parameter values.....	85

LIST OF SYMBOLS

a	Substance specific constant for Soave-Redlich-Kwong equation of state
A, a_m	Attraction parameter
A_d	Deactivated acid site
A_0	Initial acid site concentration
A_c	Crosssectional area of bed (m ²)
b	Dimensionless constant
b	Substance specific constant for Soave Redlich Kwong equation of state
B, b_m	Repulsion parameter
BP_i	Boiling point of component i (K)
$C_{\text{aromatics}\%}$	Aromatics mass percent
C_{CA}	Coke concentration on acid site
C_{CM}	Coke concentration on metal site
Ca_b	Concentration of bulk at liquid phase
Ca_g	Concentration of component at gas phase
Ca_l	Concentration of component at liquid phase at gas-liquid interphase
Ca_s	Concentration of component at solid phase
Ca_i_g	Concentration of component at gas phase at gas-liquid interphase
C_p	Specific heat (kJ/kmol.K)
C_{p_i}	Specific heat constants
Ea_j	Activation energy of reaction j (kJ/kmol)
F	Molar flow rate (kmol/h)
f_i	Coke formation on acid or metal sites
F_0	Initial molar flow rate (kmol/h)
G	Rachford rice flash equation
G'	First derivative of rachford rice equation
G''	Second derivative of rachford rice equation
K_{dehydr}	Dehydrogenation adsorption constant
k_{hi}	Coke removal rate constant metal or acid site

k_i	Distribution of coefficient of species
$k_{i,j}$	Interaction parameter between component i and j
k_{iso}	isomerization rate constant
k_j	Reaction constant of reaction j
K_j^0	Pre-exponential factor of reaction constant
K_{prot}	Protonation adsorption constant
L	Liquid molar flow rate (kmol/h)
M_0	Initial metal site concentration
M_d	Deactivated metal site
m_i	Soave Redlich Kwong equation of state parameter for component i
MW	Molecular weight
P	Pressure (kg/cm ² , psi)
P_{ci}	Critical pressure of component i (kg/cm ²)
P_i	Partial pressure of component i
$P_{n-alkane}$	Alkane partial pressure
$PAR(1)_i$	Equilibrium parameter of component i
$PAR(2)_i$	Adsorption parameter of component i
$PAR(3)_i$	Adsorption parameter of component i
$r_{i,j}$	Reaction rate for component i for reaction j (kmol/m ³ .h)
R	Ideal gas constant (kJ/kmol.K)
R	Interaction parameter calculation parameter
r_A	Reaction rate of coke formation on acid site
r_M	Reaction rate of coke formation on metal site
S	Interaction parameter calculation parameter
s_i	Vacant site of acid or metal site
T	Temperature (°C, K)
T_b	Boiling temperature (K)
T_{ci}	Critical temperature of component i (K)
T_r	Reduced temperature
V	Vapor molar flow rate (kmol/h)
V	Volume (m ³)

$V/F, VF_i$	Vapor fraction
W	Parameter estimation weight factor
x_i	Liquid molar fraction of component i
X_m	Model data
X_p	Process data
y_i	Vapor molar fraction of component i
Z^p	Compressibility factor for phase p
z_i	Molar fraction of component i
α_i	Equation of state parameter for component i
α	Reaction order
Ψ_i^p	Equation of state parameter of component i for phase p
ΔH_{form}	Heat of formation of component (kJ/mol)
ΔH_j	Heat of reaction of reaction j (kJ/mol)
ΔH_j^0	Standard heat of reaction of reaction j (kJ/mol)
ΔT	Temperature change
Δz	Length change
ε	Switching parameter for Soave Redlich Kwong equation of state
ω_i	Acentric factor of component i
ϕ_i^p	Fugacity coefficient of component i for phase p
ρ_b	Catalyst bulk density (kg/m ³)
$\vartheta_{i,j}$	Stoichiometric coefficient for component i in reaction j
Ω_A, Ω_B	Soave Redlich Kwong equation of state parameter
σ	Switching parameter for Soave Redlich Kwong equation of state

LIST OF ACRONYMS/ABBREVIATIONS

2MP	2 Methylpentane
22DMB	2,2 Dimethylbutane
23DMB	2,3 Dimethylbutane
2-D	Two dimensional
3MP	3 Methylpentane
9600PI056	Reactor inlet pressure tag number
9600PI058	Reactor outlet pressure tag number
9600TI013	First temperature along the bed tag number
9600TI014	Second temperature along the bed tag number
9600TI015	Third temperature along the bed tag number
9600TI016	Fourth temperature along the bed tag number
9600TI017	Fifth temperature along the bed tag number
9600TI018	Reactor outlet temperature tag number
9600TIC006	Reactor inlet temperature tag number
A	Acid site of the catalyst
BEN	Benzene
C ₁	Methane
C ₂	Ethane
C ₃	Propane
C ₄ , n-C ₄	Butane
C ₅ , n-C ₅	Pentane
C ₆ , n-C ₆	Hexane
C ₇ , n-C ₇	Heptane
CFD	Computational fluid dynamics
CH	Cyclohexane
C _n H _{2n+2}	Paraffin
CP	Cyclopentane
EOS	Equation of state

H ₂ /HC	Hydrogen Hydrocarbon ratio
HPA	Heteropoly Acid
i-C ₄	Isobutane
i-C ₅	Isopentane
M	Metal site of catalyst
Matlab [®]	Matrix Laboratory Program
MCP	Methylcyclopentane
MSDS	Material SafetyData Sheet
ODE	Ordinary differential equation
ODE 15s	Ordinary differential equation 1-5 Stiff
P	Products
PIBB	Process Monitoring Data Bank
PIN	Paraffin isomerization number
R	Reactants
RON	Research octane number
R&D	Research and Development
SRK	Soave-Redlich-Kwong
TIP	Total Isomerization Process
UOP	Universal Oil Products
USA	United States of America

1. INTRODUCTION

The vision of a modern oil refinery is now becoming more complex when compared with the past decades. The concerns of the public about the Earth's environment and health considerations have led to a number of new legislative measures around the world. Thus, the requirement to meet the challenge of clean fuel processing regulations must be applied accordingly. Environmental problems have become more important in refinery planning since 1970's initially in the USA. These requirements forced oil refiners to find new ways of clean oil production and octane reduction management in the gasoline pool.

Sulfur and benzene levels have been decreased in the gasoline pool in recent years; it is predicted that regulations on aromatic and olefin contents as well as vapor pressure may be introduced in the future [1]. In addition, the limitations on aromatics and vapor pressure will result in reduced use of C₄ and reformate, respectively, which makes the problem of handling toxic benzene content in the gasoline pool become more important. In this respect, gasoline production units in the petroleum industry must compensate for the requirements of these new considerations.

In general, the gasoline produced in a refinery requires a combination of different processing technologies classified as crude oil distillation, cracking, hydrocracking, reforming, polymerization and hydroisomerization. The distillation of crude oil results in light naphtha, heavy naphtha, kerosene, gas oil and reduced crude. The raw materials of gasoline production are the light and heavy naphtha which are processed by thermal, catalytic and hydro-cracking, followed by reforming and isomerization. Catalytic cracking produces blending components for high-octane gasoline and serves to improve the octane number. Hydrocracking permits wide variations in gasoline yield and furnace oils to meet seasonal demand changes and can effectively process hard-to-crack stocks. Reforming processes convert low octane gasoline-range hydrocarbons into higher-octane ones. Polymerization combines two or more low molecular weight olefin gases into higher molecular weight olefin liquids suitable for gasoline blending or for use as chemical feed stocks. Isomerization processes convert linear structured hydrocarbons into branched form

by reducing aromatics and sulfur content with increased volume. Furthermore, the isomerization unit does not need furnace and compressor facilities, thus these properties increase its importance. A well-established isomerization technology is available nowadays, with an installed capacity of about 1,500 thousand barrels per stream day, and it is growing steadily. The paraffin isomerization technology is dominated by UOP with Penex™ (C₅/C₆) and Butamer™ (C₄) units [2].

In the petroleum refining industry (downstream and marketing division), the availability of practically sulfur-free blend stocks having very low aromatics and high iso-paraffin contents is an essential criterion for maximizing profit in the production processes of engine gasoline, diesel fuels and lube base oils. These blend stocks can be produced from suitable feed stocks by using appropriate hydroisomerization catalyst(s) [3].

In refinery hydroisomerization processes, naphtha is not directly sent to the reactor as feed; it is processed and one of its components (alkanes) is fed to the reactor. Alkanes are organic compounds that are saturated hydrocarbons, known as “paraffins” in petroleum refining; they have the general chemical formula of C_nH_{n+2} and are used as an intermediate product to obtain high octane products [4]. Light alkanes which range between C₄-C₆ are important chemicals for the refinery hydroisomerization process, in which the straight chain alkanes are converted to branched-chain isomers, and the branched isomers of these hydrocarbons have higher octane numbers compared with straight chain isomers; thus, iso-alkanes are valuable additives to the fuel.

The products of hydroisomerization reaction are mainly methyl cyclopentane (MCP), 2,3-dimethyl butane (23DMB) and 3-methylpentane (3MP). Although the octane numbers of MCP and 23DMB are high, 3MP has a low octane number and, therefore, the amount of 3MP must be minimized in the product stream of the reactor by manipulating the reaction temperature. Since the hydroisomerization process is exothermic, it is very important to control the reaction temperature.

In this study, it is shown by mathematical modelling that isomerization reactions can be represented concisely and all reaction parameters can be estimated, despite the complex

reaction scheme involved. The modelling studies include the different types of reactions that define the isomerization unit and the estimation of the parameters for these reactions. The co-current, down-flow, two-phase isomerization reactors are assumed to be operating under plug flow conditions, and comprehensive models are used in modelling and simulations. In order to accomplish this aim, MATLAB© is used as the mathematical modelling tool to solve the mass and energy balance equations with a phase change algorithm.

A detailed literature search about isomerization is given in Chapter 2. In Chapter 3, modelling and simulation studies conducted for industrial isomerization reactors are presented. Results of computational simulations are reported in Chapter 4, together with the discussion of outcomes; the detailed numerical results of the simulations are given in the Appendix. Finally, major conclusions and recommendations for future studies are explained in Chapter 5.

2. LITERATURE SURVEY

2.1. Light Paraffin Isomerization

2.1.1. Isomerization Catalysts

The reduction of benzene content in fuels is forced by government environmental regulations. Thus, additional benzene reduction reactions are needed in the isomerization process. The effects of different laboratory- and industrial-scale catalysts on isopentane activity are shown in Figure 2.1, [5], where 1 represents upgraded Pt/Al₂O₃/Cl, 2 represents Pt/superacid, 3 represents Pt/Al₂O₃/Cl, 4 is Pt/sulfated metal oxide, 5 is mixed metal oxides (ZrO₂ + WO₃), 6 are different Pt/zeolites. Platinum based Al₂O₃/Cl catalysts are still best at providing the necessary benzene reduction and octane yield in the product, as seen from Figure 2.1 [3].

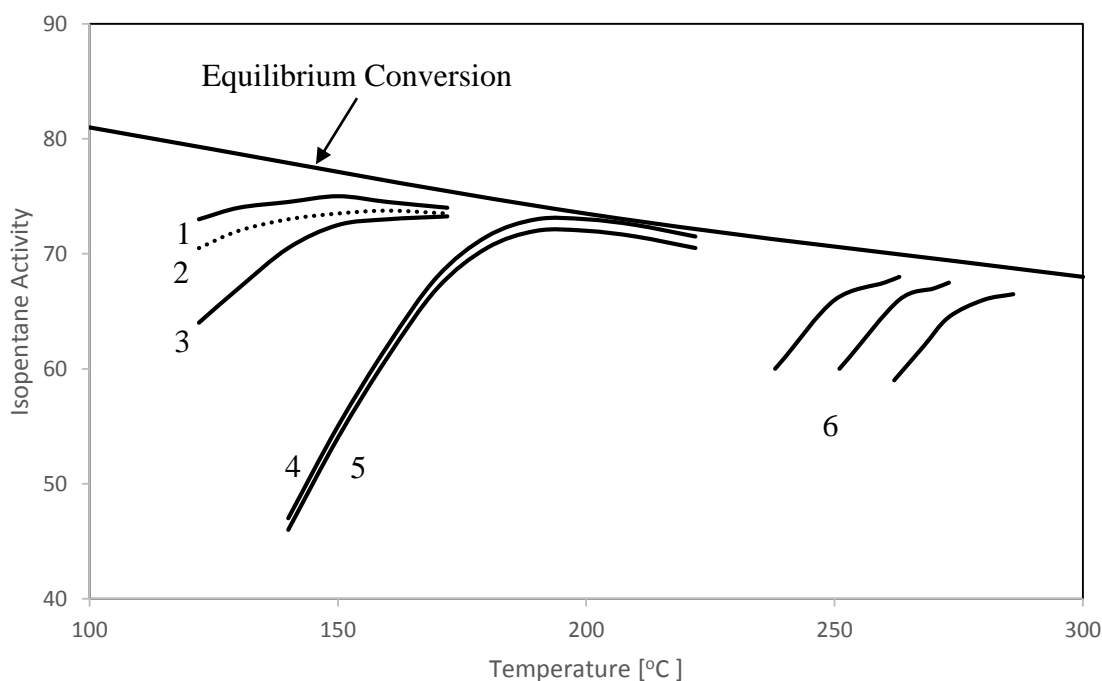


Figure 2.1. Isomerization activity comparison of several different catalysts.

Chlorided alumina and zeolite-based catalysts are the two widely utilized catalysts for naphtha isomerization process. The detailed process descriptions are discussed in the following sections. The comparison of different types of isomerization catalysts are given in Table 2.1. The detailed process descriptions are discussed in further sections.

Table 2.1. Comparison of industrially used isomerization catalysts.

Catalyst	Advantages	Disadvantages
Chlorided alumina	<ul style="list-style-type: none"> • Offers the higher activity • Yields high octane isomerate • Offers high isomerate yield 	<ul style="list-style-type: none"> • Chloride addition necessary for catalyst activity • Sensitive to poisons
Zeolitic catalysts	<ul style="list-style-type: none"> • Regenerable • Tolerant to feed poisons • Very stable 	<ul style="list-style-type: none"> • Lowest activity • Requires high temperatures and H₂/HC ratios
Sulfated zirconia	<ul style="list-style-type: none"> • Possess intermediate activity • Tolerant to catalyst poisons • Regenerable 	<ul style="list-style-type: none"> • Requires higher H₂/HC ratios

2.1.1.1. PT–Ni/H-Beta Zeolite Catalysts. The regulation on the benzene content of aromatics has a negative effect on octane number, because the removal of benzene decreases the octane number of the products. This effect has forced the consideration of skeletal isomerization in a different way. Generally, ring opening reactions are generated with isomerization processes. Many different metals have been tested for this purpose, and it was found that metal catalyst performance can be increased by adding a second metal, which is explained by metallic cluster formation [6].

First of all, nickel was introduced as the second metal while studying isomerization and cracking of n-heptane on the Ni-Mo/H-Y zeolite catalyst [7]. Later on, studies continued with n-hexane and n-heptane isomerization with different nickel contents. It was found that increasing the nickel content increases the isomerization reactions. In addition, the selectivity for the production of di-ramified alkanes increases with the Ni content [8].

2.1.1.2. Heteropoly Acid Catalysts. Heteropoly acid catalysts consist of polyoxometalate anions, and they are known to form ionic crystals comprising of heteropolyanions and

hydration water. They absorb large amounts of polar molecules like ethers and amines in bulk, resulting in heteropoly acid solvates. Studies show that these types of catalysts have higher Brønsted acidity than other solid acid catalysts; however, their thermal stability decreases with high temperature [9]. In addition, their overall catalytic activity and selectivity for isomers are similar to that of industrial zeolite catalysts under the same reaction conditions. It is also claimed that modification of this catalyst with platinum group metals increases thermal stability and regeneration features, and decreases coke formation [10]. HPAs are also important because of their economic and environmental characteristics. Compared with zeolite or metal oxide catalysts, HPAs have discrete ionic structures and they have high mobility so that anions can stabilize cationic paraffin intermediates; also, any change in chemical composition of catalyst changes its redox characteristics [11].

2.1.1.3. Molybdenum Oxide Based Catalysts. Molybdenum oxide based catalysts are also play a significant role in studies of alkane isomerization reactions. At low temperatures (300 °C), unreduced MoO₃ is found to be inactive; however, at higher temperatures (350 °C), activity and selectivity are promoted [12]. It is concluded that reduced MoO₃ catalyst successfully isomerizes n-pentane by a conventional bifunctional mechanism and that the catalyst maybe employed as a substitute to the bifunctional zeolite. Moreover, nickel content is found to be effective in stabilizing the activity of isomerization without changing the selectivity [13]. Studies also show that these catalysts have high activity and selectivity and they have potential for achieving the requirements of environmental regulations [14].

2.1.1.4. Chlorinated Platinum Alumina Catalysts. The chloride catalysts which are called Friedel crafts or Lewis acid catalysts like AlCl₃, SbCl₃, FeCl₃ were used as isomerization catalysts during earlier industrial times. Catalysts that use aluminum as metal are the most active isomerization catalysts and they are widely used in industry. They operate at low temperature which is chemically favorable because the equilibrium position shifts to the right, yielding more branched isomers at shorter reaction times; however, they are very sensitive to poisons compared to other types of isomerization catalysts [11]. Water and sulfur based materials are very poisonous for these catalysts, thus a treatment and drying process is needed in feed preparation. Continuous chloride injection is also needed during operation to maintain catalyst activity. Chlorinated Pt/Al₂O₃ catalysts usually operate at lower end of the temperature range of 130-170°C and hence do not have thermodynamic limitations.

Platinum component helps with the saturation of aromatics and ring opening of naphthenes, and aluminum metal part is involved in isomerization reactions. The negative feature of this catalyst is that it is irreversibly deactivated and regeneration is impossible [15,16].

2.1.1.5. Zeolite Based Bifunctional Catalysts. Zeolite based catalysts can be efficiently used for industrial isomerization processes by loading active metals like platinum or palladium. Reactions take place in the presence of hydrogen with medium pressure in the range of 20 – 70 kg/cm² pressure, thus, this process is also called hydroisomerization. Because acid catalysis and dehydrogenation action take place on adjacent components on the same material, these catalysts are named as bifunctional. A summary of bifunctional activity is given in Table 2.2. The metal part catalyzes hydrogenation and dehydrogenation while acidic part catalyzes the isomerization step [11]. When the influence of each alkane on catalytic activity is studied, cyclohexane is adsorbed over the zeolite part, thus, the reactions are inhibited [17]. For this reason, higher cyclohexane composition in the feed decreases the reaction activity. In addition, zeolite-based catalysts have low activity and operate at relatively high temperatures of 250-300 °C which is not thermodynamically favorable for the formation of branched isomers. The main advantage of using these catalysts is that they are not sensitive to water or chemical compounds, as in the case of alumina-based catalysts. Since zeolite based catalysts are resistant to feed poisons, extensive feed pretreatment steps are not required, and thus, these catalysts offer lower capital investment; a typical zeolite-based catalyst operates for a period of 10-15 years [15,16].

2.1.1.6. Sulfated Zirconia. The activity of these types of catalysts is between that of zeolites and chlorinated alumina catalysts. Unlike chlorinated alumina catalysts, sulfated zirconia catalysts are tolerant of oxygenates such as water and CO in the feed. These catalysts do not require a halide promoter, so there is no chloride injection or caustic scrubber, and they are also regenerable [15].

Studies show that sulfated zirconia catalysts become strongly acidic when treated with H₂SO₄ and calcinated at high temperatures, and are active for n-butane isomerization at room temperature [18]. In addition, platinum has positive effect on the isomerization selectivity on these catalysts in the presence of hydrogen [19]. It is clear that the platinum content

stabilizes catalytic activity and ensures higher selectivity for hydroisomerization; however, some research findings show that the isomerization activity of zirconia catalysts declines rapidly at lower temperatures [20]. This was thought to be due to coke formation, reduction of Zr_4^+ to Zr_3^+ by reacting hydrocarbons, H_2S formation due to reduction of surface sulfate groups, and surface poisoning by water. Similarly, the acidity and activity relationship has not yet been fully understood [11].

2.1.1.7. Benzene Saturation Catalysts. Benzene saturation reactions are as important as isomerization reactions because of environmental regulations. Most commonly used catalysts for this purpose are nickel or platinum based. Platinum based catalysts are generally advised by licensor companies because they are not permanently poisoned [15].

Table 2.2. Isomerization reaction steps and required catalyst function.

Step No	Reaction Step	Catalyst function
1	Dehydrogenation of paraffin to intermediate olefin	Metal
2	Carbonium ion formation from the olefin	Acid
3	Rearrangement of carbonium ion to isocarbonium ion	Acid
4	Formation of iso-olefins from isocarbonium ion	Acid
5	Hydrogenation of isoolefin to isoparaffin	Metal

2.1.2. Reactions and Mechanisms

Isomerization processes aim to convert n-C₄, n-C₅, and n-C₆ into their branched isomers. In addition to isomerization reactions, there are additional reactions that occur during this process, such as benzene saturation. The most important reactions occurring in the isomerization process are summarized in Table 2.3 [16].

Table 2.3. Important isomerization reactions and their characteristics.

Reaction	Characteristics
Isomerization of n-paraffins	<ul style="list-style-type: none"> • Desirable reaction and limited by equilibrium • High activity catalysts result in low temperature operation and thus improve isomer yield
Ring opening of naphthenes	<ul style="list-style-type: none"> • Favored by high temperatures high catalyst activity
Benzene saturation	<ul style="list-style-type: none"> • Desirable reaction • Occurs over hydrogenation sites of the catalyst • Highly exothermic resulting in high reactor ΔT
Hydrocracking	<ul style="list-style-type: none"> • Favored by high reactor temperature • Result in yield loss

A general sequence of steps for solid-catalyzed reactions can be expressed together with physical transport steps in the following manner [21]:

- Heat and mass transport from the bulk fluid to catalyst outer surface,
- Heat and mass transport from the outer surface to catalyst pores,
- Adsorption, chemical reaction and desorption of products from catalyst active site,
- Heat and mass transport from the catalyst pores to outer surface,
- Heat and mass transport from the outer surface to bulk fluid.

The rate determining step in this sequence is the chemical reaction on the active site; therefore, the chemical reaction mechanism for catalytic reactions is considered here.

Catalysts that were used previously for reforming reactions had only the acid function. The reason for having acidic activity was to increase the resistance for coke formation. Afterwards, when platinum loaded catalysts were developed, it was seen that they were more active and selective than the monofunctional acidic catalysts. Studies on bifunctional catalysts aimed to explain the reaction mechanism; and the first reaction mechanism claimed for n-paraffins given in Figure 2.2 [22].

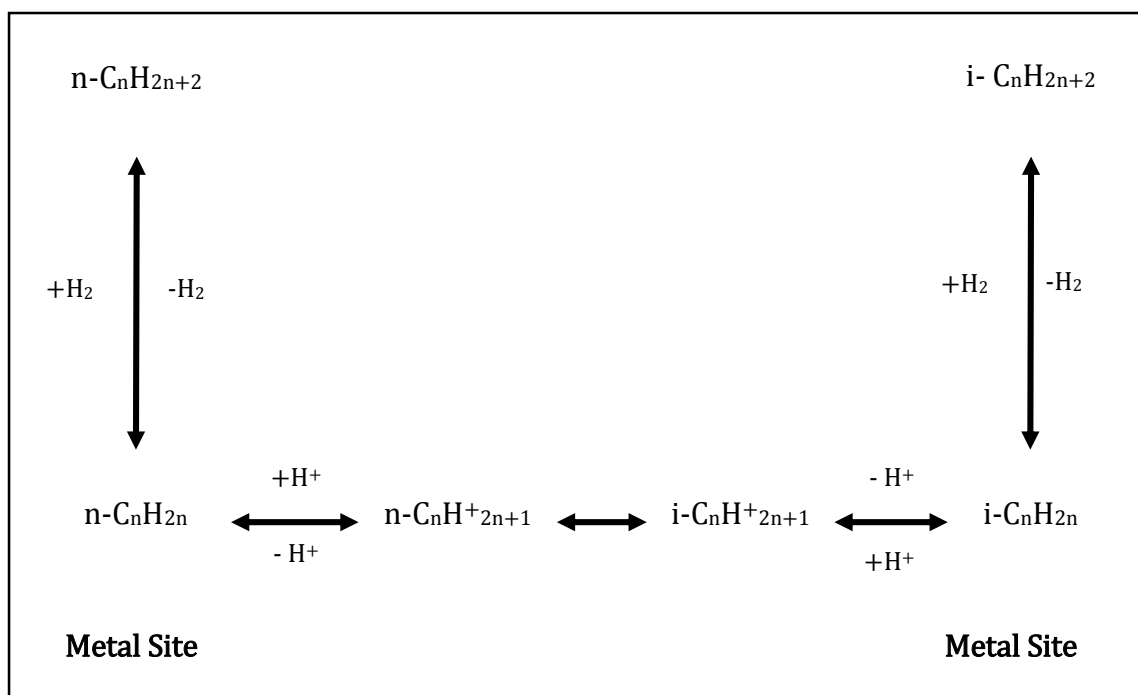


Figure 2.2. Classical bifunctional mechanism for hydroisomerization of n-alkanes.

Bifunctional solid acid catalysts loaded with platinum began to be widely used in the industrial isomerization processes later on. One site acts as an acid catalyst, the other site acts as a hydrogenation–dehydrogenation catalyst. Paraffins are dehydrogenated on metallic sites to the corresponding alkenes, which are isomerized by acid sites to branched alkenes. The branched alkene is then hydrogenated into the branched alkane again on the metallic sites [18]. As seen from the Figure 2.2, the metal sites are involved in the difficult step of alkane activation. The hydrogenation–dehydrogenation steps reach equilibrium in the presence of hydrogen on the metal component. The carbonium ion rearrangement step is the rate determining step of isomerization reactions, thus it is the most important step of the mechanism on the acidic sites that must be clearly understood. In addition, there are studies showing that isomerization activity is controlled by paraffin diffusion between active sites [23]. Besides isomerization reactions, ring opening, benzene saturation, and hydrocracking reactions also occur on the catalyst surface. All these reactions are schematically represented in Figure 2.3 [24].

The advantage of using bifunctional catalysts is the high catalytic activity observed in the presence of hydrogen, and because of equilibrium reactions, hydrogen shifts the reactions

to the product side [22]. Studies prove that isomerization reactions obey the three elementary steps in the reaction mechanism, which are dehydrogenation, isomerization and hydrogenation. Despite the establishment of this theory, there are many unsolved points to be studied and further investigations are necessary to clarify the reaction mechanism [11].

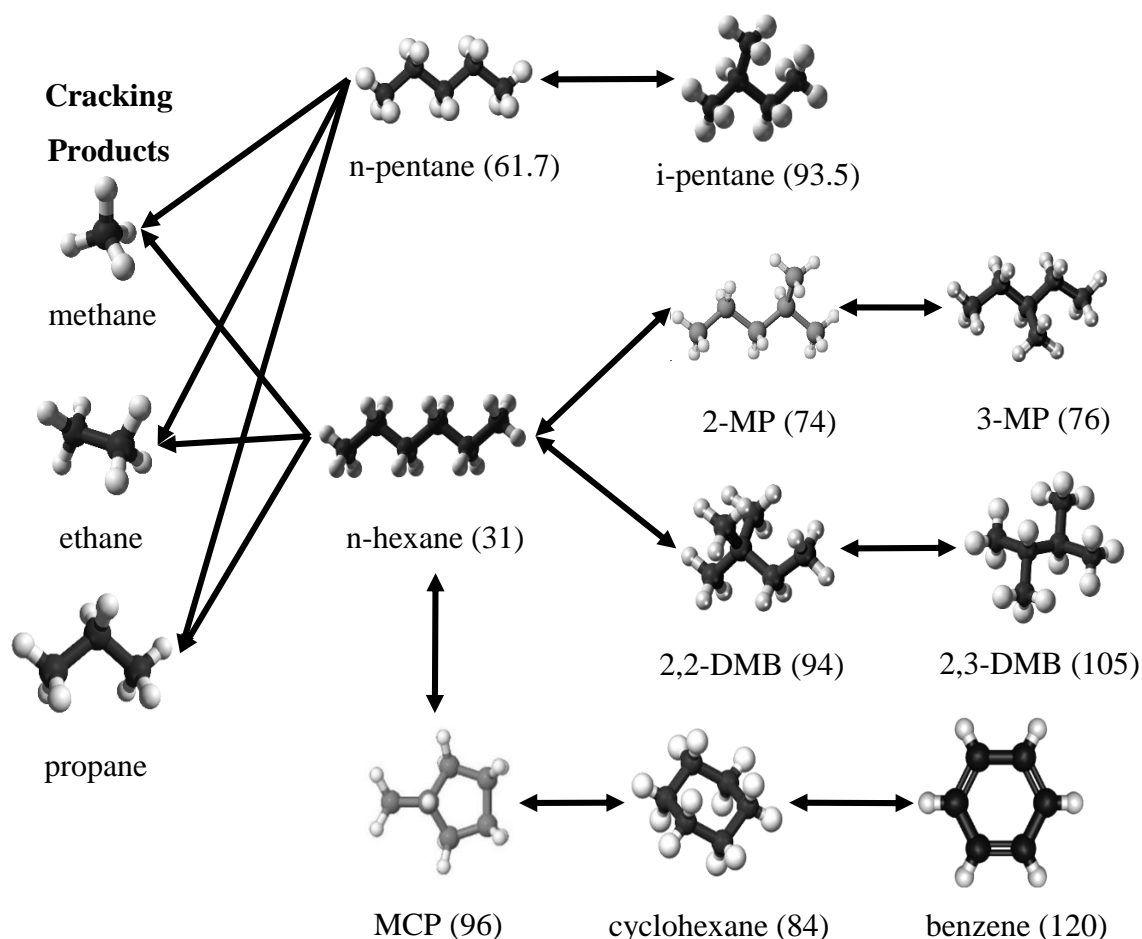


Figure 2.3. Reaction pathways of hydrocarbons and benzene.

2.1.3. Kinetics

The most important parameter for isomerization reactions is reaction temperature. For this reason, thermodynamics of the various reactions must be considered carefully. The first factor that must be considered is that isomerization reactions are equilibrium reactions and that lower reaction temperatures mean higher isoparaffin yields. On the other hand, the reactions are exothermic and when the temperature increases, reaction rates also increase;

however, high temperatures limit the yield by thermodynamic equilibrium. The schematic representation of this phenomenon is given in Figure 2.4 [25].

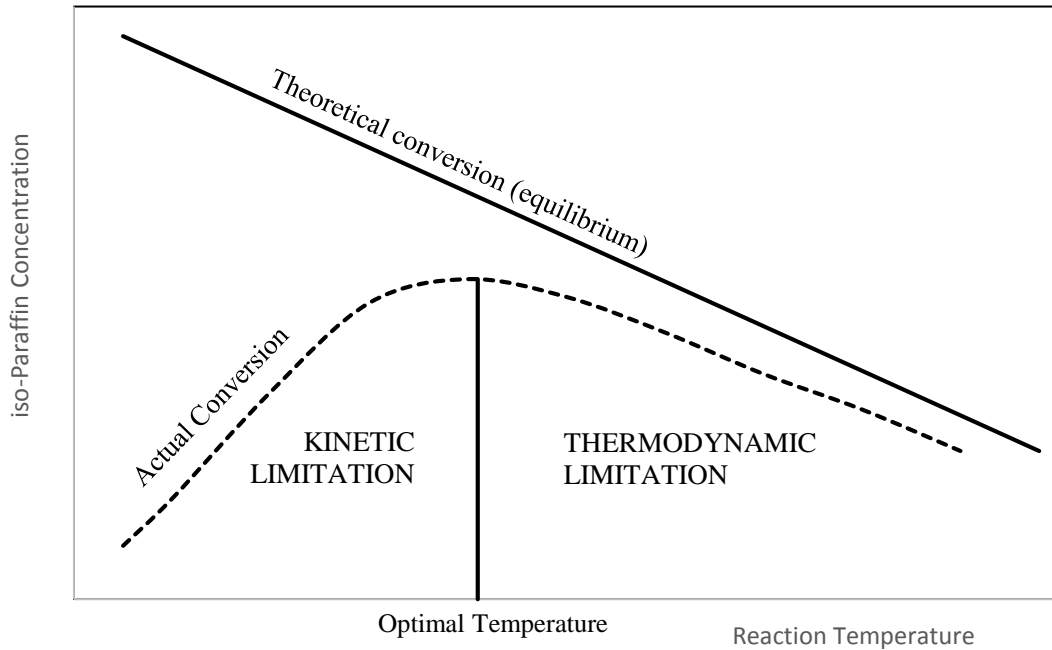


Figure 2.4. Dependence of n-paraffins conversion on reaction temperature.

In ideal bifunctional behavior, the isomerization reaction step is rate determining, and the hydrocarbon concentrations inside the catalyst are in equilibrium with the gas phase. Generally, these reactions obey the Langmuir-Hinshelwood mechanism and various reaction rate expressions were obtained in different studies. An overall rate expression given in the literature for hexane isomerization is as follows, and the order of reaction, α , is equal to or smaller than unity [26].

$$r = k_{iso} \frac{K_{dehydr} K_{prot} \left(\frac{P_{nC6}}{P_{H2}} \right)}{1 + K_{dehydr} K_{prot} \left(\frac{P_{nC6}}{P_{H2}} \right)} \approx k_{iso} \left(K_{dehydr} K_{prot} \left(\frac{P_{nC6}}{P_{H2}} \right) \right)^\alpha \quad (2.1)$$

When the pores of the catalyst are completely covered with reactant, this inhibits diffusion and equilibrium between hydrocarbons and gas phase is no longer attainable. In

this circumstance, the proposed general form of the rate expression becomes [27]:

$$r = k_{iso} \frac{PAR(1) \cdot P_{n-alkane}}{P_{H_2} + PAR(2) \cdot P_{H_2} \cdot P_{n-alkane} + PAR(3) \cdot P_{n-alkane}} \quad (2.2)$$

Where PAR(1), PAR(2), and PAR(3) are equilibrium and adsorption parameters. This rate expression is studied and confirmed on n-alkane isomerization reaction kinetics.

Many studies have been conducted on the kinetics of isomerization of n-alkanes. In addition to individual alkanes, binary mixtures were also studied and some of the best representing results were acquired as [28]:

For n-C₅ / n-C₆ mixtures:

$$r_{n-C_5} = k_{iso} \frac{PAR(1)_{nC5} \cdot P_{nC5}}{P_{H_2} + PAR(2)_{nC5} \cdot P_{nC5} + PAR(2)_{nC6} \cdot P_{nC6}} \quad (2.3)$$

$$r_{n-C_6} = k_{iso} \frac{PAR(1)_{nC6} \cdot P_{nC6}}{P_{H_2} \cdot (1 + PAR(3)_{nC6} \cdot P_{nC6} + PAR(3)_{nC5} \cdot P_{nC5})} \quad (2.4)$$

For n-C₆ / n-C₇ mixtures:

$$r_{n-C_6} = k_{iso} \frac{PAR(1)_{nC6} \cdot P_{nC6}}{P_{H_2} \cdot (1 + PAR(2)_{nC6} \cdot P_{nC6} + PAR(2)_{nC7} \cdot P_{nC7})} \quad (2.5)$$

$$r_{n-C_7} = k_{iso} \frac{PAR(1)_{nC7} \cdot P_{nC7}}{P_{H_2} \cdot (1 + PAR(2)_{nC7} \cdot P_{nC7} + PAR(2)_{nC6} \cdot P_{nC6})} \quad (2.6)$$

For n-C₆ / c-C₆ mixtures:

$$r_{n-C_6} = k_{iso} \frac{PAR(1)_{nC6} \cdot P_{nC6}}{P_{H_2} \cdot (1 + PAR(2)_{nC6} \cdot P_{nC6} + PAR(2)_{cC6} \cdot P_{cC6})} \quad (2.7)$$

$$r_{c-C_6} = k_{iso} \frac{PAR(1)_{cC_6} \cdot P_{cC_6}}{P_{H_2} \cdot (1 + PAR(2)_{cC_6} \cdot P_{cC_6} + PAR(2)_{nC_6} \cdot P_{nC_6})} \quad (2.8)$$

The kinetic parameters determined for these binary mixture isomerization reactions at 200 °C, are given in Table 2.4.

Table 2.4. Kinetic constants determined for binary mixtures.

Mixture	PAR(1)	PAR(2)	PAR(3)
n-C ₅ / n-C ₆	8.0 · 10 ⁻⁶	19.7	34.3
n-C ₆ / n-C ₅	3.4 · 10 ⁻⁴	58.4	231.1
n-C ₆ / n-C ₇	2.0 · 10 ⁻⁶	0.5	-
n-C ₇ / n-C ₆	5.3 · 10 ⁻⁴	1.3	-
n-C ₆ / c-C ₆	4.2 · 10 ⁻⁴	1.8	-
c-C ₆ / n-C ₆	5.8 · 10 ⁻⁶	7.1	-

2.1.4. Coke Formation and Deactivation

A simplified mechanism for the coke formation process can be schematically represented as:

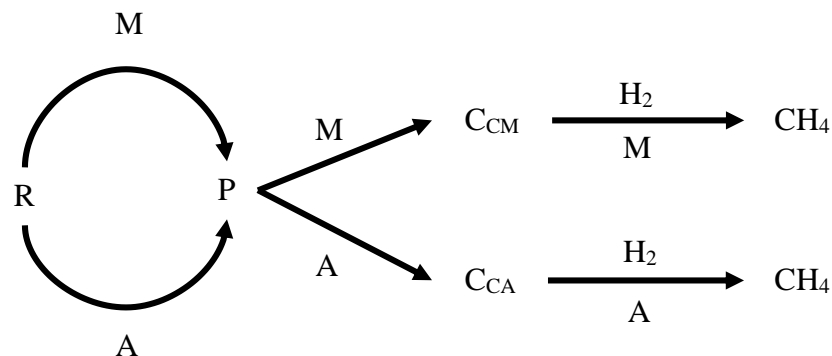


Figure 2.5. Simplified mechanism of coke formation.

According to Figure 2.5, R represents the reactants, and they undergo chemical

reaction on metal and acid sites denoted by M and A respectively. During the chemical reactions, coke precursor is produced (P) which is then transformed to coke form on a metal or acid site. Regeneration can happen in the presence of hydrogen, thus methane can be produced. In order to understand the kinetic definition of this process, precursor concentration is assumed to be proportional to the initial metal and acid concentration with dimensionless constant ($M_0 + bA_0$). By this assumption, rate of metal and acid coke formation can be defined with [29]:

$$r_M = f'_M M_0 s_M (M_0 + bA_0) - k_{HM} M_d C_{H_2} \quad (2.9)$$

$$r_A = f'_A A_0 s_A (M_0 + bA_0) - k_{HA} A_d C_{H_2} \quad (2.10)$$

Here f'_i represents the coke formation, s is the vacant sites, k_{Hi} is the coke removal rate constant.

In laboratory scale experiments, it is concluded that coke formation rate is directly affected by the ratio of metal and acid sites. In addition, because coking can be regarded as a polymerization reaction of olefins, the steady state level of deactivation increases with increasing partial pressure of n-paraffins and decreasing partial pressure of hydrogen. Coke formation directly affects the selectivity of products. Studies also show that acid part of the bifunctional catalyst is more attractive to be deactivated than metallic parts [29]. Under industrial conditions, the deactivation is low because of high operation pressure [22].

Besides coke formation, activation is decreased by the poisons coming from the feed which can be sulfur, nitrogen, and water. These materials directly affect catalyst activity and poison active sites. For this reason, before the process, a pretreatment and drying procedure is applied to protect the catalyst against these poisoning agents [22].

2.1.5. Unit Performance

The performance of an isomerization unit is measured by the resulting high octane components. The most important indicator is ratio of isoparaffin to n-paraffin named as the paraffin ratio, which can be expressed for a C₅-C₆ isomerization unit as follows [30]:

$$\text{Isopentane ratio} = \frac{i-C_5}{\sum(i-C_5 + n-C_5)} \quad (2.11)$$

In addition to the isomerization ratio, selectivity is another indicator to measure the unit performance. It is generally used for the butane isomerization and C₅-C₆ isomerization units; paraffin isomerization number (PIN) used as a performance indicator is defined as;

$$\text{PIN} = \frac{i-C_5}{\sum(i-C_5 + n-C_5)} + \frac{22\text{DMB} + 23\text{DMB}}{\sum(i-C_6 + n-C_6)} \quad (2.12)$$

Selectivity of the catalyst to iso-alkane molecules increases with decreasing alkane chain length. In addition, temperature is the major parameter that affects the selectivity. Figure 2.6 shows the relationship between temperature and alkane selectivity [31].

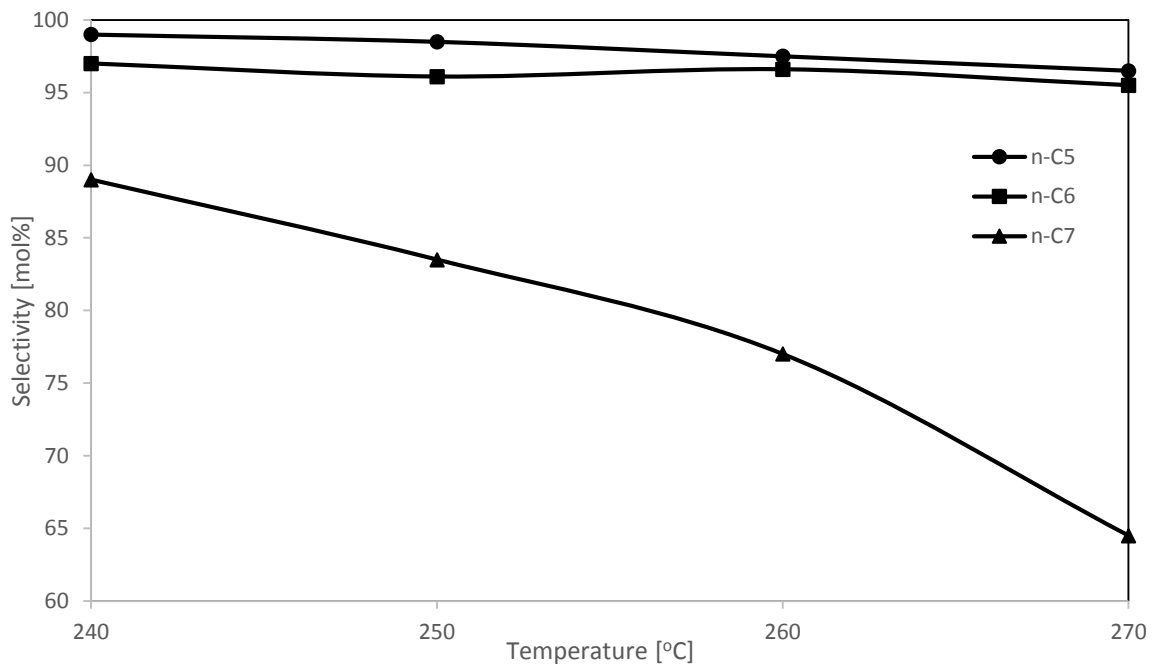


Figure 2.6. Selectivity to total isomers at different temperatures.

2.2. Industrial Isomerization Processes

There are five types of different isomerization processes used worldwide. These are, medium-temperature isomerization process (250-300 °C) on zeolite catalysts [32] given in Figure 2.7, low-temperature isomerization process on chlorinated-alumina catalysts given in Figure 2.8, sulfated metal oxides given in Figure 2.9, low-temperature butamer process on chlorinated-alumina catalysts [33] given in Figure 2.10, and total isomerization process given in Figure 2.11.

There are different types of isomerization processes used commercially given below. These are for butane isomerization and pentane/hexane isomerization processes. When historical development of the processes and use of most developed technologies are studied, it can be seen that nowadays UOP is the leader licensing company that has more than 200 operation units all over the world. Big companies refinery industry such as Shell, BP, and UOP have been supporting for development of this processes for many years. Development of isomerization processes can be divided into four historical groups. A brief summary of these commercial processes are given in Table 2.5 [33].

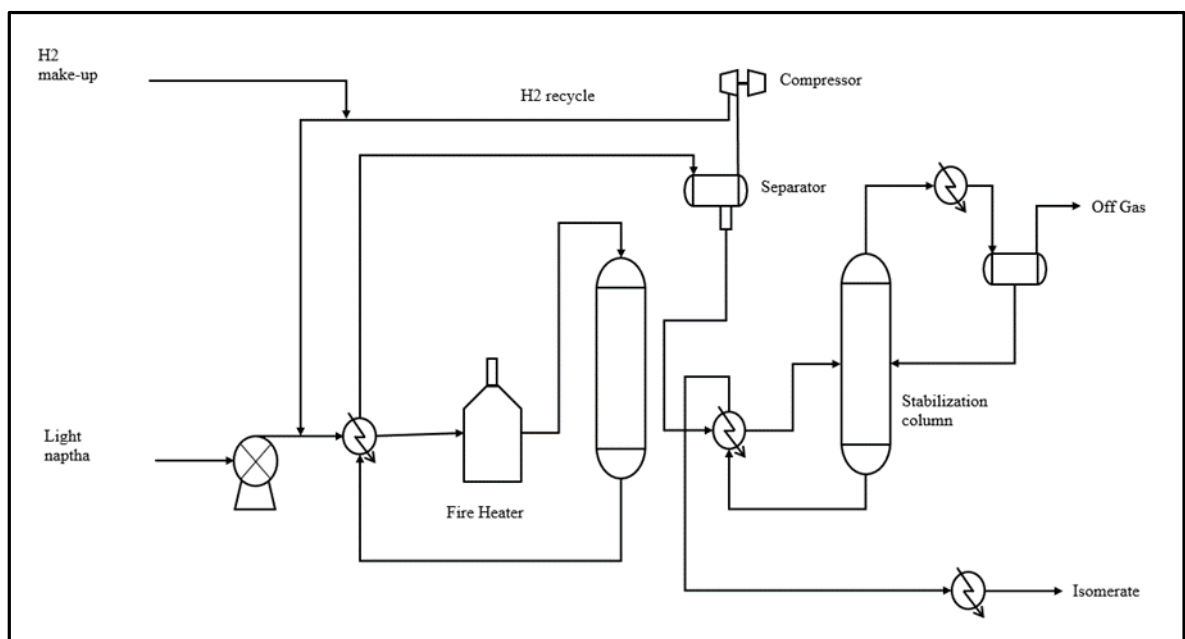


Figure 2.7. Process flow diagram of zeolite catalyst based isomerization.

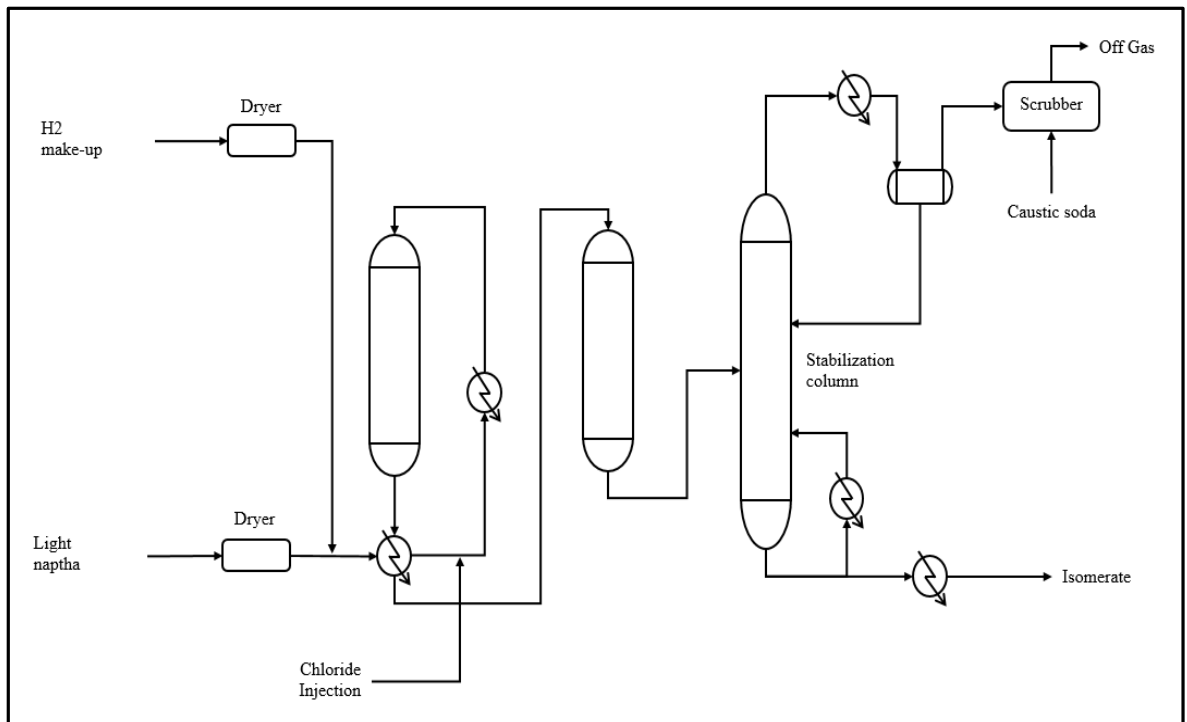


Figure 2.8. Low-temperature isomerization process on chlorinated-alumina catalysts.

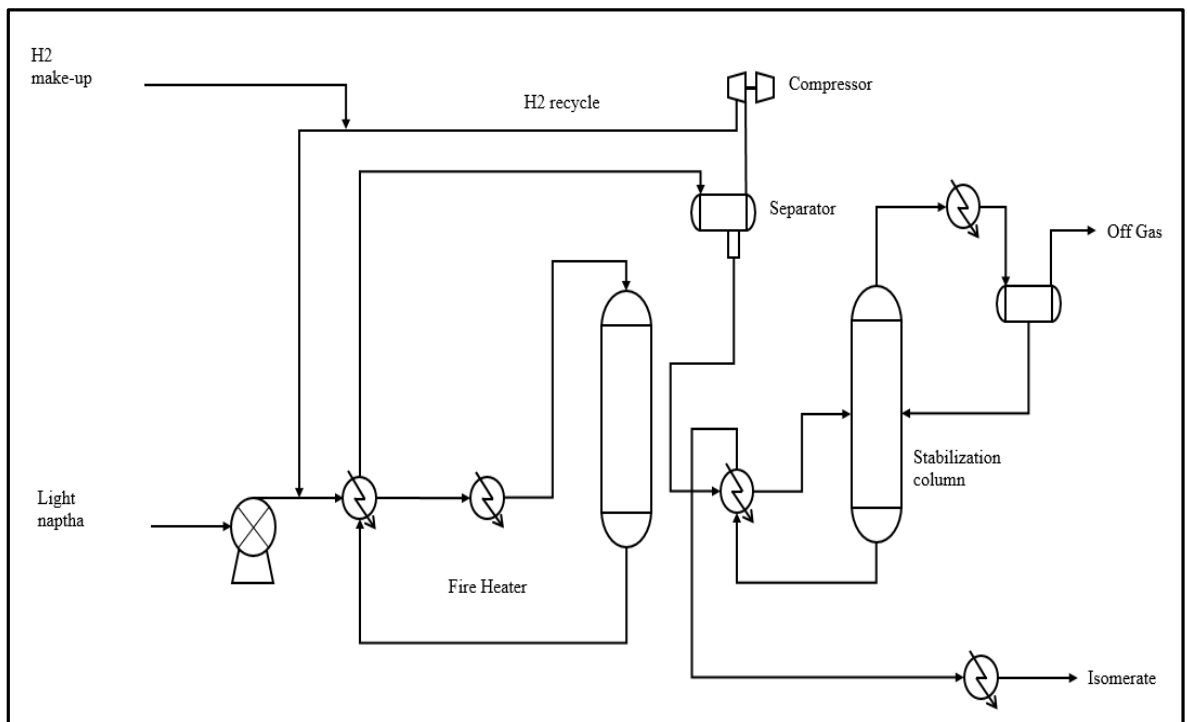


Figure 2.9. Process flow diagram of sulfated zirconia catalyst based isomerization.

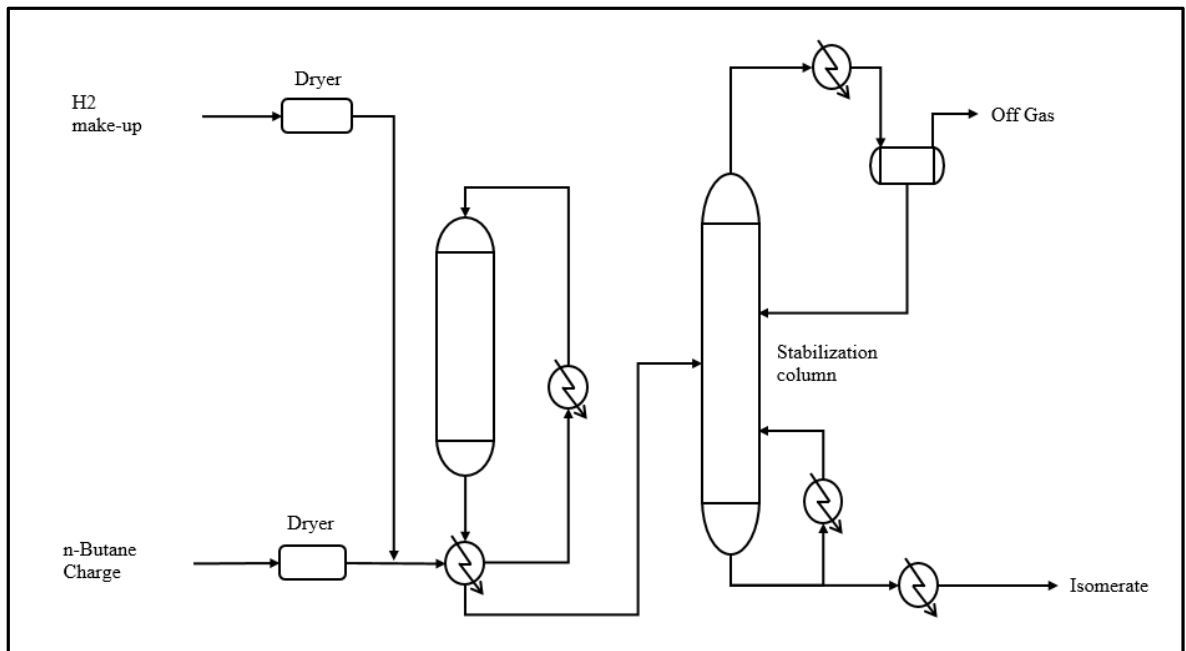


Figure 2.10. Process flow diagram of Butamer process.

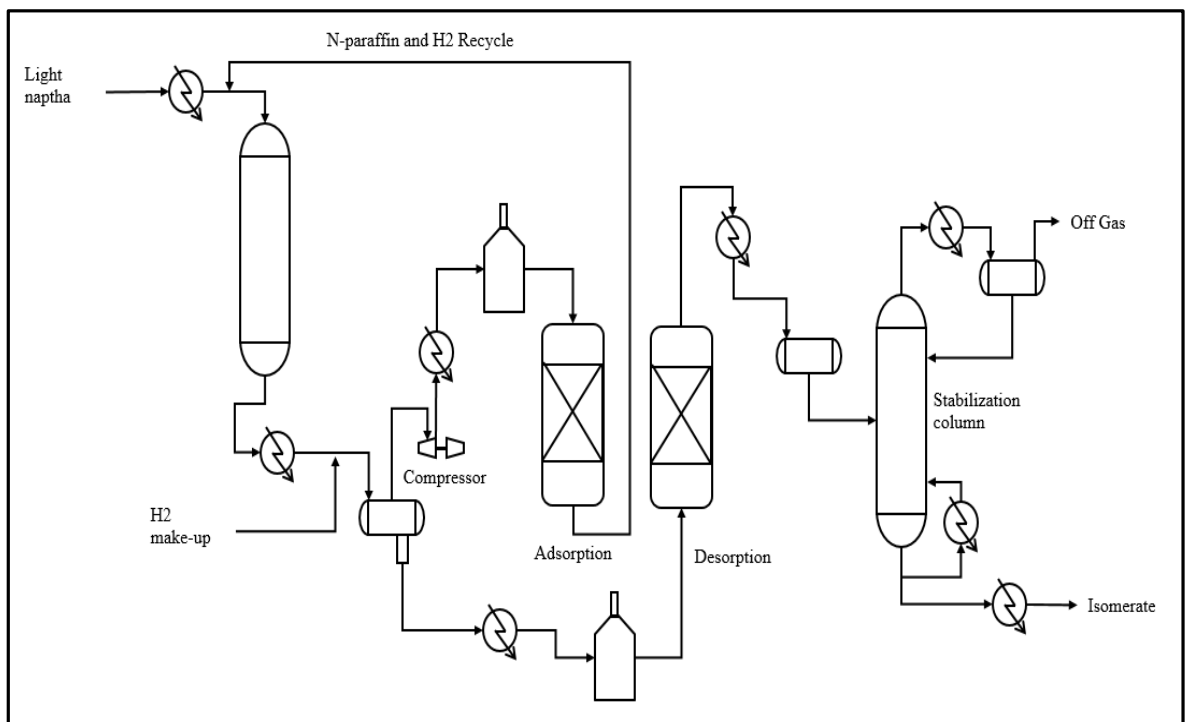


Figure 2.11. Process flow diagram of TIP process.

Table 2.5. Processes for light naphtha isomerization.

Generation	Licensors	Feed	Phase	T(°C)	P(kg/cm ²)	Catalyst
I	Shell	C ₄	Gas	95-150	-	AlCl ₃ / bauxite / HCl
	UOP	C ₄	Liquid	-	-	AlCl ₃ / HCl
	Standard Oil	C ₅ / C ₆	Liquid	80-100	-	AlCl ₃ / HCl
	Shell	C ₄ , C ₅ / C ₆	Liquid	-	-	AlCl ₃ / SBF ₃ / HCl
II	UOP: Butamer	C ₄	Gas	375	-	Pt / Support
	Kellogg: Iso-Kel	C ₅ / C ₆	Gas	400	20-40	Group (VIII) / Support
	Pur Oil: Isomerase	C ₅ / C ₆	Gas	420	50	Not noble metal / Support
	UOP: Penex HT	C ₅ / C ₆	Gas	400	20-70	Pt / Support
	Linde	C ₅ / C ₆	Gas	320	30	Pt / Si-Al
	Atlantic Refining Pentafining	C ₅ / C ₆	Gas	450	50	Pt / Si-Al
III	UOP: Penex BT	C ₄ , C ₅ / C ₆	Gas	110-180	20-70	Pt / Al ₂ O ₃ ; AlCl ₃
	BP	C ₄ , C ₅ / C ₆	Gas	110-180	10-25	Pt / Al ₂ O ₃ ; CCl ₄
	IFP	C ₄ , C ₅ / C ₆	Gas	110-180	25-50	Pt / Al ₂ O ₃ ; AlR _x Cl _y
	UOP: Butamer	C ₄	Gas	110-180	20-30	Pt / Al ₂ O ₃ ; AlCl ₃
IV	Shell: Hysomer	C ₅ / C ₆	Gas	230-300	30	Pt / H-modernite
	Mobil	C ₆	Gas	315	20	H-modernite (Pt, Pd)
	UOP	C ₆	Gas	150	-	H-modernite + PtRe / Al ₂ O ₃
	Sun Oil	C ₅ / C ₆	Gas	325	30	PtHY
	Norton	C ₅	Gas	250	30	Pd / modernite
	IFP	C ₅ / C ₆	Gas	240-260	15-30	Pt / H-modernite

2.3. Packed Bed Reactors

Packed bed reactors consist of uniformly sized catalyst particles distributed regularly or randomly in a tube or vessel. The fluid stream sent to the reactor flows through the catalyst particles and undergoes chemical reaction on the catalyst active sites resulting in heat absorption or heat release. In some systems, heat addition or removal is needed by quench flow or through the tube wall. Examples of the simple packed bed reactor and multitubular fixed bed reactor are given in Figure 2.12 respectively [34].

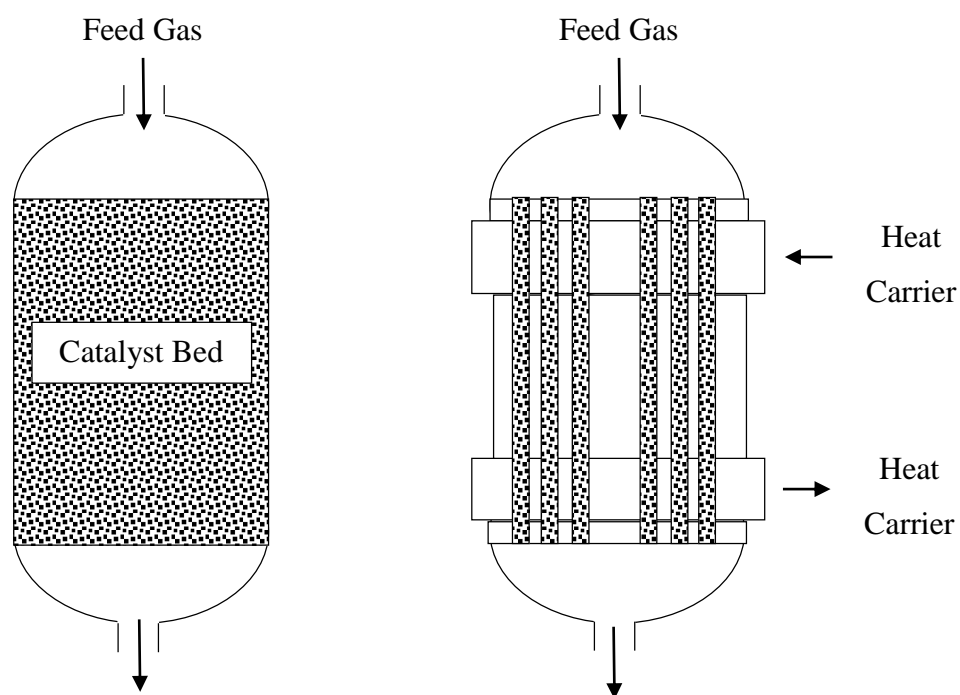


Figure 2.12. Basic types of catalytic packed bed reactors.

The main element of packed bed reactors, as the term “packed” implies, is the solid catalyst placed in the reactor tube. There are many types of solid catalysts that are used for different types of chemical processes. The catalyst makes the processes specific for a given type of production and is like the fingerprint of the process. Some examples of catalysts are listed in Table 2.6 to indicate their area of use [35].

Table 2.6. Catalyst types used for different chemical reactions.

Catalyst	Reaction
Metals (Ni, Pd, Pt as powders or on supports) or metal oxides (Cr ₂ O ₃)	C=C bond hydrogenation olefin + H ₂ → paraffin
Metals (Cu, Ni, Pt)	C=O bond hydrogenation acetone + H ₂ → isopropanol
Metal (Pd, Pt)	Complete oxidation of hydrocarbons, oxidation of CO
Fe (supported and promoted with alkali metals)	3H ₂ + N ₂ → 2NH ₃
Ni	CO + 3H ₂ → CH ₄ + H ₂ O (methanation)
Fe or Co (supported and promoted with alkali metals)	Fischer Tropsch reaction
Cu (supported on ZnO, with other components, Al ₂ O ₃)	CO + 2H ₂ → CH ₃ OH
Re + Pt (supported on η-Al ₂ O ₃ or γ-Al ₂ O ₃ promoted with chloride)	Paraffin dehydrogenation, isomerization and dehydrocyclization
Solid acids (SiO ₂ -Al ₂ O ₃ , zeolites)	Paraffin cracking and isomerization
γ-Al ₂ O ₃	Alcohol → olefin + H ₂ O
Pd supported on acidic zeolite	Paraffin hydrocracking
Metal oxide supported complexes of Cr, Ti, Zr	Olefin polymerization ethylene → polyethylene
Metal oxide supported complexes of W or Re	Olefin metathesis 2 propylene → ethylene + butene
Ag (on inert support, promoted by alkali metals)	Ethylene + ½ O ₂ → ethylene oxide
V ₂ O ₅ or Pt	2SO ₂ + O ₂ → 2 SO ₃
V ₂ O ₅ (on metal oxide support)	Naphthalene + 9/2 O ₂ → phthalic anhydride + 2CO ₂ + 2H ₂ O
Bismuth molybdate	Propylene + ½ O ₂ → acrolein
Mixed oxides of Fe and Mo	CH ₃ OH + O ₂ → formaldehyde
Fe ₃ O ₄ or metal sulfides	H ₂ O + CO → H ₂ + CO ₂

In the majority of fixed-bed reactors used for industrial synthesis reactions, direct or indirect supply or removal of heat in the catalyst bed is utilized to adapt the temperature profile over the flow path to the requirements of an optimal reaction pathway as much as possible.

Packed bed reactors have complex physical and chemical phenomena, thus exact mathematical description of these reactors is not possible. Instead, simplified models are used to define the problem. Moreover, nonlinear reaction rate expressions also complicate the solution of differential and algebraic set of equations. Therefore the problem is usually handled by numerical or approximate solutions. In packed bed reactors, convection is generally dominant to conductional heat and diffusional mass transfer, thus defining these terms is very important. Considering the complexity of the equations involved, techniques treating various phenomena in one algorithm that solves the entire set of equations are needed. Each individual technique should be flexible and simple enough to allow incorporation in a large program and at the same should be robust and efficient enough to solve the problem in a reliable and efficient way [36].

Different types of numerical methods were developed to solve these complex problems. Ordinary differential equations are mostly solved by the Runge-Kutta technique or by Gear's method [37]. Parabolic partial differential equations are often transformed to ordinary differential equation by using the method of lines [38]. Collocation methods are also widely used for solution of the packed bed reactor model [39].

2.3.1. Trickle Bed Reactors

Trickle bed reactors are one example of packed bed reactors that have liquid and gas trickles over solid catalyst particles. They are commonly used in petroleum refineries and petrochemical plants that have mass production. Generally they are 3-6 m in length and up to 3 m in diameter. Commonly used processes are hydrocracking, hydrodesulphurization, hydrotreating, and isomerization in refineries. There are several transport resistances in these type of reactors. These resistances are shown in Figure 2.13 [40].

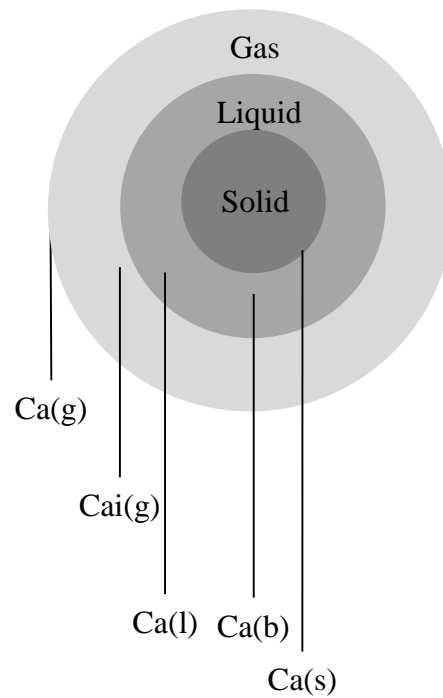


Figure 2.13. Transport resistances in trickle bed reactor catalyst.

Transport steps can be summarized as follows [41]:

- Transport from the bulk gas phase to the gas-liquid interface
- Equilibrium at gas-liquid interface
- Transport from interface to bulk liquid
- Transport from bulk liquid to external catalyst surface
- Diffusion and reaction in the pellet
- Transport of products from bulk liquid to solid catalyst interface
- Transport from bulk liquid to interface
- Equilibrium at liquid - gas interface
- Transport from the gas-liquid interface to the bulk gas phase

2.3.2. Plug Flow Reactor Model

A mathematical model for an industrial trickle bed reactor is necessary for understanding reactor behavior and for deciding on the operating conditions for optimum

production. An ideal reactor generally operates isothermally; however, since industrial reactors operate non-isothermally, heat balance should also be considered while modelling [42]. General heat and mass balances are obtained with the assumptions listed below:

- Reactor operates at steady state conditions,
- There is no catalyst deactivation,
- One dimensional model is valid (because there is generally no information available to make a two dimensional model),
- Complete wetting of catalyst is assumed,
- Pressure is constant along the reactor.

When a trickle bed reactor is operated at high temperatures and pressures, the liquid reactants vaporize and the two-phase behavior creates a complex reaction system. In order to meet the requirements of the model, the volatility effect must also be taken into account. A study made with first and second order power law and Langmuir-Hinshelwood kinetics shows that there is more than 30% difference between volatile and nonvolatile cases [43]. Reactions take place in the liquid phase thus concentrations of components are taken from liquid phase. Detailed formulization of reactor model is given in Section 3.3.

3. REACTOR MODELING

Mathematical model constructed for isomerization reactor is explained in detail in this chapter. Matlab© ODE (Ordinary Differential Equation) solvers are used to solve heat and mass balance equations used for this reactor system. Isomerization reactions that take place on chlorinated Pt/Al₂O₃ catalyst are examined and the parameters of reactions are calculated in this work. Dimensions of reactors, inlet feed conditions (temperature, pressure, composition) are taken from the process historian database, catalyst information is used from UOP's I-8 catalyst MSDS and initial reaction parameters are taken from literature and Aspen HYSYS ISOM reactor modules.

3.1. Thermodynamic Analysis

The objective of light naphtha isomerization unit all over the world is to increase the research octane number (RON) of mixture of C₅/C₆ paraffin. The octane numbers of hydrocarbons given in Table 3.1 shows the effect of isomerization reactions on octane number change [15].

Table 3.1. Light naphtha blending components octane numbers.

Component	RON
i-pentane	93.5
n-pentane	61.7
2,2 dimethylbutane	94.0
2,3 dimethylbutane	105.0
2 methylpentane	74.4
3 methylpentane	75.5
n-hexane	31.0
Benzene	120.0
Cyclohexane	84.0
Methylcyclopentane	96.0

Isomerization of straight lined hydrocarbons to their branched isomers is slightly exothermic. Thermodynamic calculations show that the yield of branched alkanes is thermodynamically favored at low temperatures. These calculations are done by ASPEN HYSYS© software using Soave-Redlich-Kwong (SRK) equation of state by Gibbs reactor. The equilibrium compositions of C₄, C₅, and C₆'s shown in Figure 3.1, Figure 3.2, and Figure 3.3 are in accordance with the results given in literature [31,44].

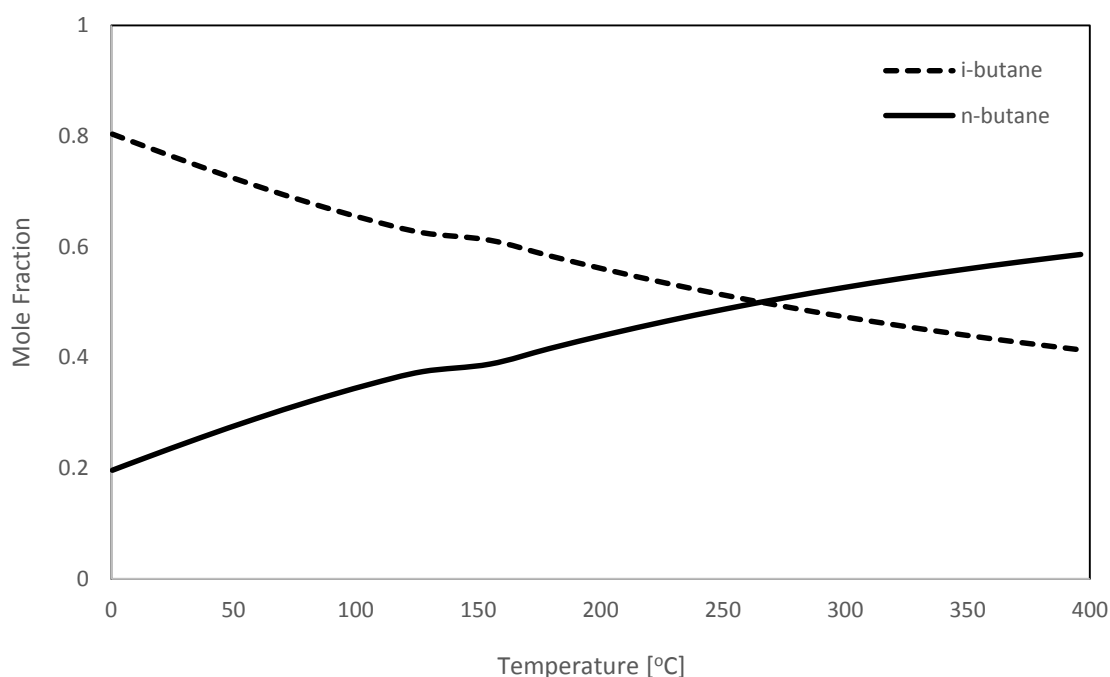


Figure 3.1. Thermodynamic equilibrium for butane and its isomers.

As seen from the Figure 3.1, isobutene composition is highly affected by temperature and it is favored at low temperatures. However, n-butane is favored at higher temperatures. Branched isomers have higher octane numbers, thus, low reaction temperature is desired for reaction media.

Figure 3.2 shows that, production of branched hydrocarbons, isopentane and neopentane, is favored at lower temperatures, whereas n-pentane formation is favored at high temperatures.

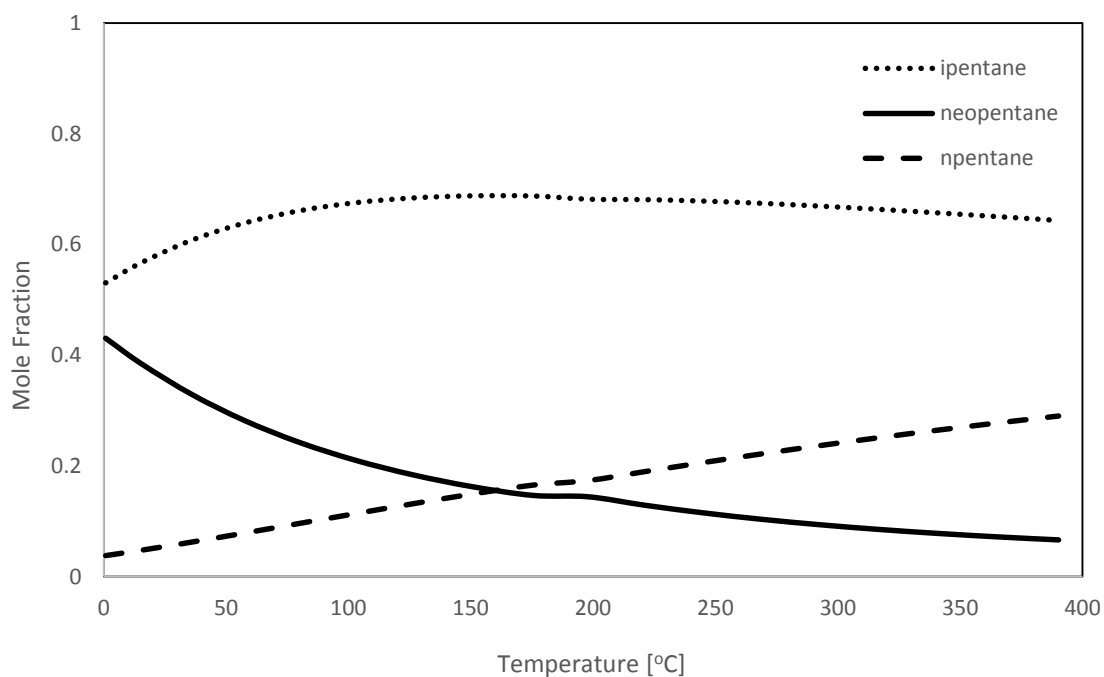


Figure 3.2. Thermodynamic equilibrium for pentane and its isomers.

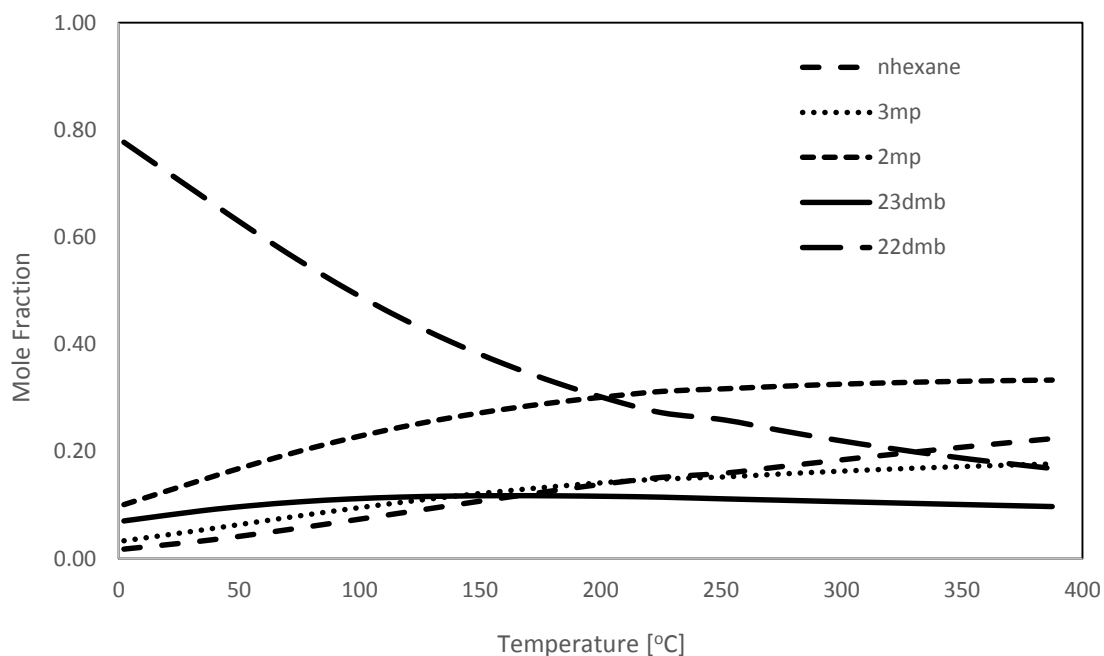


Figure 3.3. Thermodynamic equilibrium for hexane and its isomers.

The most temperature sensitive isomer is 2,2-dimethylbutane and it is

thermodynamically favored at low temperatures. However, 2,3-dimethylbutane is nearly unchanged for the temperature range. In addition, n-hexane and the methyl pentanes are favored at higher temperatures.

3.2. Vapor Liquid Equilibrium

Vapor-liquid equilibrium calculations are very important for processes including two phases. A typical system which needs flash calculation is shown in Figure 3.4.

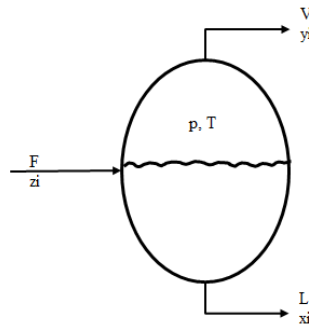


Figure 3.4. A general flash process.

Mass balance equations written for the system is done for every single component:

$$Fz_i = Lx_i + Vy_i \quad (3.1)$$

The vapor and liquid is assumed to be in equilibrium, thus:

$$y_i = K_i x_i \quad (3.2)$$

In addition to equations above, Equations 3.3 and 3.4 can be used for trial-error calculation procedure and properties of liquid and vapor phase can be calculated.

$$\sum x_i = 1 \quad (3.3)$$

$$\sum y_i = 1 \quad (3.4)$$

$$\sum(y_i - x_i) = 0 \quad (3.5)$$

Studies done for this calculation techniques show that Equation 3.5 gives better numeric results and when it is updated with Equations 3.3 and 3.4, Rachford-Rice flash equation is obtained [45]:

$$G = \sum \frac{z_i (K_i - 1)}{1 + \frac{V}{F} (K_i - 1)} = 0 \quad (3.6)$$

Rachford-Rice flash equation is solved by trial error according to V/F ratio. Cubic iteration method named Householder's method, shown below, is used for this solution [46].

$$VF_{n+1} = VF_n - \frac{G}{G'} \left[1 + \frac{G \cdot G''}{2G'^2} \right] \quad (3.7)$$

G' , and G'' are first and second derivatives of G function given in Equation 3.6 with respect to V/F ratio:

$$G' = -\sum \frac{z_i (K_i - 1)^2}{\left(1 + \frac{V}{F} (K_i - 1)\right)^2} \quad (3.8)$$

$$G'' = \sum \frac{2z_i (K_i - 1)^3}{\left(1 + \frac{V}{F} (K_i - 1)\right)^3} \quad (3.9)$$

First estimation of K_i is calculated by Wilson correlation [47]:

$$K_i = \frac{P_{ci}}{P} \exp \left[5.37(1 + \omega_i) \left(1 - \frac{T_{ci}}{T} \right) \right] \quad (3.10)$$

In preceding iterations, thermodynamic equation of state is used to calculate K_i values. The feed for isomerization processes is classified as light naphtha. Thus, the most suitable equation of state used for such mixtures is defined by Soave-Redlich-Kwong (SRK) [48]:

$$P = \frac{RT}{V-b} - \frac{a}{V(V+b)} \quad (3.11)$$

By this equation, molar volume, molar density, compressibility factor, specific heat, enthalpy and fugacity coefficient can be calculated by knowing the stream's molar component fraction, temperature and pressure.

When Equation 3.11 is rearranged with respect to compressibility factor, a 3rd order equation can be obtained.

$$Z^3 + a_2 Z^2 + a_1 Z + a_0 = 0 \quad (3.12)$$

With the solution of this equation, three roots are obtained. The maximum valued root gives the compressibility factor of vapor phase, and the minimum valued root gives the liquid phase compressibility factor. Temperature and pressure based parameters of this equation are;

$$a_2 = (\varepsilon + \sigma - 1)B - 1 \quad (3.13)$$

$$a_1 = A - (\varepsilon + \sigma)B - (\varepsilon + \sigma - \varepsilon\sigma)B^2 \quad (3.14)$$

$$a_0 = -AB - \varepsilon\sigma(1+B)B^2 \quad (3.15)$$

ε and σ are switching parameters and for SRK equation of state, their values are $\varepsilon = 0$ and $\sigma = 1$.

A and B are attraction and repulsive parameters respectively and they are dimensionless;

$$A = \frac{P}{(RT)^2} a_m \quad (3.16)$$

$$B = \frac{P}{RT} b_m \quad (3.17)$$

$$a_m = \sum x_i \Psi_i \quad (3.18)$$

$$b_m = \sum x_i b_i \quad (3.19)$$

$$\Psi_i = \sum x_j a_{ij} \quad (3.20)$$

$$a_{ij} = \sqrt{a_i a_j \alpha_i \alpha_j} (1 - k_{ij}) \quad (3.21)$$

$$a_i = \Omega_a R^2 \frac{T_{ci}^2}{P_{ci}} \quad (3.22)$$

$$b_i = \Omega_b R \frac{T_{ci}}{P_{ci}} \quad (3.23)$$

For SRK equation of state, $\Omega_b = 0.427480$ and $\Omega_a = 0.086640$. Other parameters are:

$$\alpha_i = \left[1 + m_i (1 - \sqrt{T_r}) \right]^2 \quad (3.24)$$

$$m_i = 0.480 + 1.574\omega_i - 0.176\omega_i^2 \quad (3.25)$$

The interaction parameters k_{ij} are generally assumed to be zero for easy calculation, however, studies show that when H₂-HC interaction parameters are estimated, better physical property results are achieved [49]. According to the correlation given, interaction parameters can be calculated as follows:

$$k_{iH_2} = S + R \cdot BP_i \quad (3.26)$$

$$S = 0.3852 - 0.00241 C_{aromatics\%} \quad (3.27)$$

$$R = 0.002245 + 1.96 \cdot 10^{-5} C_{aromatics\%} \quad (3.28)$$

In isomerization system, the only aromatic component is benzene and its mass fraction is used to calculate the interaction parameters. By these interaction parameters, the vapor fraction and composition results became closer to ASPEN HYSYS results. By using Equations 3.13 to 3.28, the coefficients of Equation 3.12 are obtained and the root of it gives the molar volume. Compressibility factor then calculated as:

$$Z = \frac{P \times V}{R \times T} \quad (3.29)$$

As last step, fugacity coefficient is calculated by:

$$\ln \phi_i^p = \frac{B_i}{B} (Z^p - 1) - \ln(Z^p - B) - \left(\frac{A}{(\varepsilon - \sigma)B} \right) \left[2 \frac{A_{ij}}{A} - \frac{B_i}{B} \right] \ln \left(\frac{Z^p + \varepsilon B}{Z^p + \sigma B} \right) \quad (3.30)$$

$$B_i = \frac{P}{RT} b_i \quad (3.31)$$

$$A_{ij}^p = \frac{P}{(RT)^2} \Psi_i^p \quad (3.32)$$

New K_i values by liquid and vapor fugacity coefficient can be calculated as:

$$K_i = \frac{\phi_i^L}{\phi_i^V} \quad (3.33)$$

The solution procedure of flash calculation is shown in Figure 3.5 in detail. The results of flash calculations are given in Figure 3.6.

The calculations defined above are done separately for 58 days. Figure 3.6 shows the results of these 58 data inlet flash calculation. Black line is the result of ASPEN HYSYS calculations. There are used to check the accuracy of calculation. Dotted line shows the first completed flash procedure. The result are in agreement at most of the days but at some days, the difference is very big that cannot be ignored. With these results, it is concluded that modification is needed for better vapor fraction estimation. Equations 3.26 to 3.28 are defined for interaction parameters of binary components. As the result, black dots are acquired which has high accuracy with ASPEN HYSYS results.

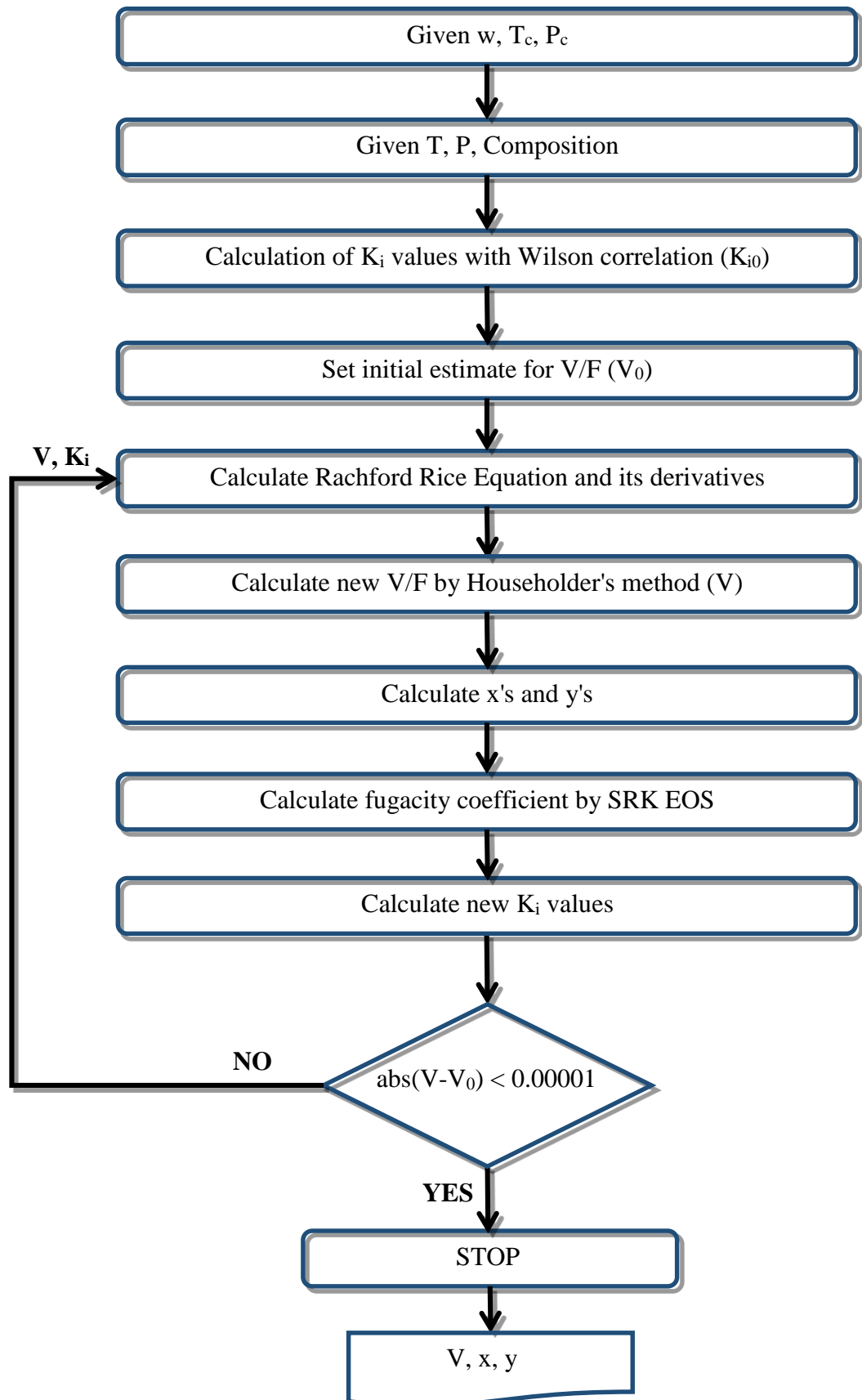


Figure 3.5. Flow chart of flash calculation procedure.

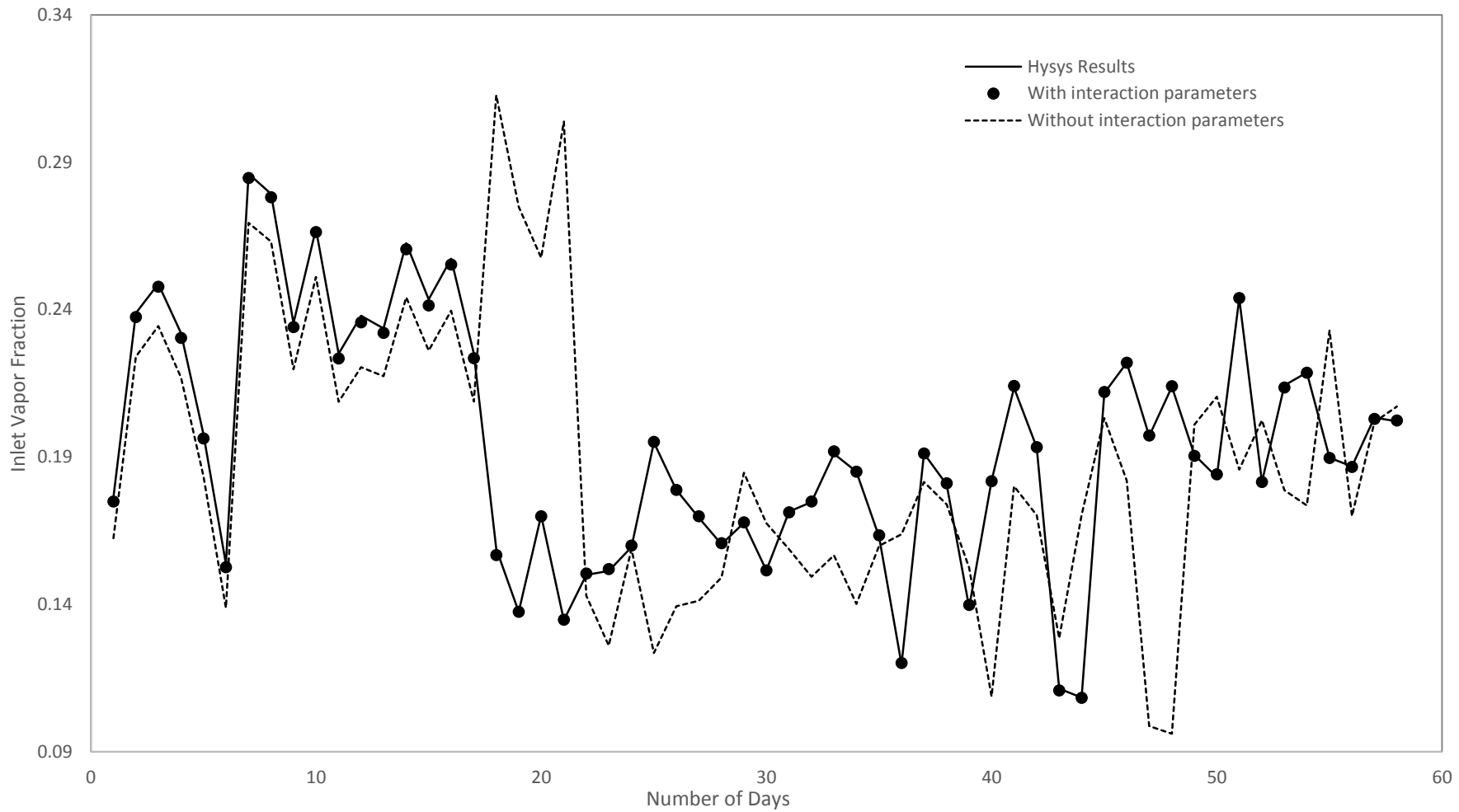


Figure 3.6. Comparison of flash calculations with ASPEN HYSYS.

3.3. Plug Flow Reactor Model

3.3.1. Mass Balance

System boundaries must be determined to be able to write mass balance or mole balance on any system. A general mole balance is represented by the formula below:

$$\begin{bmatrix} \text{Rate of} \\ \text{flow of } i \\ \text{into the} \\ \text{system} \end{bmatrix} - \begin{bmatrix} \text{Rate of} \\ \text{flow of } i \\ \text{out of the} \\ \text{system} \end{bmatrix} + \begin{bmatrix} \text{Rate of} \\ \text{generation of } i \\ \text{within the} \\ \text{system} \end{bmatrix} = \begin{bmatrix} \text{Rate of} \\ \text{accumulation of} \\ i \text{ within the} \\ \text{system} \end{bmatrix} \quad (3.34)$$

The system is assumed to be at steady state, thus the accumulation term goes to zero. As shown below, shell balance is written for a control volume whose thickness is equal to Δz and mole balance is accomplished. The schematic representation of shell balance is shown in Figure 3.7.

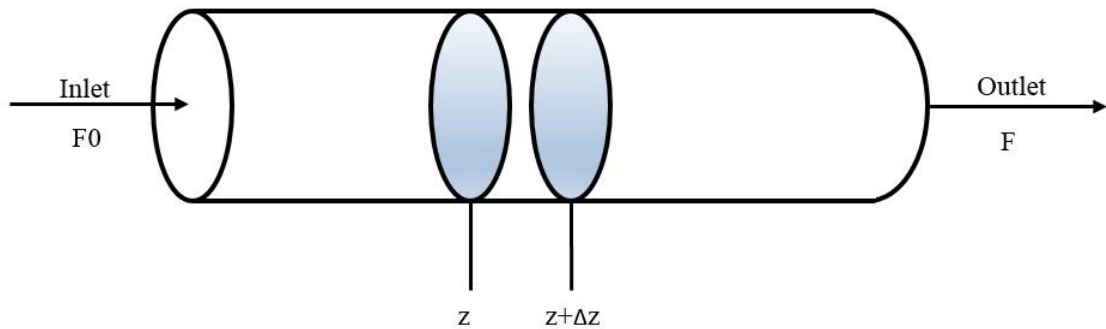


Figure 3.7. Control volume of a plug flow reactor system.

$$F_{i|z} - F_{i|z+\Delta z} + r_{i,j} A_c \rho_b \mathcal{G}_{i,j} \Delta z = 0 \quad (3.35)$$

$$\frac{F_{i|z} - F_{i|z+\Delta z}}{\Delta z} = -r_{i,j} A_c \rho_b \mathcal{G}_{i,j} \quad (3.36)$$

$$\frac{dF_i}{dz} = r_{i,j} A_c \rho_b \vartheta_{i,j} \quad (3.37)$$

For multiple reaction systems:

$$\frac{dF_i}{dz} = A_c \rho_b \sum r_{i,j} \vartheta_{i,j} \quad (3.38)$$

Reaction rate is defined as power law:

$$r_j = k_j \cdot C_i^a \cdot C_{H_2}^b \quad (3.39)$$

Reaction constant is defined with Arrhenius equation:

$$k_j = k_j^o \cdot \exp\left(\frac{-E_{A,j}}{R \cdot T}\right) \quad (3.40)$$

3.3.2. Energy Balance

The general energy balance for a system shown in Figure 3.7 can be written as follows:

$$\begin{bmatrix} \text{Rate of} \\ \text{flow of} \\ \text{heat to} \\ \text{the system} \\ \text{from} \\ \text{surr.} \end{bmatrix} - \begin{bmatrix} \text{Rate of} \\ \text{work} \\ \text{done} \\ \text{the} \\ \text{system} \\ \text{on surr.} \end{bmatrix} + \begin{bmatrix} \text{Rate of} \\ \text{energy} \\ \text{added} \\ \text{to the} \\ \text{system} \\ \text{by mass} \\ \text{flow} \\ \text{into the} \\ \text{system} \end{bmatrix} + \begin{bmatrix} \text{Rate of} \\ \text{energy} \\ \text{leaving} \\ \text{the system} \\ \text{by} \\ \text{mass flow} \\ \text{out of the} \\ \text{system} \end{bmatrix} = \begin{bmatrix} \text{Rate of} \\ \text{acc.} \\ \text{of energy} \\ \text{within the} \\ \text{system} \end{bmatrix} \quad (3.41)$$

The system is assumed to be steady state, thus the accumulation term goes to zero. Shell balance is written for a Δz thickness control volume and energy balance is

accomplished. After necessary steps, the final form of the energy balance for the packed bed reactor shown in Figure 3.7 can be expressed as follows:

$$\frac{dT}{dz} = A_c \rho_b \frac{\sum r_{i,j} \Delta H_j}{F_{vap} C_{p,vap} + F_{liq} C_{p,liq}} \quad (3.42)$$

3.3.3. Reactor Model

Trickle bed reactors are widely used in refinery and in petrochemical companies. Refineries use this type of reactors for sulfur, nitrogen, oxygen and metal removal, olefins and aromatic saturation, isomerization and cracking activities. These processes need high temperature and pressure media and, under these conditions, hydrogen-hydrocarbon mixture exists in vapor-liquid equilibrium. In this type of reactors, reaction only occurs in liquid phase.

Isomerization reactors typically operate at 30-35 kg/cm² pressure and 130-180 °C temperature range with vapor-liquid equilibrium conditions established. Literature survey shows that modelling studies are generally done without vapor-liquid equilibrium assumption. Thus, this area of study is open to development in isomerization reactor modelling.

General assumption that are used to start reactor modelling can be classified as follows [50]:

- System is at steady state (no catalyst deactivation),
- One-dimensional flow occurs (radial change is zero),
- Mass and heat transfer occurs by convection,
- Plug flow reactor,
- Adiabatic operation,
- Constant pressure,
- Complete catalyst wetting,
- Formalized mechanism of reaction scheme,

- Reactions occur only in liquid phase,
- Reaction rates are described by empirical, power law type expressions.

With these assumptions, first of all, a reaction scheme is identified. The most complex reaction scheme studied nowadays has 36 reactions identified [50]. By defining additional cracking reactions, finally 48 reactions are acquired and these reactions are shown in Figure 3.8.

Isomerization reactions are equilibrium reactions and they are reversible. Thus, every isomerization reaction is defined as two different irreversible reactions. 8 equilibrium reactions are defined by 16 reactions, which are given in Table 3.2.

Table 3.2. Isomerization reactions defined for reactor model.

$nC_4 \rightarrow iC_4$	$iC_4 \rightarrow nC_4$	$nC_5 \rightarrow iC_5$	$iC_5 \rightarrow nC_5$
$nC_6 \rightarrow 2MP$	$2MP \rightarrow nC_6$	$nC_6 \rightarrow 3MP$	$3MP \rightarrow nC_6$
$23DMB \rightarrow 2MP$	$2MP \rightarrow 23DMB$	$23DMB \rightarrow 22DMB$	$22DMB \rightarrow 23DMB$
$MCP \rightarrow CH$	$CH \rightarrow MCP$	$3MP \rightarrow 2MP$	$2MP \rightarrow 3MP$

Benzene saturation and ring opening reactions are defined by 9 different reactions, which are given in Table 3.3.

Table 3.3. Benzene saturation and ring opening reactions.

$CP + H_2 \rightarrow nC_5$	$CP + H_2 \rightarrow iC_5$	$CH + H_2 \rightarrow nC_6$
$MCP + H_2 \rightarrow 2MP$	$MCP + H_2 \rightarrow 3MP$	$MCP + H_2 \rightarrow 23DMB$
$MCP + H_2 \rightarrow 22DMB$	$BEN + 3H_2 \rightarrow MCP$	$BEN + 3H_2 \rightarrow CH$

Apart from those given above, 23 reactions, given in Table 3.4, are used to describe cracking:

Table 3.4. Cracking reactions defined for reactor model.

$nC_4 + H_2 \rightarrow C_1 + C_3$	$nC_4 + H_2 \rightarrow 2C_2$	$iC_4 + H_2 \rightarrow C_1 + C_3$
$nC_5 + H_2 \rightarrow C_1 + nC_4$	$nC_5 + H_2 \rightarrow C_2 + C_3$	$iC_5 + H_2 \rightarrow C_1 + nC_4$
$iC_5 + H_2 \rightarrow C_1 + iC_4$	$iC_5 + H_2 \rightarrow C_2 + C_3$	$nC_6 + H_2 \rightarrow C_1 + nC_5$
$nC_6 + H_2 \rightarrow C_2 + nC_4$	$nC_6 + H_2 \rightarrow 2C_3$	$2MP + H_2 \rightarrow C_1 + nC_5$
$2MP + H_2 \rightarrow C_1 + iC_5$	$2MP + H_2 \rightarrow C_2 + iC_4$	$2MP + H_2 \rightarrow 2C_3$
$3MP + H_2 \rightarrow C_1 + nC_5$	$3MP + H_2 \rightarrow C_1 + iC_5$	$3MP + H_2 \rightarrow C_2 + nC_4$
$23DMB + H_2 \rightarrow C_1 + iC_5$	$23DMB + H_2 \rightarrow 2C_3$	$23DMB + H_2 \rightarrow C_1 + iC_5$
$22DMB + H_2 \rightarrow C_2 + iC_4$	$nC_7 + H_2 \rightarrow C_1 + nC_6$	

Totally with 48 reactions, the reaction scheme for isomerization reactor is completed.

After all of the reactor model equations are decided and completed, the codes are written in Matlab© program. The sequence of codes are given in detail below.

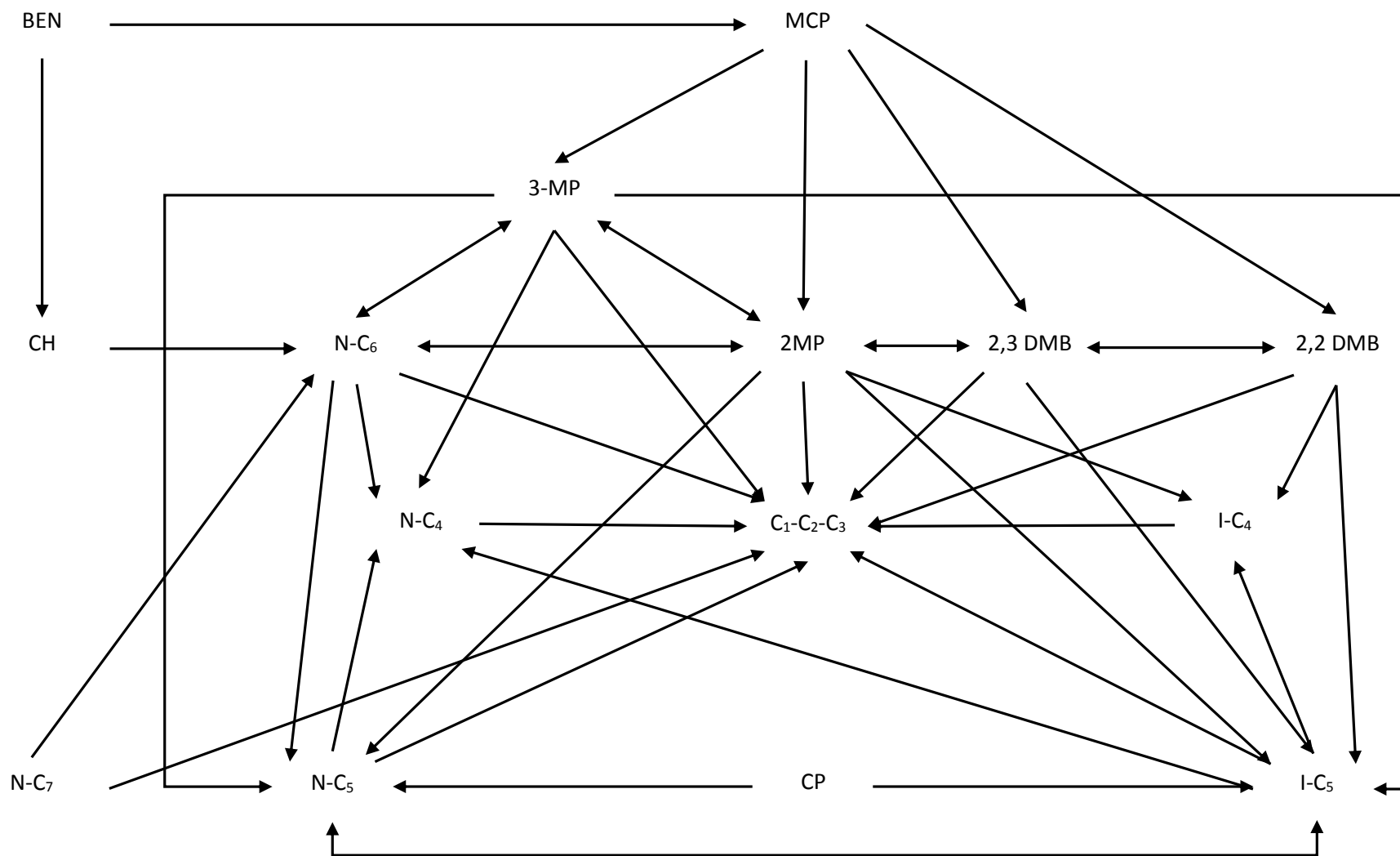


Figure 3.8. Completed reaction scheme for isomerization reactions.

3.3.3.1. Data Files. Before starting to write the codes, the data should be introduced to the program. In this study, 5 different input data are formed and implemented into the codes.

Input Data: Input data file contains reactor inlet data from the process. These data are reactor inlet temperature ($^{\circ}\text{C}$), reactor inlet pressure ($\text{kg}/\text{cm}^2\text{-g}$) and inlet composition (tonmol/day). There are 35 components defined for isomerization unit feed in ASPEN HYSYS, with inlet temperature and inlet pressure, the input data is formed. Thus for 58 days of data, the input data is 37×58 matrix. Data are given in Table A.2.

Plant Data: Plant data file contains reactor data from the process. The data represent temperatures taken from 5 different points along the reactor, reactor outlet temperature ($^{\circ}\text{C}$), reactor outlet pressure ($\text{kg}/\text{cm}^2\text{-g}$), and outlet composition for 35 components (tonmol/day). Thus for 58 days of data, the plant data is represented as a 42×58 matrix. Data are given in Table A.3.

Thermochemical Data: This file contains the heat of formations, specific heat constants, acentric factors, critical temperatures, critical pressures, boiling points and molecular weights of the components involved in the reaction network which results in 10 specific properties. Thus for 35 components, 35×10 matrix is identified for thermochemical properties. Data are given in Table A.4.

Coefficient Data: This file contains the stoichiometric coefficients of the reactions. When a component is consumed in a reactor, its coefficient is negative, otherwise its coefficient is positive. There are 35 components and 48 reactions defined in this study. Thus, a 35×48 matrix is defined for reactions according to given reaction scheme. Data are given in Table A.5.

Reaction Parameters: This file contains the activation energies and pre-exponential factors of the reactions. As 48 reactions are identified for the reactor, a 48×2 matrix is defined for these parameters. Data are given in Table A.6.

3.3.3.2. Model.M. All the necessary information for reactor model is defined in this file.

Codes are written in a manner that they can be easily updated for a different reactor.

First of all reactor and catalyst properties are defined. These are catalyst bulk density, length of reactor bed, diameter and cross sectional area of the reactor. All these data are set as global parameters. Then thermochemical data, reaction coefficients, inlet data and plant data given in data files are identified and imported to the main file. The flowchart is given in Figure B.1.

3.3.3.3. Simulation.M. This file is written to be able to show the profiles of selected properties along the reactor. It can show the temperature profile along the reactor for given number of days or the outlet concentration comparison between model data and plant data. Inlet and plant data are taken from main file and reaction parameters are taken from data files. It sends the information to plant model file and takes the results from this file. Flow chart is given in Figure B.2.

3.3.3.4. Plant Model.M. This file is written for calculating temperature and concentration along the reactor. Inlet and parameters data are taken from simulation file, needed physical properties to solve the ODE's are taken from SRK file, explained in Section 3.3.3.5, and flash file, explained in Section 3.3.3.6. Ordinary differential equations are solved by the 'ode15s' solver in MATLAB. Flow chart is given in Figure B.3.

3.3.3.5. Srk Eos.M. This file is written for calculating the equation of state properties. Inlet are taken from plant model and thermochemical properties are taken from data files. The formulas given in Section 3.2, are calculated here. Flow chart is given in Figure B.4.

3.3.3.6. Flash.M. This file is written for calculating the equation of state properties. Inlet data are taken from plant model file and thermochemical properties are taken from data files. The Rachford-Rice equation, defined with Equation 3.6, is calculated here. Flow chart is given in Figure B.5.

3.3.3.7. Reactor Model.M. This file is written for solving the reactor model equations. It is one of the main codes in this study because it includes the differential equations written for heat and mass balance calculations. Differential equations are defined as:

$$\frac{dC_i}{dz} = A_c \cdot \rho_b \cdot \sum (stoich_{coeff_i} \cdot rate_j) \quad (3.43)$$

$$\frac{dT}{dz} = \frac{A_c \cdot \rho_b \cdot \sum (rate_j \cdot \Delta H_{rxn_j})}{\sum (F_{liq} \cdot Cp_{liq} + \sum F_{vap} \cdot Cp_{vap})} \quad (3.44)$$

$$\frac{dP}{dz} = 0 \quad (3.45)$$

It takes the plant information from plant model file and calculates reaction rates and heat of reaction, then calculates the differential equation values given in Equations 3.43 to 3.45. Flow chart is given in Figure B.6.

3.3.3.8. Rxn Rates.M. This file is written to be able to calculate reaction rates of 48 reactions. Rates are defined in terms of power law type expressions. For the jth reaction, the rate is written at given temperature T as follows:

$$r_j = k_{0j} \cdot \exp\left(-\frac{Ea_j}{R \cdot T}\right) \cdot C_{ij}^{order} \quad (3.46)$$

This file takes the information from reactor model file and stoichiometric coefficient file. Flow chart is given in Figure B.7.

3.3.3.9. Heat of Reaction.M. This file is written for computing the heat of reaction data. For the jth reaction, heat of reaction is calculated at given temperature T (converted to K):

$$\Delta H_{rxn_j} = \Delta H_{rxn_j}^o + \int_{T^o}^T Cp_j \cdot dT \quad (3.47)$$

This file takes the information from reactor model file, stoichiometric coefficient and thermochemical properties file data is also used. Flow chart is given in Figure B.8.

3.3.4. Parameter Estimation

Parameter estimation is used to predict the model parameters – which are activation energy and reaction constants for this study – by using the plant data. Under normal conditions, up to three months of data can be used to estimate parameters, otherwise the catalytic activity change must be integrated to the model. In this study, however, the catalyst is nearly fully deactivated; thus 1-2 years data can be used to do parameter estimation.

At the first stage of data collection, the composition data are taken from weekly laboratory reports, and flow rates are taken from PIBB (Process Monitoring Data Bank) files between 2012 and 2014. 08:00-16:00 shift average data are used for flow rate data, because laboratory samples are taken in this shift. For gross error detection and data validation, the days that have incomplete laboratory data are discarded. After this filtering, the days that have outlier temperature and flow rate data are discarded. Finally 58 days data are left to start the parameter estimation and simulation studies for which nonlinear least squares method is used:

$$F = \min_{\varnothing} \left(X_p - X_m(\varnothing) \right)^T W \left(X_p - X_m(\varnothing) \right) \quad (3.48)$$

In Equation 3.48, X_p 's are process variables that are temperature and composition, X_m 's are the calculated process variables by the reactor model, and W is the weighting factor. Process variables that are used for parameter estimation are temperatures taken along the reactor, outlet temperature, and compositions of products and of the unconverted normal paraffins. Generally, the reaction rate definition decides the type of parameters. Since power law reaction rate is used, the parameters to be estimated are activation energies and reaction constants only. Weight factor is chosen according to statistical importance of measurements [51].

Initial guess of parameters are given to the codes after checking the literature and the ASPEN HYSYS Isom reactor parameters which are given in Table A.7. Optimization of objective function is solved by 'fminsearch' algorithm in MATLAB and steady state reactor model is used for solution of minimization problem. The objective function that must be

minimized is given in Equation 3.48 and it is defined for temperature and composition as follows:

$$\begin{aligned}
 F(Temp) = & 0.15 \cdot (T_p(1) - T_m(1))^2 + 0.05 \cdot (T_p(2) - T_m(2))^2 + \dots \\
 & 0.00 \cdot (T_p(3) - T_m(3))^2 + 0.10 \cdot (T_p(4) - T_m(4))^2 + \dots \\
 & 0.05 \cdot (T_p(5) - T_m(5))^2 + 0.15 \cdot (T_p(out) - T_m(out))^2
 \end{aligned} \quad (3.49)$$

For $w = 0.045$ and at outlet conditions:

$$\begin{aligned}
 \frac{F(Comp)}{w} = & (C_p(nC_4) - C_m(nC_4))^2 + (C_p(iC_5) - C_m(iC_5))^2 + \dots \\
 & (C_p(nC_5) - C_m(nC_5))^2 + (C_p(22DMB) - C_m(22DMB))^2 + \dots \\
 & (C_p(23DMB) - C_m(23DMB))^2 + (C_p(2MP) - C_m(2MP))^2 + \dots \\
 & (C_p(3MP) - C_m(3MP))^2 + (C_p(nC_6) - C_m(nC_6))^2 + \dots \\
 & (C_p(MCP) - C_m(MCP))^2 + (C_p(cC_6) - C_m(cC_6))^2 + \dots \\
 & (C_p(nC_7) - C_m(nC_7))^2
 \end{aligned} \quad (3.50)$$

$$F = \sqrt{F(Temp) + F(Comp)} \quad (3.51)$$

As stated by the process engineers of the plant, temperature estimation is enough to predict the unit behavior because temperature data is collected at every second by temperature indicators; however, composition data is collected once a week. In addition, because of the time limitation at laboratory, every component is not measured; only the important components are quantified. Thus, the weight of composition in objective function is given by considering this situation.

3.3.4.1. Par Est.M. This file is written for executing parameter estimation for 96 parameters by using 'fminsearch' algorithm in MATLAB. It saves the calculated parameters after finishing the given number of iterations. Inlet and plant data are taken from main file and reaction parameters are taken from data files. It sends the information to objective function file and takes the results from this file. Flow chart is given in Figure B.9.

3.3.4.2. Objective Function.M. This file is written for calculating the value of given objective function. It gives the calculated objective function value to parameter estimation file to solve minimization problem. Inlet and plant data are taken from parameter estimation file and model output are taken from plant model file. Flow chart is given in Figure B.10. Flowchart of complete reactor model and parameter estimation studies are given in Figure B.11.

There are 48 reactions and 96 parameters defined in this study. Because of the high number of reactions and parameters, computational time is also higher than a simple study. Total computational time required for simulation of 58 days is about 1.5 minutes and for parameter estimation, about 10000 iterations, required time is four months.

4. RESULTS AND DISCUSSION

Isomerization reactions are modeled according to the procedure described in Section 3. After parameter estimation is completed, the effects of different process conditions on hydrogen consumption, conversion of paraffins and production of isomers are investigated. Totally, 24 cases are investigated for different inlet temperature, inlet pressure, and inlet flow rate. Default case results are given in APPENDIX A, and studied parameters are given in Table 4.1.

Table 4.1. Parameters studied in reactor model.

Reactor inlet temperature [°C]	100, 110, 120, 130, 140, 150, 160, 170, 180, 190, 200
Reactor inlet pressure [bar_g]	25, 30, 35, 40, 45, 50
Reactor inlet flow rate multiplier	0.1, 0.5, 1.0, 2.0, 3.0, 4.0, 5.0

4.1. Simulation of the Isomerization Reactor

After parameter estimation studies are completed, reactor is simulated and an example result for one of the 58 days is given in Figure 4.1. The black line represents the model result and black dots represent the plant data. It can be clearly seen that temperature profile is correctly estimated and predicted. Additional results are given in Appendix section.

The plant outlet temperature is given as 177.6 °C and model prediction is 177.1 that corresponds to 0.3 % computational error which is in acceptable error range. For the whole simulation, the highest outlet temperature estimate error is calculated as 5.2 % which is again considered as acceptable. These results are shown in Figure 4.2.

The working reactors are nearly fully deactivated and major reaction occurring at the reactor media is benzene reduction at the reactor inlet. Other reactions are not as effective as

reduction reactions. Thus sharp temperature increase at reactor inlet can be explained by sudden benzene reduction reaction. Small temperature rise along the reactor shows that other reactions i.e, isomerization, occurs slower than reduction.

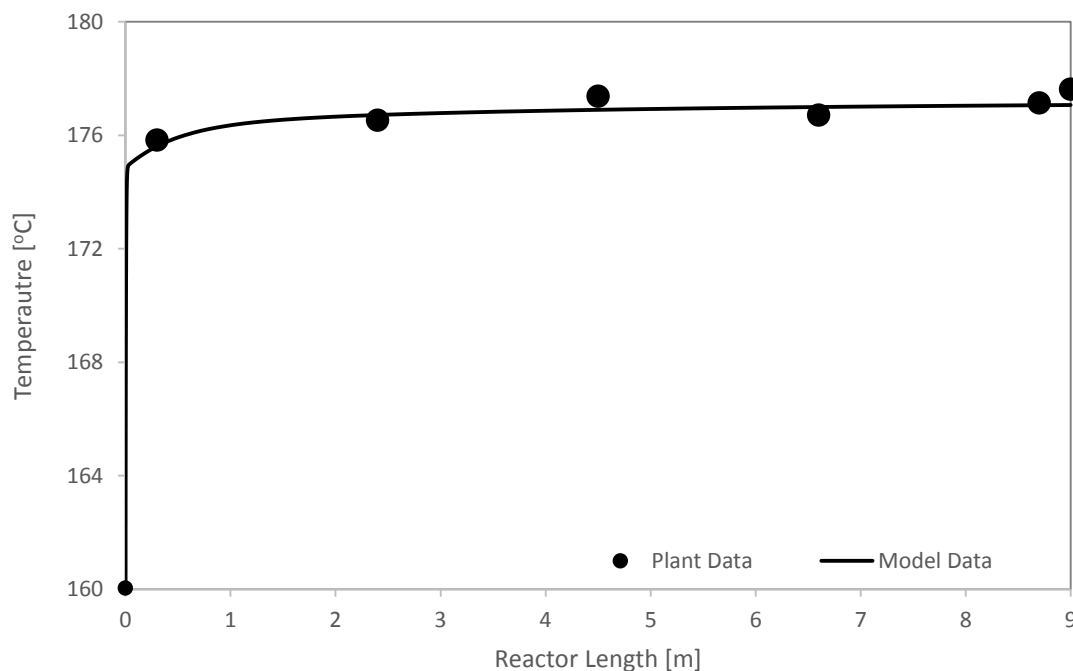


Figure 4.1. Reactor simulation temperature profile for 57. Day.

As stated by the process engineers of the plant, temperature estimation is enough to predict the unit behavior because temperature data is collected at every second by temperature indicators. However, composition data is collected once a week. In addition, because of the time limitation at laboratory, every component is not measured, only important components are measured and there is also measurement errors that must be considered. Thus, good temperature estimation is the best check point to see the unit performance.

Outlet compositions of important components are also shown in this study in addition to temperature. Despite measurement problems, most of the model data is in consistent with plant data except some components.

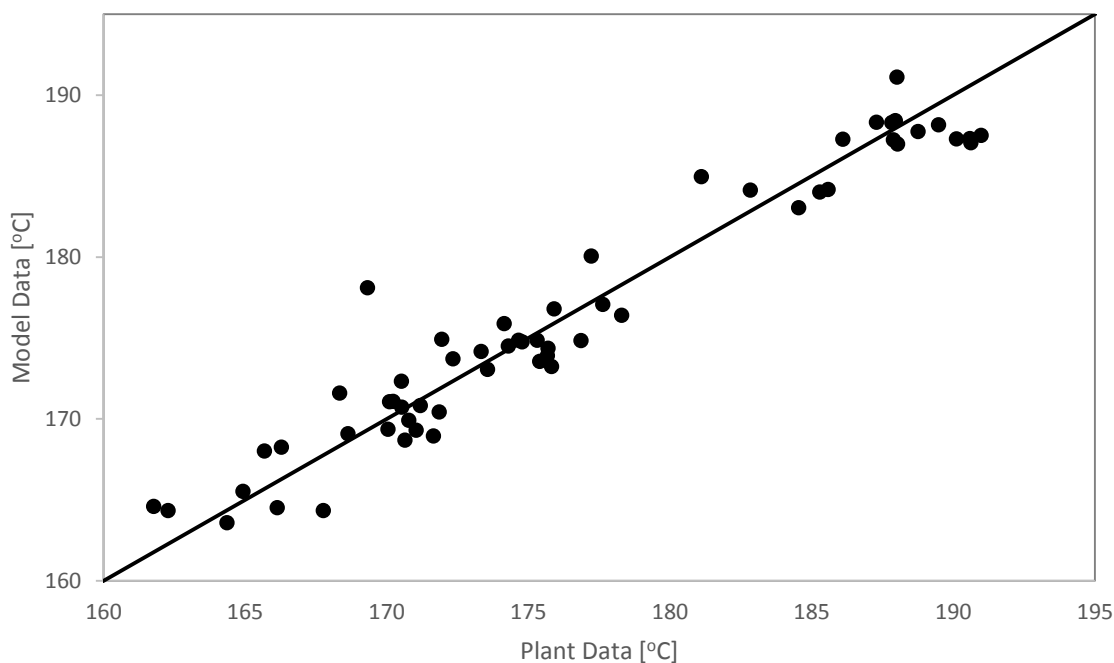


Figure 4.2. Comparison of outlet temperature at 58 days.

N-pentane outlet composition comparison for model and plant data is shown in Figure 4.3. Dotted data show the plant vs. model data and black line is $y=x$ line. As seen from the figure, data points lie on the $y=x$ line with a maximum error of 20 %. In Figure 4.4, it is seen that n-hexane outlet composition is not well estimated. Model estimates are higher than those of the laboratory results. In Figure 4.5, iso-pentane outlet composition is better estimated than n-hexane, and data are clustered around the $y=x$ line. In Figure 4.6, 22DMB composition is estimated like n-hexane. Model predictions are monotonically higher than plant data. In Figure 4.7, 23DMB composition is estimated to be lower than the plant data. In Figure 4.8, 2MP composition is estimated like 22DMB, and model results are higher than plant data. Additionally, benzene concentration is also estimated however, because the laboratory measurement at reactor outlet does not contain benzene, all outlet composition data is zero thus benzene composition could not be compared. Major reason for difference in plant and model data comes from measurement errors. First of all, temperature profile given in Figure 4.1 shows that 4th temperature is lower than 3rd one. In real operation, it is an impossible situation which that temperature must continuously increase along the reactor. This effect can be eliminated by the weight constants of objective function. However for compositions, it is not so easy to determine the weight constants because laboratory analysis is not enough

to be able to do perfect parameter estimation.

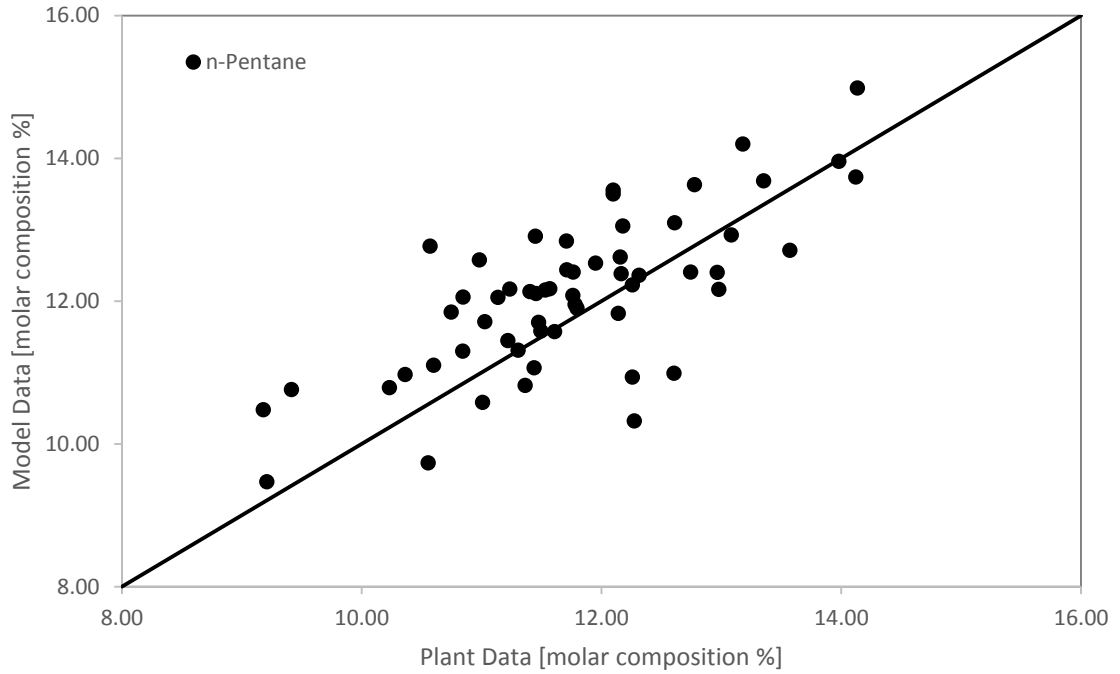


Figure 4.3. Comparison of n-Pentane outlet compositions for 58 days.

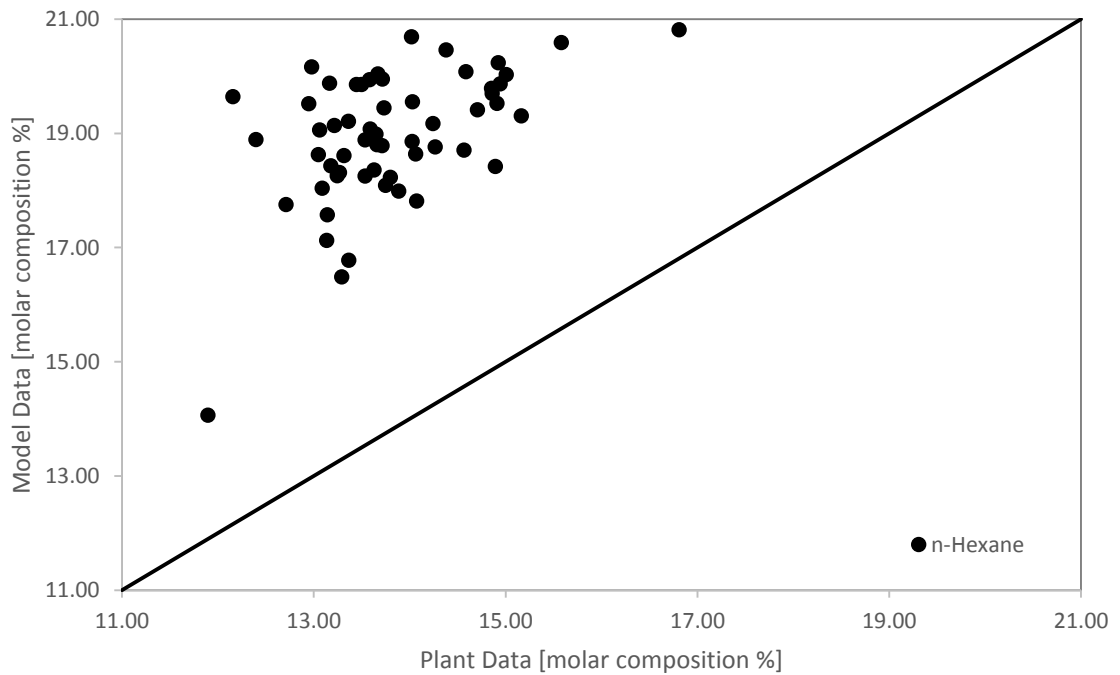


Figure 4.4. Comparison of n-Hexane outlet compositions for 58 days.

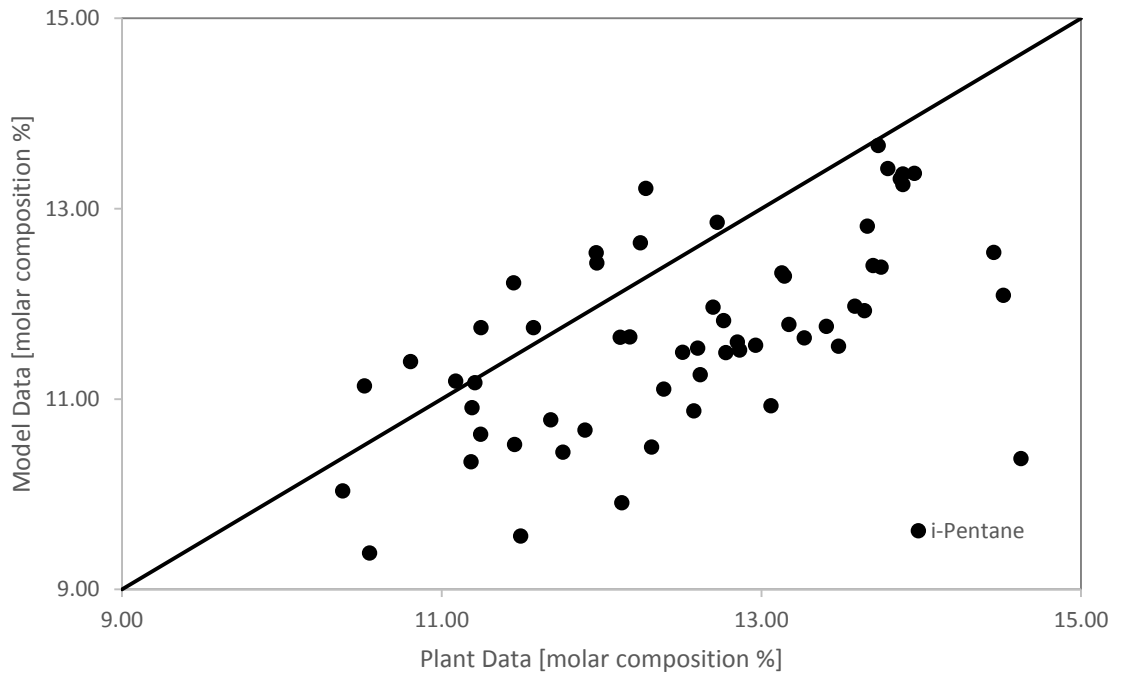


Figure 4.5. Comparison of i-Pentane outlet compositions for 58 days.

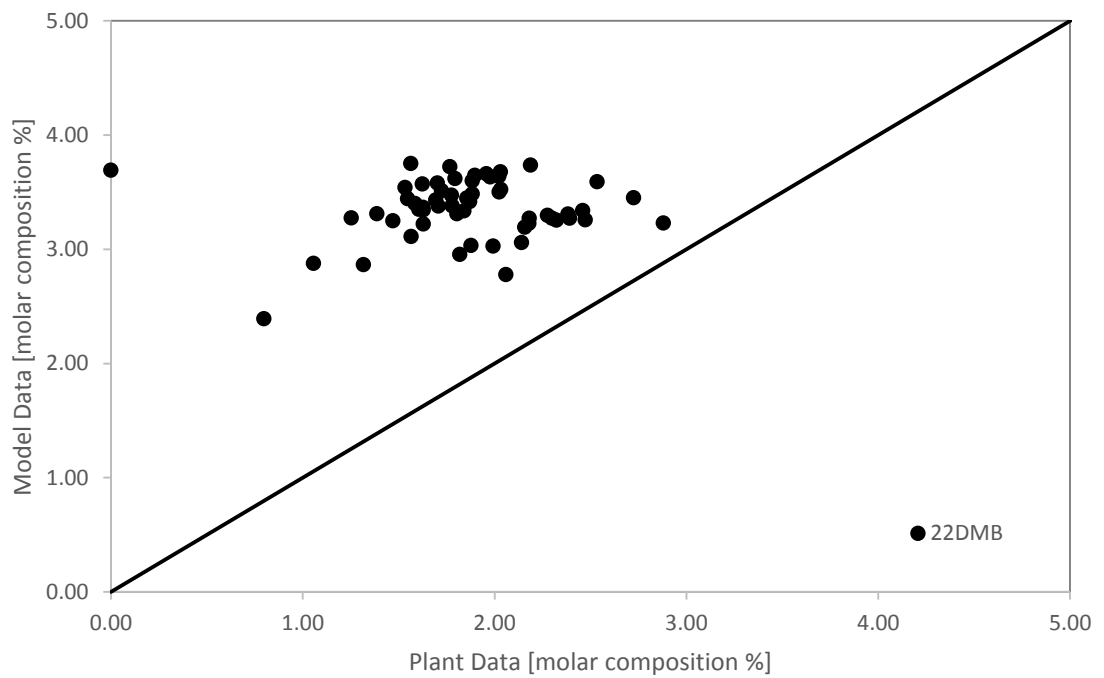


Figure 4.6. Comparison of 22DMB outlet compositions for 58 days.

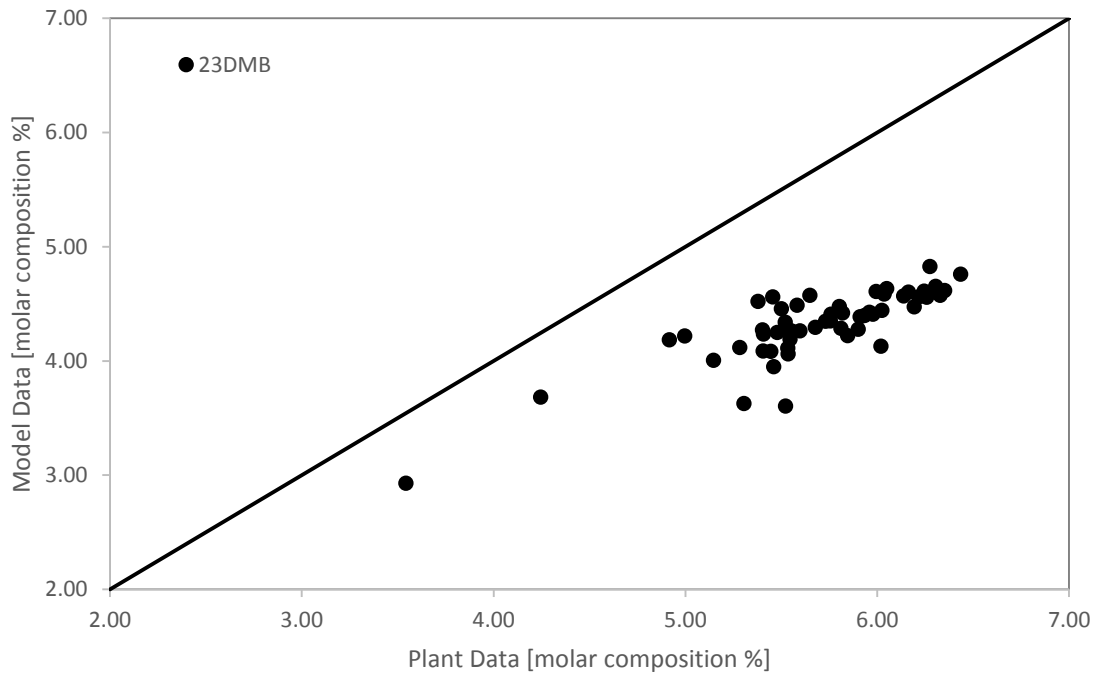


Figure 4.7. Comparison of 23DMB outlet compositions for 58 days.

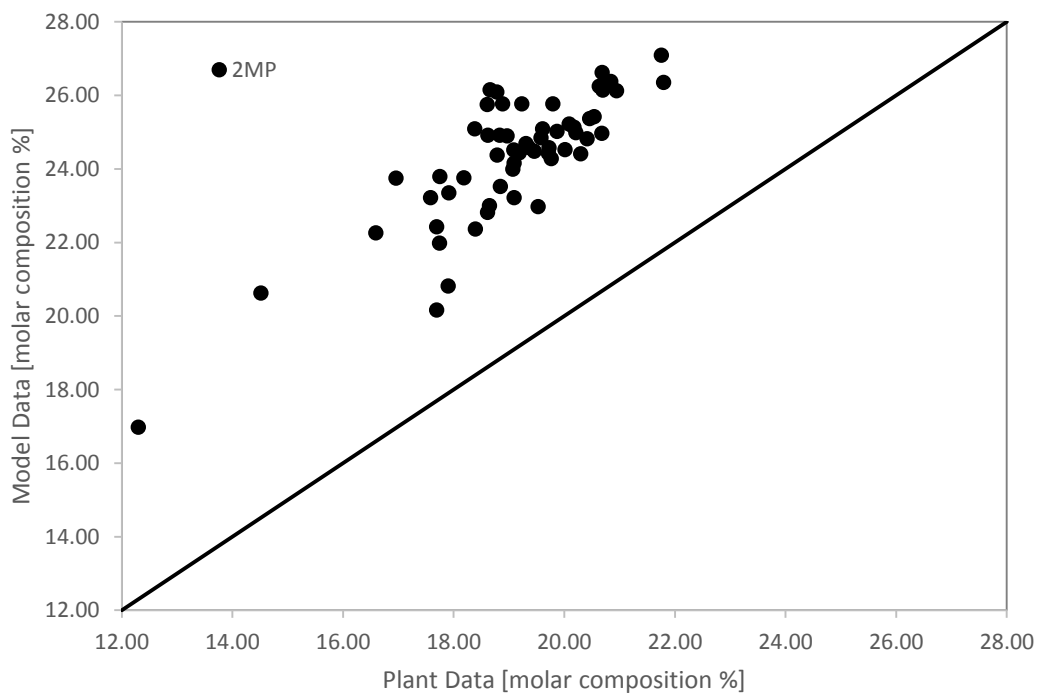


Figure 4.8. Comparison of 2MP outlet compositions for 58 days.

4.2. Effect of Reactor Inlet Temperature

The effect of reactor inlet temperature is examined in reactor simulations. Different temperatures are tested to see the effect of inlet temperature from 100 °C to 200 °C by increasing 10 °C. With these simulations, the maximum hydrogen consumption is obtained at 160 °C with flow rate of 36.3 kmol/h. When conversion of paraffins are analyzed, maximum conversion of n-butane is reached at lower temperatures while those of n-pentane is at 180 °C and of n-hexane is 160 °C with 2.46% and 18.2%, respectively. Maximum production rate of high octane components is obtained at 160 °C for isopentane with 9.8 kmol/h and at 130 °C for 22DMB and 23DMB with 38.5 kmol/h and 6.7 kmol/h, respectively. Methylcyclopentane and cyclohexane are also examined and it is observed that they are produced at lower reactor inlet temperatures. At the lowest inlet temperature of 100 °C, the production rates are found to be 142.2 kmol/h and 118.2 kmol/h respectively.

Hydrogen consumption is highly affected from temperature change as seen from Figure 4.9. Increase in consumption means that the ring opening and cracking reactions are becoming more dominant. The maximum consumption is reached at 160 °C and the profile is in consistent with conversion of paraffins data given in Figure 4.10.

It is observed from Figure 4.10 that n-butane is not highly affected from inlet temperature change until about 170°C. After this temperature, the conversion of n-butane decreases suddenly. The profile continuously decreases, and, as a result, the maximum n-butane conversion is reached at 100°C with 6.6 % conversion. N-pentane shows a slightly different profile compared with n-butane: it increases until 180 °C, reaches its maximum at 2.5 kmol/h, and then starts to decrease, as stated in literature. N-hexane also shows similar profile with n-pentane, but it is more sensitive to temperature change compared with n-pentane. It reaches to its maximum conversion at 160 °C with 18.3% conversion and then starts to decrease. Isomerization reactions are equilibrium reactions and they show maximum activity in a middle temperature range. At very low and very high temperatures these reactant conversions decrease. This study also shows similar results with the literature.

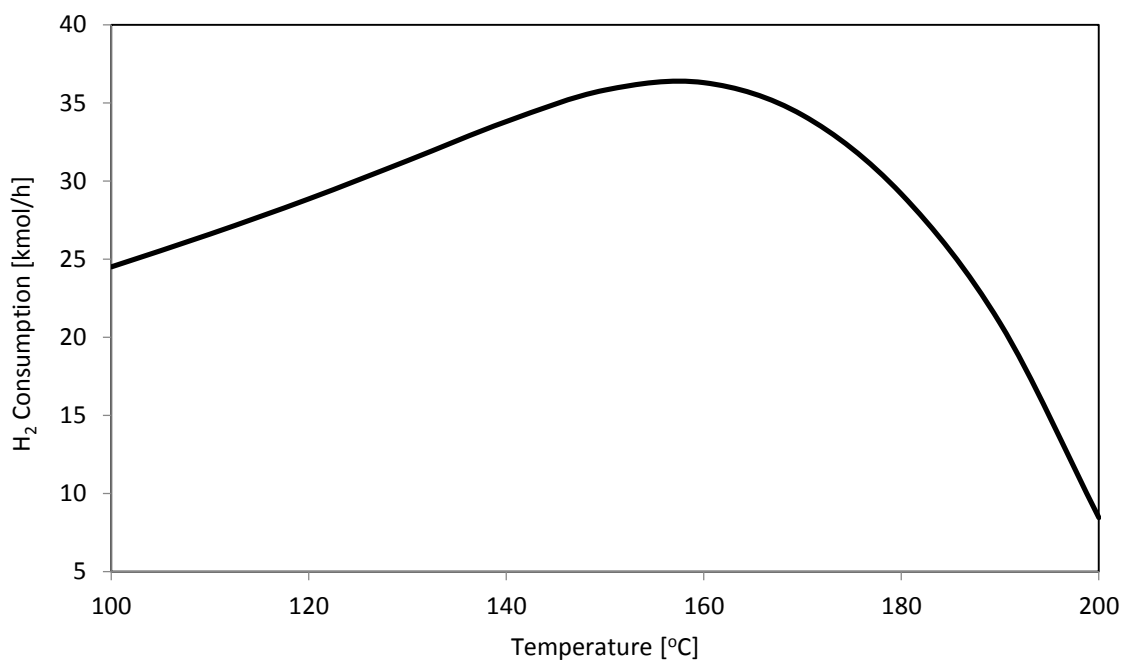


Figure 4.9. Effect of reactor inlet temperature on hydrogen consumption.

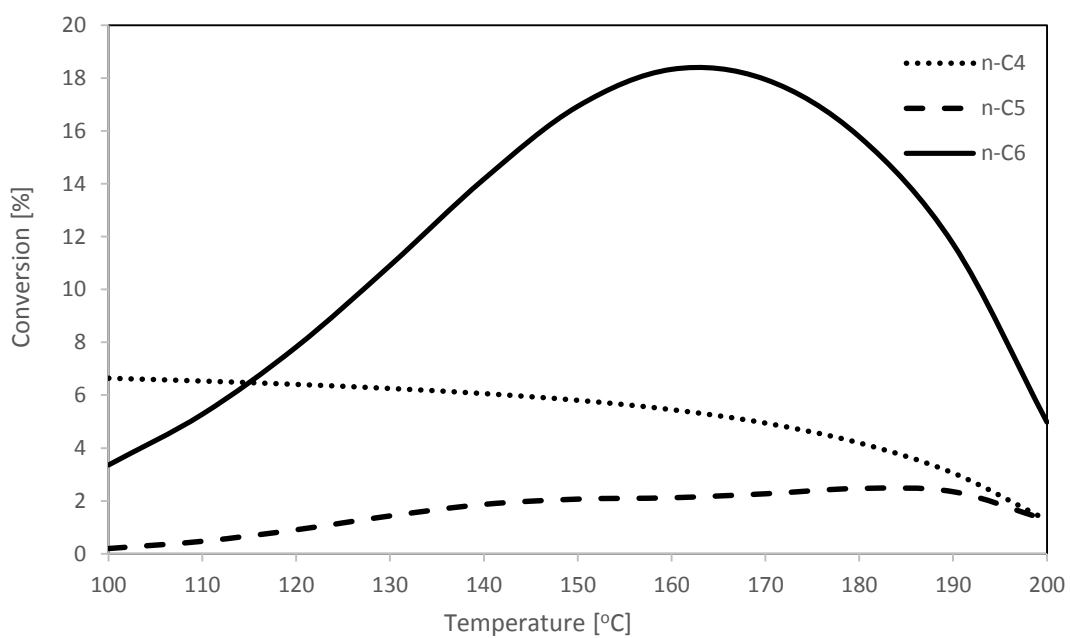


Figure 4.10. Effect of reactor inlet temperature on paraffin conversion.

Figure 4.11, Figure 4.12, and Figure 4.13 show the high octane component production rates. Isopentane, 2,2-dimethylbutane, 2,3-dimethylbutane, methylcyclopentane and cyclohexane have higher octane numbers compared with other paraffins and branched components. As seen from figures, isopentane is very sensitive to reactor inlet temperature and it shows an increasing trend until 160 °C and then decreases in accordance with equilibrium reactions. Its maximum production rate is 9.8 kmol/h.

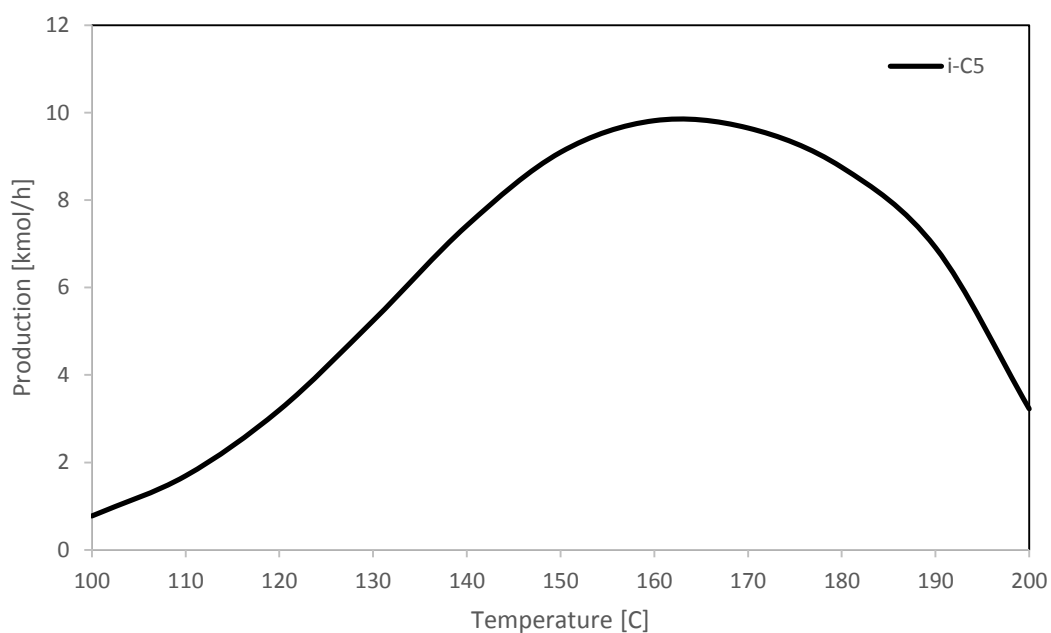


Figure 4.11. Effect of reactor inlet temperature on isopentane production.

2,2-dimethylbutane is also sensitive to temperature changes. It shows the same trend with isopentane and reaches its maximum at 130 °C with 38.5 kmol/h flow rate, which then decreases. However, 2,3-dimethylbutane is not as sensitive to temperature changes as isopentane and 2,2-dimethylbutane, do. It is not affected until 180 °C, after which the flow rate decreases slowly. Its maximum rate is calculated as 6.7 kmol/h at 130 °C.

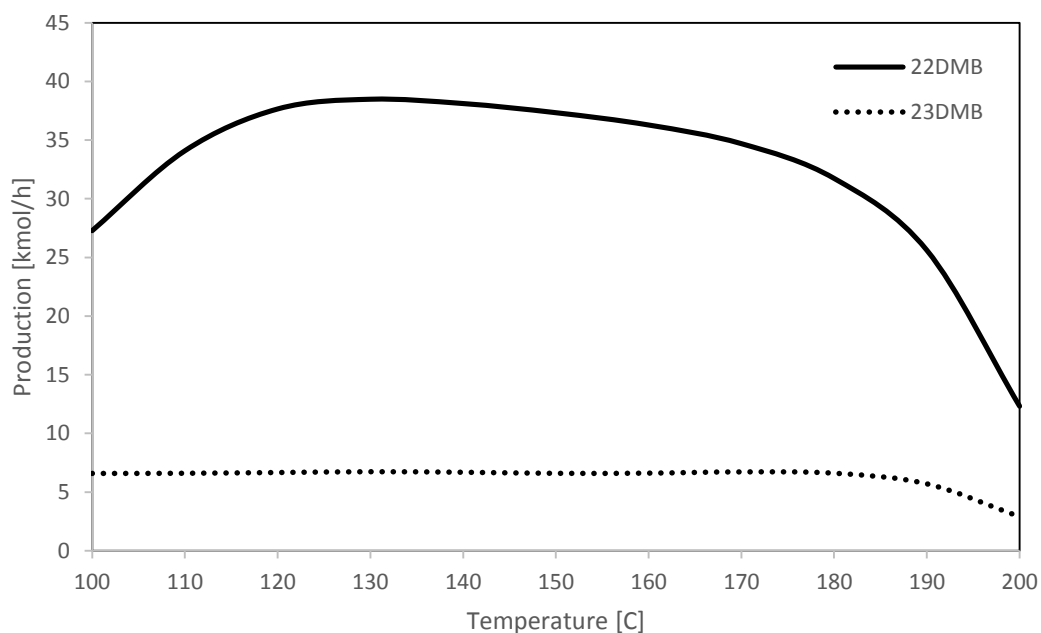


Figure 4.12. Effect of reactor inlet temperature on 22DMB and 23DMB production.

Methylcyclopentane and cyclohexane also shows similar results with 23DMB as shown in Figure 4.3. Their flow rate change slightly until 170 °C, and then starts to decrease more rapidly. Their maximum flow rate is calculated at 100 °C as 142.2 kmol/h and 118.2 kmol/h respectively.

It can be clearly seen from results that 160 °C is optimum reactor inlet temperature for maximization of high octane components with maximum hydrogen consumption, maximum n-hexane, n-pentane and n-butane conversions. The production rate of isopentane is also maximum at this temperature as well as 22DMB, 23DMB, MCP and cyclohexane.

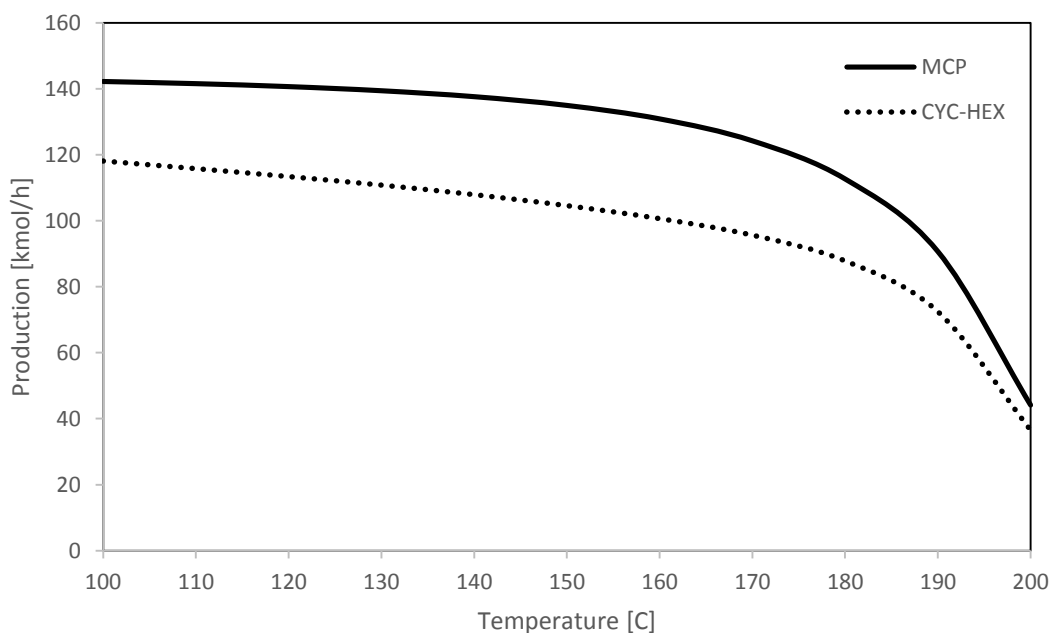


Figure 4.13. Effect of reactor inlet temperature on MCP and CYC-HEX production.

4.3. Effect of Reactor Inlet Pressure

The effect of reactor inlet pressure is examined in reactor simulations. Different pressures are tested to see the effect of inlet pressure from 25 bar_g to 50 bar_g by with increments of 5 bar. With these simulations, it is observed that hydrogen consumption is linearly conversions are found to increase with pressure. When conversion of paraffins are analyzed, maximum conversion of n-pentane is reached at a pressure of 30 bar_g with 2.4 %, while n-butane and n-hexane increasing with increasing pressure. Production rate of isopentane increases with increasing pressure, but that of 22DMB is not affected from pressure. 23DMB remains almost unaffected by pressure and stays at average value of 7.1 kmol/h. Methylcyclopentane and cyclohexane are also examined and it is observed that while MCP rate is increasing, cyclohexane production rate is decreasing with pressure.

Hydrogen consumption is highly affected from pressure change as seen from Figure 4.14. Increase in consumption means ring opening and cracking reactions are increasing. The maximum consumption is reached at maximum parameter study value of 50 bar_g with

77.4 kmol/h.

It is observed from Figure 4.15 that n-butane conversion is affected from inlet pressure change. With total 25 bar pressure increase, the n-butane conversion increases nearly 50% and reaches to 6.6 %. N-pentane is inversely affected by pressure, and after 45 bar_g, it starts to be produced instead of being consumed. Like n-butane, n-hexane conversion is affected from the pressure change. It shows an increasing trend during pressure increase, and conversion increases nearly by 50% and reaches to 23.8% conversion.

Figure 4.16, Figure 4.17, and Figure 4.18 show the production rates of high octane components. Compared with other paraffins and branched components, isopentane, 2,2-dimethylbutane, 2,3-dimethylbutane, methylcyclopentane and cyclohexane have higher octane numbers. As seen from figures, isopentane is very sensitive to reactor inlet pressure and it shows an increasing trend with maximum value of 16.8 kmol/h at 50 bar_g pressure.

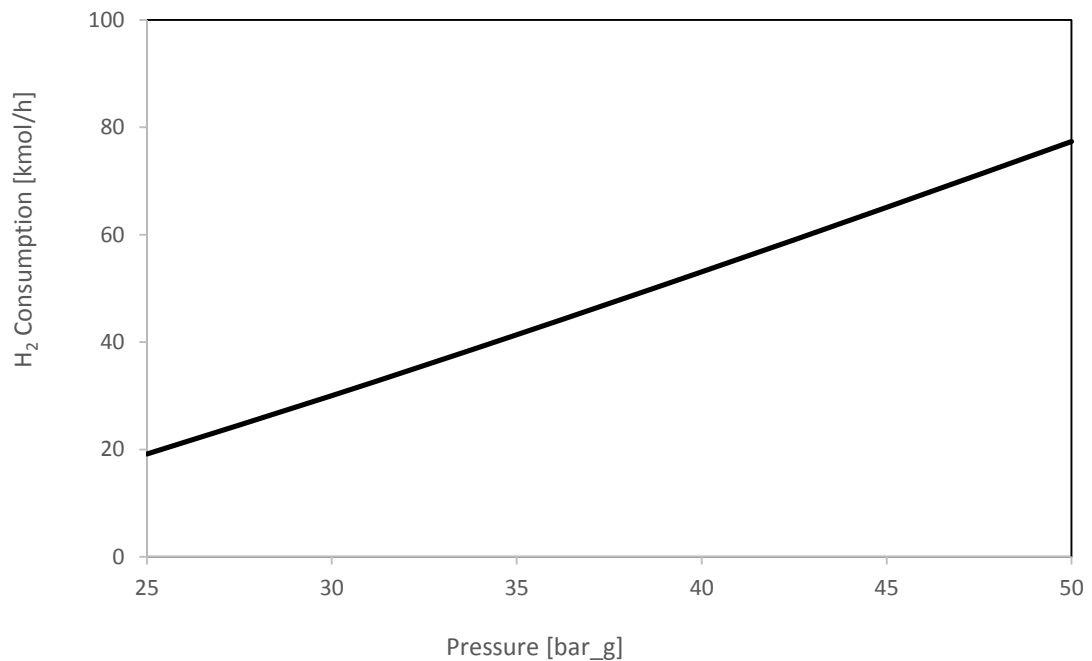


Figure 4.14. Effect of reactor inlet pressure on hydrogen consumption.

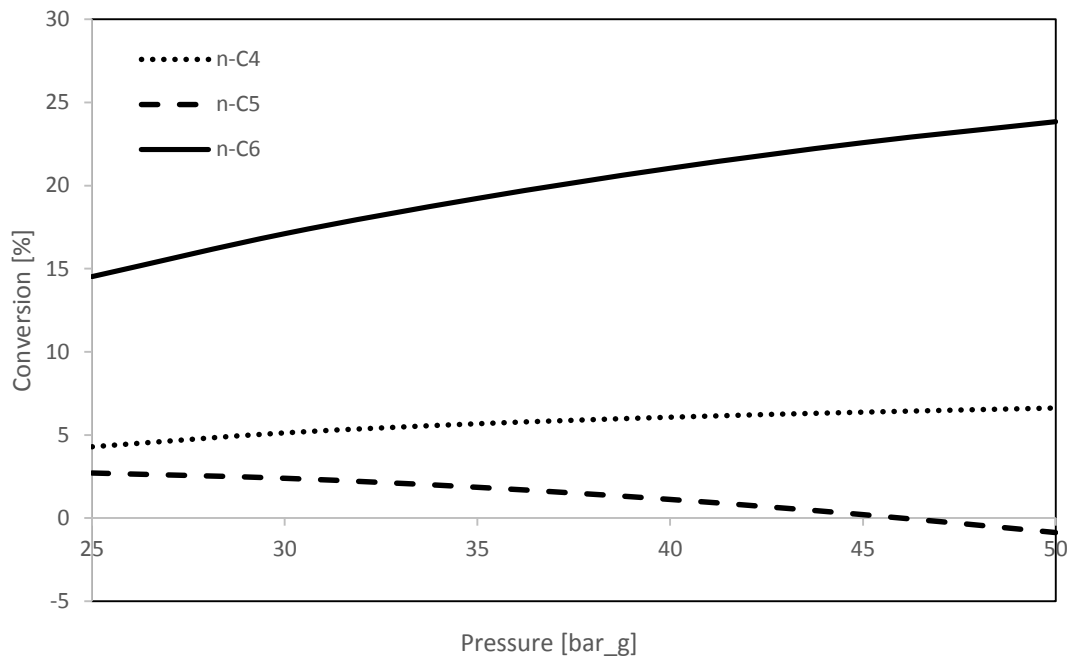


Figure 4.15. Effect of reactor inlet pressure on paraffin conversion.

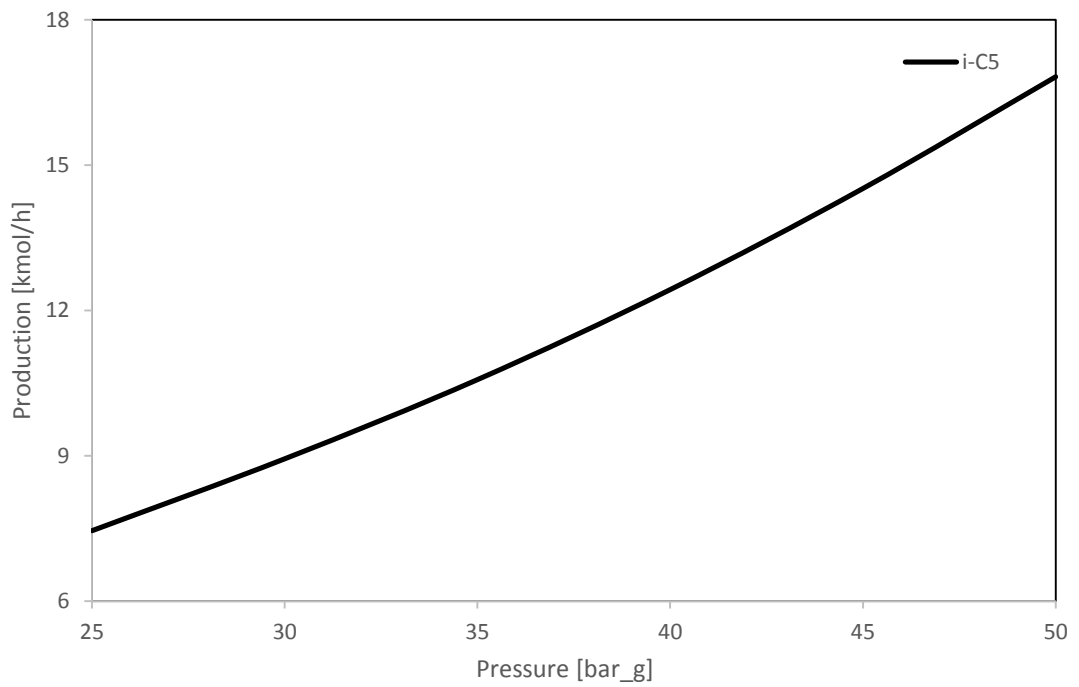


Figure 4.16. Effect of reactor inlet pressure on isopentane production.

2,2-dimethylbutane and 2,3-dimethylbutane are not as feed pressure sensitive as isopentane. They show an increasing trend and increases by 25.9% and 62.0% from their initial values respectively. Their maximum production rates are reached at 50 bar_g with 40.3 kmol/h and 8.5 kmol/h, respectively.

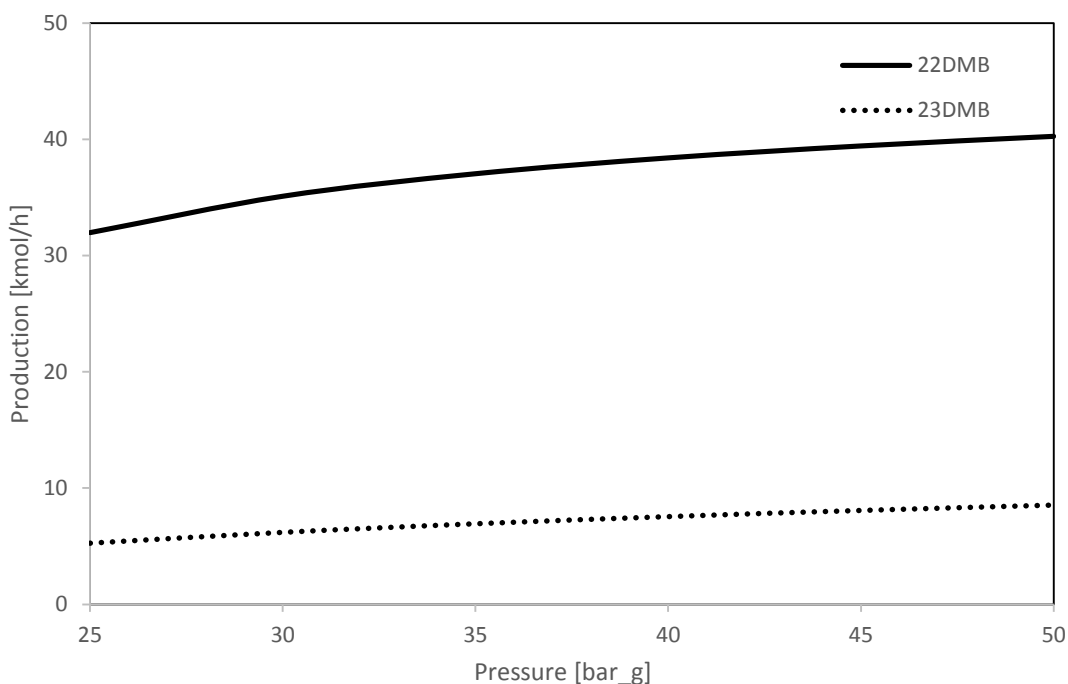


Figure 4.17. Effect of reactor inlet pressure on 22DMB and 23DMB production.

Methylcyclopentane shows increasing trend as the other components: it increases by 16.4% with pressure range and reaches its maximum value of 139.0 kmol/h. However, cyclohexane production decreases with increasing pressure. It decreases by 21.7% and reaches its minimum with 80.5 kmol/h.

It can be clearly seen from results that pressure range of 30-35 bar_g pressure range is the optimum range for maximization of high octane components with maximum hydrogen consumption, maximum n-hexane, n-pentane and n-butane conversion. The production rate of all components is at their optimum as well.

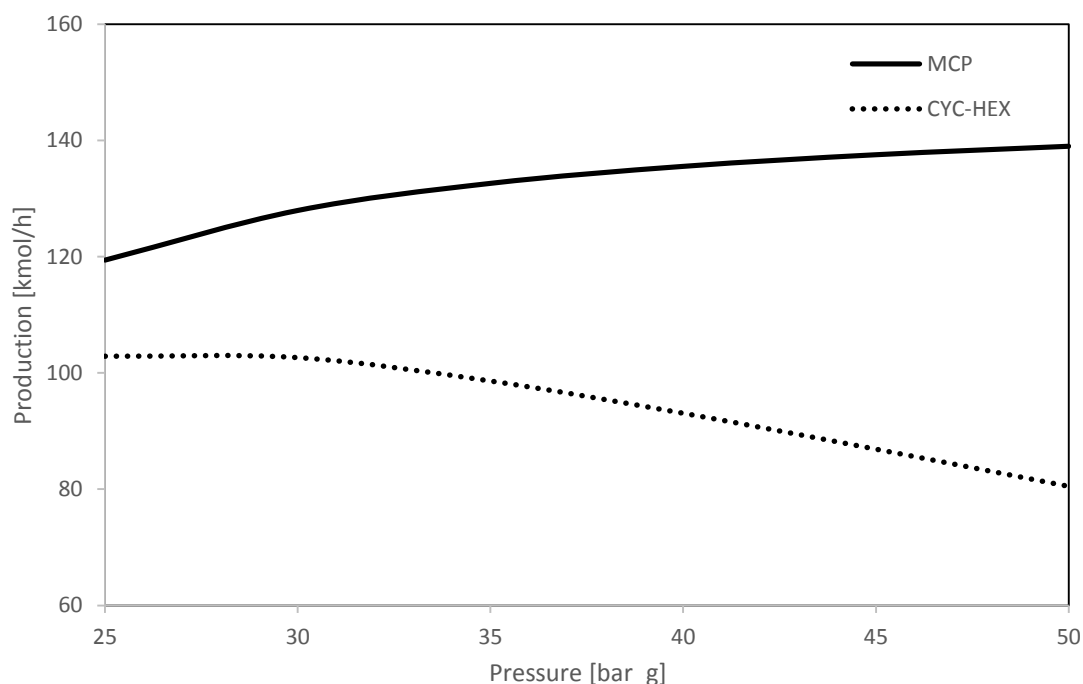


Figure 4.18. Effect of reactor inlet pressure on MCP and CYC-HEX production.

4.4. Effect of Reactor Inlet Flow Rate

The effect of reactor inlet flow rate is also examined in reactor simulations. Different flow rates are tested to see the effect of inlet flow with multiplying total flow rate of average 1501.5 kmol/h by 0.1, 0.5, 1.0, 2.0, 3.0, 4.0, and 5.0. With these simulations, it is observed that hydrogen consumption is linearly increasing with increasing flow rate. When conversion of paraffins are analyzed, n-butane is nearly not affected by increasing flow rate, while n-pentane is affected a little bit more and reached to its maximum conversion at 3003.3 kmol/h (total flow rate multiplied by 2.0) with 2.4%. N-hexane is highly affected and it reaches to its maximum conversion at 750.8 kmol/h (total flow rate multiplied by 0.5) with 20.4%. Production rate of i-pentane increases with increasing flow rate as the other components do.

Hydrogen consumption is highly affected from the change in inlet flow rate as seen from Figure 4.19. Increase in consumption means ring opening and cracking reactions are increasing. The maximum consumption of 155 kmol/h is reached at the highest inlet flow rate studied (7508 kmol/h, i.e. total flow rate multiplied by 5.0).

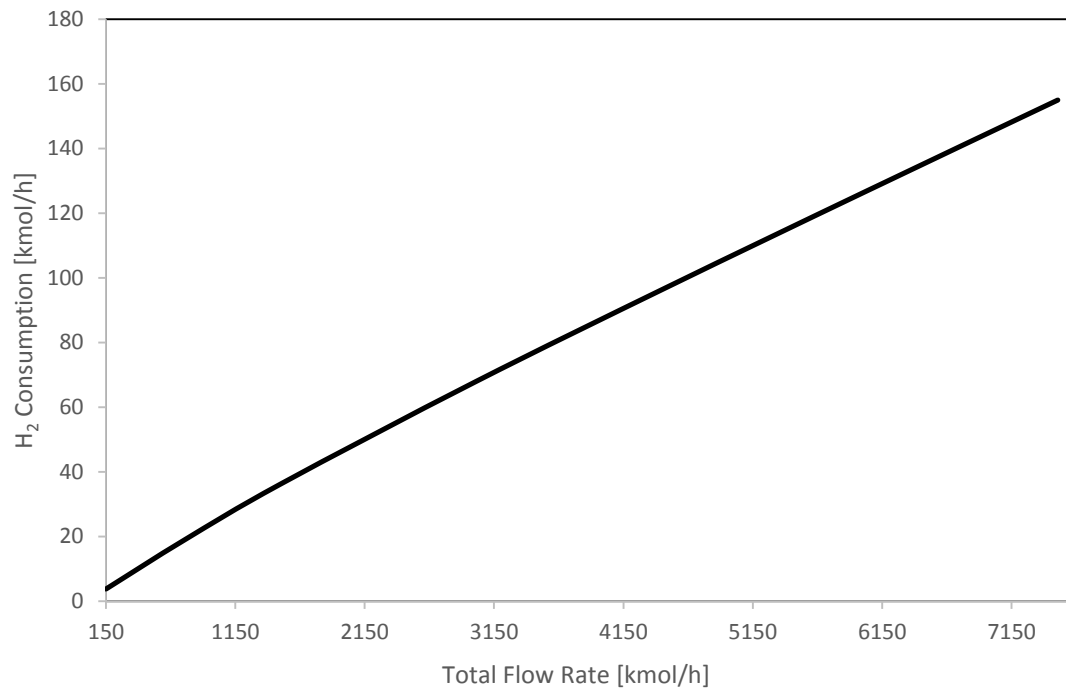


Figure 4.19. Effect of reactor inlet flow rate on hydrogen consumption.

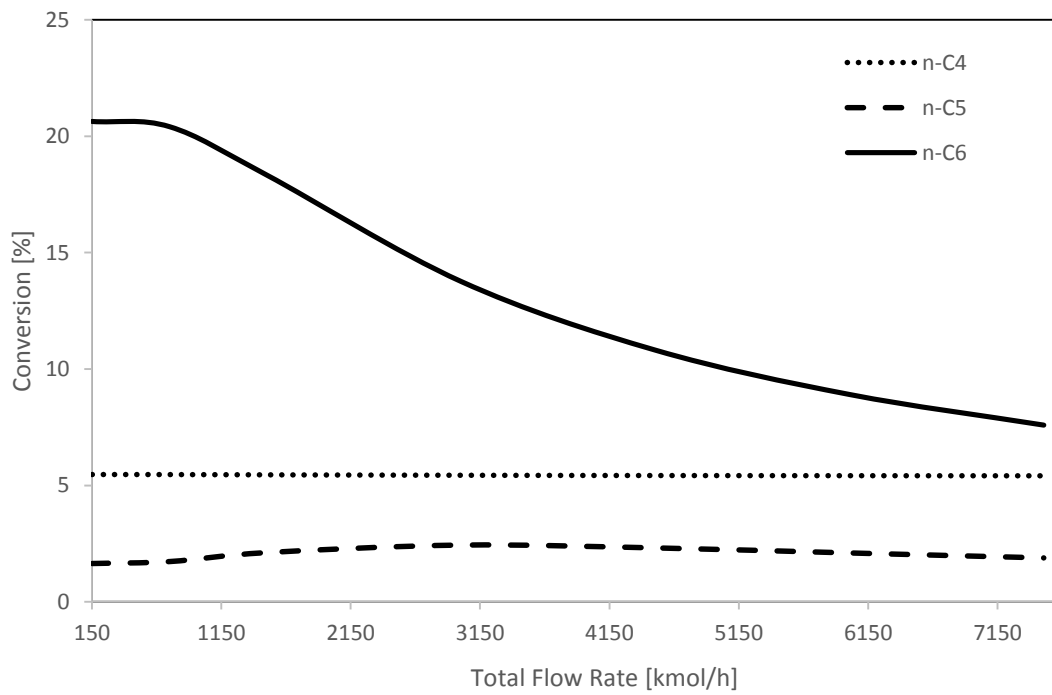


Figure 4.20. Effect of reactor inlet flow rate on paraffin conversion.

It is observed from Figure 4.20 that n-butane is not affected from the inlet flow rate change. With totally 50 times increase in flow rate, the n-butane conversion decreases nearly by 1.0% and reaches to 5.4%. N-pentane is affected by flow rate; it first increases until 3003.3 kmol/h and then starts to decrease. N-hexane is the most sensitive component to the flow rate change. It shows a decreasing trend during flow rate increase and conversion decreases nearly 63% and reaches 7.6% conversion finally.

Figure 4.21, Figure 4.22, and Figure 4.23 show the production rates of the high octane components. Isopentane, 2,2-dimethylbutane, 2,3-dimethylbutane, methylcyclopentane and cyclohexane have higher octane numbers compared with other paraffins and branched components. As seen from figures, all the components are sensitive to reactor inlet flow rate and they show increasing trends. I-pentane is very sensitive to reactor inlet flow rate and it shows an increasing trend with maximum value of 28.1 kmol/h at 7508 kmol/h total feed.

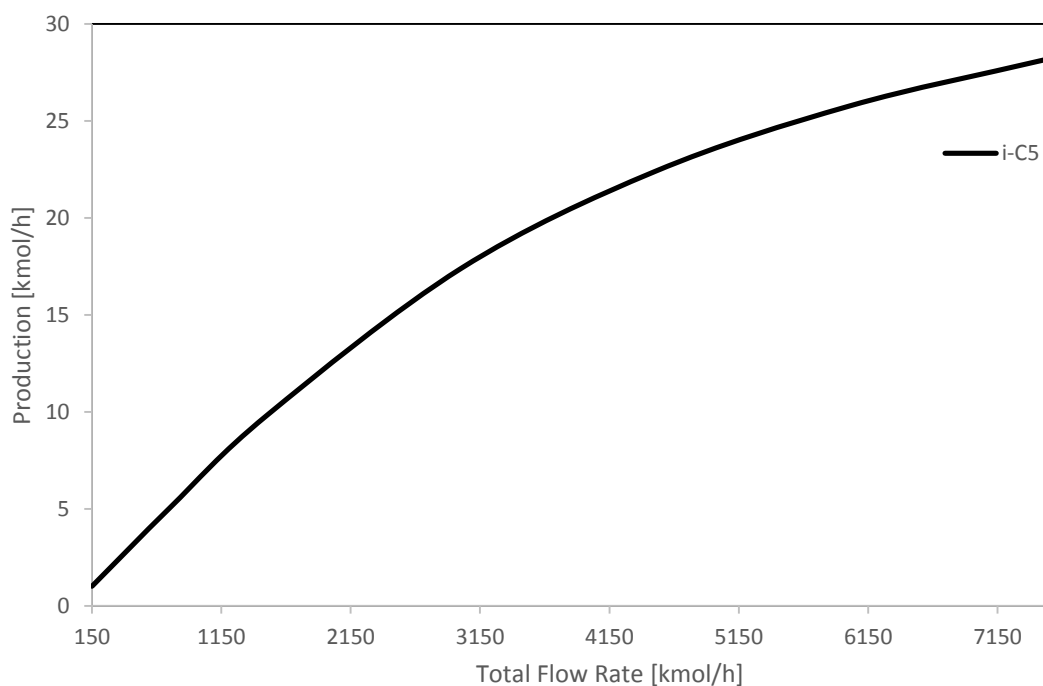


Figure 4.21. Effect of reactor inlet flow rate on isopentane production.

2,2-dimethylbutane and 2,3-dimethylbutane are also sensitive to flow rate. They show an increasing trend and increase up to 191.4 kmol/h and 47.7 kmol/h, respectively. Note that

these are the maximum production rates.

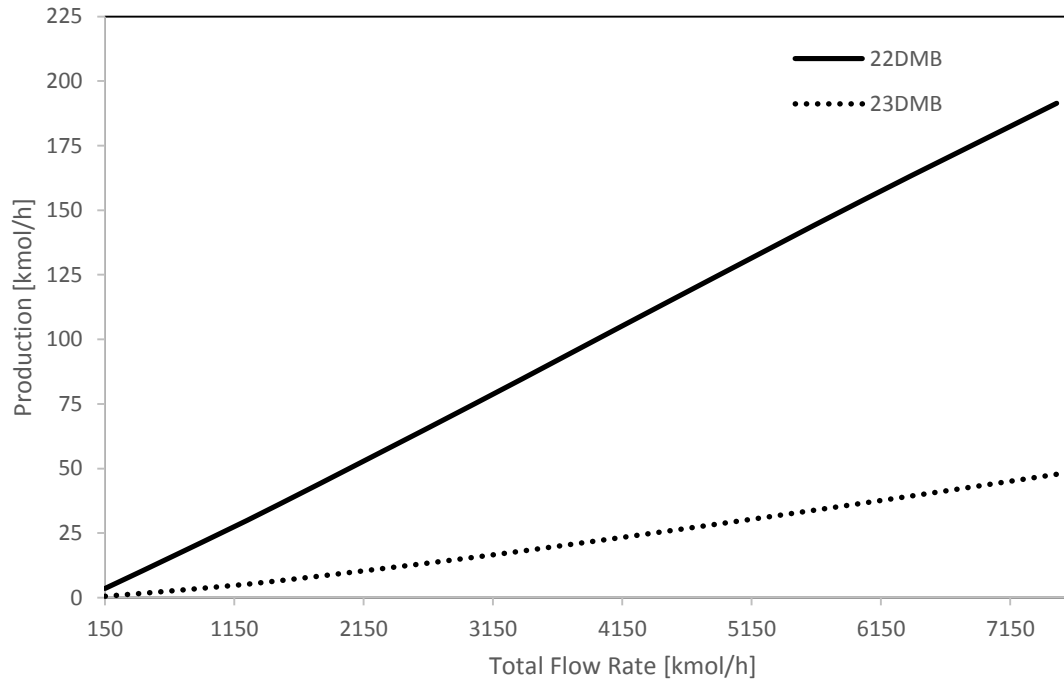


Figure 4.22. Effect of reactor inlet flow rate on 22DMB and 23DMB production.

Similar to other components, methylcyclopentane and cyclohexane production rates also show increasing trends. They reach their maximum values of with 654.2 kmol/h and 510.6 kmol/h, respectively, when the flow rate is at its highest value.

It can be clearly seen from results that flow rate range of 1.0 and 2.0 multiplier of the total flow rate is optimum reactor inlet flow range for maximization of high octane components with maximum hydrogen consumption, maximum n-hexane, n-pentane and n-butane conversion. The production rate of all components are at their optimum values as well. This shows that the reactors are able to support any capacity increase in the refinery.

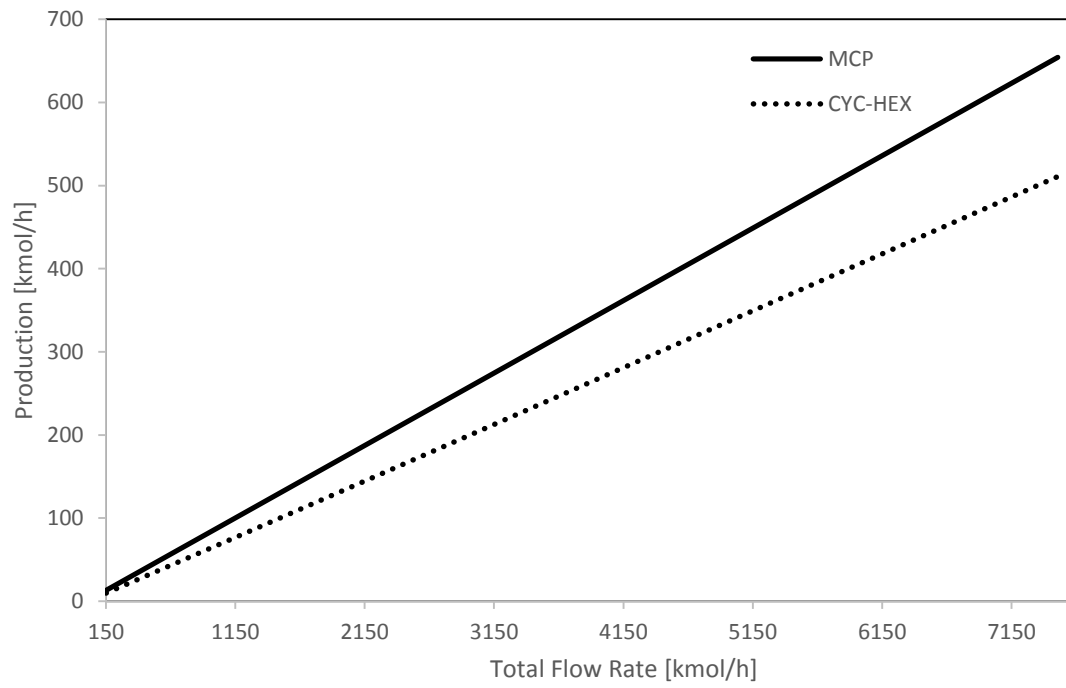


Figure 4.23. Effect of reactor inlet flow rate on MCP and CYC-HEX production.

5. CONCLUSIONS AND RECOMMENDATIONS

5.1. Conclusions

The objectives of this study are to understand the effects of operating conditions on an industrial isomerization reactor by the help of a parametric study and to understand the ways of improving the reactor performance by differences in the temperature, pressure and flow rate at the reactor inlet. The conclusions obtained by this study are summarized below.

Reactor inlet temperature has a significant impact on the hydrogen consumption, conversion of n-paraffins and production of high octane components because of the thermodynamic equilibrium limitation of the isomerization reactions. It is seen that 160 °C is the optimum inlet temperature to obtain maximum octane number at reactor effluent.

Reactor inlet pressure has also significant effect on hydrogen consumption. It also effects conversion of paraffins. However, after a certain value of pressure, conversion decreases and reverses through the production. Production rate of i-pentane, 22DMB, 23DMB, MCP, and cyclohexane increases. It is concluded that 30-35 bar_g range is the optimum reactor inlet pressure to get high octane number at effluent.

Total inlet flow rate is found to have a significant impact on the production rates, reactant conversion, and hydrogen consumption. While hexane conversion is inversely affected by flow rate, other paraffins directly affected from it. Production rates are found to increase with the feed flow rate. However, high flow rates are not preferred because of the capacity of reactor, and thus it is found that 1500-3000 kmol/h flow rate range is the optimum to get high octane number at effluent.

5.2. Recommendations

The recommendations to develop this study and advices for future work are summarized below.

Isomerization processes have two reactors working in series thus modelling of second reactor would give better results to see the complete unit performance. In addition, dynamic reactor model can be studied to see the effect of advanced process control applications on industrial reactors.

Besides thermodynamic and complex models, cognitive learning methods are at center of interest nowadays. Models with less than 1% error can be obtained with these studies by just using the process data. Some of these methods are artificial neural network and fuzzy logic models.

Computational fluid dynamics (CFD) applications are also in area of interest at reactor engineering. 2-dimensional or 3-dimensional reactor behavior can be investigated by CFD studies.

APPENDIX A. DETAILED SIMULATION RESULTS

Table A.1. Flash calculation results comparison with ASPEN HYSYS results.

Day Number	Hysys vapor fraction	Without interaction parameters	With interaction parameters
1	0.1763	0.1624	0.1749
2	0.2388	0.2240	0.2375
3	0.2488	0.2344	0.2478
4	0.2320	0.2170	0.2304
5	0.1977	0.1835	0.1963
6	0.1538	0.1388	0.1526
7	0.2861	0.2694	0.2847
8	0.2793	0.2631	0.2781
9	0.2354	0.2197	0.2341
10	0.2674	0.2511	0.2663
11	0.2250	0.2087	0.2234
12	0.2379	0.2205	0.2357
13	0.2336	0.2174	0.2321
14	0.2625	0.2442	0.2605
15	0.2435	0.2261	0.2414
16	0.2573	0.2396	0.2553
17	0.2251	0.2088	0.2235
18	0.1588	0.3128	0.1567
19	0.1374	0.2749	0.1375
20	0.1701	0.2576	0.1699
21	0.1346	0.3038	0.1348
22	0.1500	0.1429	0.1504
23	0.1513	0.1260	0.1520
24	0.1594	0.1588	0.1599
25	0.1950	0.1235	0.1951
26	0.1788	0.1393	0.1788
27	0.1695	0.1412	0.1699

Table A.1. Flash calculation results comparison with ASPEN HYSYS results (cont.).

28	0.1604	0.1491	0.1607
29	0.1676	0.1846	0.1678
30	0.1515	0.1675	0.1515
31	0.1715	0.1587	0.1712
32	0.1747	0.1494	0.1749
33	0.1911	0.1566	0.1919
34	0.1850	0.1401	0.1850
35	0.1629	0.1598	0.1634
36	0.1196	0.1638	0.1201
37	0.1912	0.1815	0.1912
38	0.1806	0.1739	0.1811
39	0.1389	0.1524	0.1398
40	0.1820	0.1087	0.1818
41	0.2135	0.1801	0.2141
42	0.1933	0.1702	0.1933
43	0.1114	0.1285	0.1108
44	0.1084	0.1703	0.1083
45	0.2117	0.2032	0.2120
46	0.2220	0.1820	0.2220
47	0.1970	0.0987	0.1973
48	0.2138	0.0961	0.2140
49	0.1907	0.2009	0.1904
50	0.1832	0.2104	0.1841
51	0.2438	0.1857	0.2439
52	0.1815	0.2025	0.1815
53	0.2143	0.1787	0.2136
54	0.2187	0.1735	0.2186
55	0.1898	0.2329	0.1897
56	0.1868	0.1700	0.1866
57	0.2034	0.2018	0.2029
58	0.2021	0.2071	0.2024

Table A.2. Reactor inlet data for 58 days*.

No of Day	1	2	3	4	5	6	7	8	9	10	11	12
9600TIC006	173.23	173.16	173.13	173.14	173.18	178.28	178.33	178.26	178.26	178.24	178.18	178.26
9600PI056	33.46	33.54	33.44	33.40	33.60	33.53	33.62	33.54	33.53	33.53	33.53	33.67
H ₂	2.25	3.54	4.19	3.80	3.39	2.76	4.48	4.36	3.82	4.44	3.07	3.09
CH ₄	0.11	0.08	0.11	0.11	0.10	0.00	0.00	0.12	0.11	0.00	0.08	0.10
C ₂ H ₆	0.12	0.10	0.12	0.14	0.13	0.00	0.17	0.14	0.15	0.14	0.09	0.12
C ₃ H ₈	0.07	0.07	0.08	0.08	0.09	0.08	0.14	0.08	0.08	0.09	0.07	0.07
C ₄ H ₁₀	0.09	0.16	0.10	0.17	0.21	0.12	0.27	0.17	0.09	0.12	0.07	0.06
C ₄ H ₁₀	1.14	1.44	1.20	1.87	1.96	1.37	1.38	1.34	1.23	1.27	1.00	1.24
C ₅ H ₁₂	2.67	3.50	3.34	3.26	3.31	3.17	3.40	3.16	3.25	3.41	3.04	3.05
C ₅ H ₁₂	3.14	3.67	4.06	4.13	3.81	4.08	3.44	3.75	4.12	3.89	3.55	3.83
C ₅ H ₁₀	0.25	0.33	0.28	0.00	0.28	0.25	0.00	0.00	0.00	0.00	0.00	0.00
C ₆ H ₁₄	0.13	0.16	0.15	0.23	0.23	0.11	0.13	0.17	0.13	0.12	0.09	0.05
C ₆ H ₁₄	0.98	0.89	1.11	1.40	1.22	1.01	1.33	1.39	1.54	1.44	1.40	1.35
C ₆ H ₁₄	4.09	4.08	4.85	5.13	5.15	4.53	5.13	5.00	5.71	5.30	5.13	5.11
C ₆ H ₁₄	2.75	2.84	3.49	3.67	3.60	3.44	3.62	3.58	3.88	3.83	3.41	3.46
C ₆ H ₁₄	3.23	3.49	4.53	4.74	4.52	4.95	4.38	4.57	4.83	4.68	3.95	4.09
MCP	1.82	2.48	2.36	2.06	2.89	2.68	2.38	2.60	2.21	2.50	1.68	1.42
C ₆ H ₆	0.00	0.21	0.42	0.39	0.00	0.31	0.37	0.32	0.38	0.30	0.35	0.32
CH	0.00	1.35	1.25	1.11	0.02	1.44	1.09	1.45	1.16	1.42	0.77	0.73
C ₇ H ₁₆	1.55	1.69	1.67	1.39	2.31	1.85	2.37	1.98	1.70	2.04	1.18	0.97

Table A.2. Reactor inlet data for 58 days* (cont.).

No of Day	13	14	15	16	17	18	19	20	21	22	23	24
9600TIC006	178.20	178.21	178.21	178.25	178.35	178.24	152.77	152.77	152.76	152.71	152.77	152.86
9600PI056	33.78	33.56	33.68	33.70	33.67	33.60	33.53	33.46	33.54	33.46	33.44	33.40
H ₂	2.80	2.84	3.35	3.56	2.84	2.07	3.33	4.08	3.40	3.81	3.90	4.11
CH ₄	0.09	0.07	0.08	0.08	0.06	0.08	0.08	0.11	0.09	0.11	0.11	0.14
C ₂ H ₆	0.11	0.10	0.11	0.10	0.08	0.11	0.09	0.11	0.10	0.12	0.13	0.15
C ₃ H ₈	0.07	0.07	0.07	0.06	0.05	0.06	0.06	0.03	0.07	0.07	0.08	0.08
C ₄ H ₁₀	0.06	0.03	0.07	0.10	0.11	0.04	0.10	0.12	0.27	0.13	0.10	0.22
C ₄ H ₁₀	0.83	0.69	1.38	1.37	1.09	0.95	1.66	2.14	1.95	1.40	0.83	1.68
C ₅ H ₁₂	2.45	2.49	3.06	3.04	2.78	2.95	3.67	4.11	3.31	3.40	3.49	3.08
C ₅ H ₁₂	3.13	4.03	3.86	3.79	3.04	3.86	4.54	4.48	3.94	4.07	4.17	3.84
C ₅ H ₁₀	0.00	0.00	0.00	0.00	0.00	0.01	0.00	0.00	0.00	0.00	0.00	0.27
C ₆ H ₁₄	0.11	0.03	0.09	0.09	0.07	0.05	0.12	0.09	0.09	0.17	0.12	1.19
C ₆ H ₁₄	1.28	1.16	1.44	1.47	1.09	1.19	1.50	1.54	1.63	1.57	1.31	1.19
C ₆ H ₁₄	4.63	4.40	5.30	5.46	4.46	4.69	5.57	5.80	5.93	5.92	4.98	5.39
C ₆ H ₁₄	3.06	2.86	3.53	3.53	3.29	3.27	3.63	3.85	3.88	3.94	3.60	3.81
C ₆ H ₁₄	3.70	3.70	4.27	4.23	3.88	4.30	4.25	4.38	4.39	4.81	4.99	4.61
MCP	1.31	0.96	1.70	1.69	1.54	1.32	1.91	2.04	2.16	2.07	3.03	2.66
C ₆ H ₆	0.27	0.18	0.45	0.45	0.25	0.32	0.34	0.29	0.40	0.42	0.48	0.49
CH	0.58	0.28	0.88	0.93	0.90	0.45	0.97	0.93	1.17	1.15	1.72	1.43
C ₇ H ₁₆	0.99	0.84	0.95	0.97	1.11	0.40	0.62	0.73	0.76	0.90	0.94	1.31

Table A.2. Reactor inlet data for 58 days* (cont.).

No of Day	25	26	27	28	29	30	31	32	33	34	35	36
9600TIC006	152.86	157.87	157.87	157.76	157.88	157.80	157.91	157.90	157.88	157.90	157.89	158.03
9600PI056	33.60	33.53	33.62	33.54	33.53	33.53	33.53	33.67	33.78	33.56	33.68	33.70
H ₂	4.91	4.27	4.23	4.02	4.15	3.73	4.07	4.31	4.96	4.45	4.20	3.21
CH ₄	0.15	0.12	0.12	0.12	0.11	0.12	0.12	0.11	0.13	0.13	0.13	0.16
C ₂ H ₆	0.17	0.14	0.14	0.16	0.15	0.14	0.16	0.14	0.13	0.15	0.16	0.19
C ₃ H ₈	0.11	0.09	0.09	0.11	0.11	0.10	0.11	0.09	0.08	0.09	0.10	0.12
C ₄ H ₁₀	0.21	0.17	0.12	0.09	0.13	0.15	0.12	0.14	0.13	0.13	0.07	0.10
C ₄ H ₁₀	1.96	1.79	1.26	1.16	1.46	1.94	1.76	1.63	1.47	1.57	0.85	1.02
C ₅ H ₁₂	3.49	3.20	3.43	3.31	3.16	3.16	3.54	3.15	3.32	3.92	3.26	3.61
C ₅ H ₁₂	4.62	4.50	4.15	4.60	4.31	4.05	5.24	3.94	3.23	4.36	3.91	4.63
C ₅ H ₁₀	0.00	0.00	0.34	0.00	0.00	0.00	0.00	0.00	0.29	0.00	0.00	0.00
C ₆ H ₁₄	0.09	0.27	0.35	0.12	0.16	0.19	0.11	0.21	0.07	0.19	0.18	0.12
C ₆ H ₁₄	1.51	1.75	1.34	1.70	1.74	1.68	1.58	1.59	0.66	1.58	1.62	1.49
C ₆ H ₁₄	5.61	6.35	5.77	6.31	6.34	6.36	5.93	5.84	3.54	5.83	6.12	5.58
C ₆ H ₁₄	3.87	4.16	3.92	4.28	4.19	4.32	4.06	4.08	2.85	4.03	4.21	3.92
C ₆ H ₁₄	4.65	5.18	4.92	5.24	5.05	5.28	5.22	5.06	4.12	4.56	4.98	4.73
MCP	2.57	1.89	2.99	2.12	2.02	1.98	1.89	2.70	5.58	2.29	2.54	2.42
C ₆ H ₆	0.35	0.34	0.22	0.43	0.41	0.37	0.30	0.40	0.39	0.31	0.40	0.45
CH	1.19	1.02	1.70	1.02	1.10	1.04	0.87	1.45	3.20	0.99	1.23	2.42
C ₇ H ₁₆	1.61	0.86	1.03	1.04	1.32	0.87	0.97	1.21	2.83	1.75	1.80	1.17

Table A.2. Reactor inlet data for 58 days* (cont.).

No of Day	37	38	39	40	41	42	43	44	45	46	47	48
9600TIC006	157.89	158.05	157.93	162.46	163.04	163.02	162.99	162.87	162.98	163.02	163.02	162.98
9600PI056	33.67	33.31	33.61	33.71	33.75	33.63	33.63	33.78	33.80	33.74	33.64	33.81
H ₂	4.60	3.93	3.84	4.22	5.16	4.41	2.79	2.90	4.92	5.02	4.60	5.20
CH ₄	0.14	0.12	0.10	0.13	0.14	0.15	0.09	0.09	0.17	0.15	0.11	0.15
C ₂ H ₆	0.16	0.12	0.11	0.15	0.15	0.17	0.11	0.11	0.20	0.18	0.14	0.18
C ₃ H ₈	0.10	0.07	0.08	0.09	0.09	0.10	0.07	0.08	0.11	0.12	0.08	0.10
C ₄ H ₁₀	0.08	0.09	0.05	0.10	0.10	0.09	0.18	0.07	0.07	0.04	0.05	0.06
C ₄ H ₁₀	1.44	0.90	0.55	1.22	0.93	1.39	2.10	1.10	1.09	0.96	0.66	0.92
C ₅ H ₁₂	3.92	3.08	2.90	4.08	3.18	3.06	3.71	3.57	2.98	3.92	3.66	3.71
C ₅ H ₁₂	4.57	3.11	3.32	4.24	3.83	4.03	4.59	5.15	3.96	4.44	4.19	4.21
C ₅ H ₁₀	0.00	0.00	0.00	0.00	0.00	0.00	0.00	0.00	0.00	0.00	0.00	0.00
C ₆ H ₁₄	0.13	0.11	0.20	0.20	0.09	0.09	0.08	0.18	0.12	0.11	0.08	0.14
C ₆ H ₁₄	1.56	1.38	1.51	1.68	1.15	1.64	1.53	1.64	1.55	1.72	1.69	1.90
C ₆ H ₁₄	5.84	5.21	5.86	6.28	4.44	6.30	5.93	6.15	5.80	6.34	6.49	7.08
C ₆ H ₁₄	4.10	3.64	4.39	4.23	3.43	4.33	4.23	4.24	4.19	4.18	4.39	4.86
C ₆ H ₁₄	4.72	4.04	5.39	4.51	4.90	5.16	4.93	5.23	5.23	4.56	5.02	5.48
MCP	2.64	2.55	2.86	2.28	4.32	2.24	2.10	1.71	2.83	2.32	2.17	2.08
C ₆ H ₆	0.47	0.32	0.20	0.39	0.42	0.38	0.31	0.41	0.46	0.37	0.40	0.40
CH	1.08	1.35	1.43	1.00	2.33	1.09	0.81	0.77	1.42	0.99	1.05	1.05
C ₇ H ₁₆	1.14	1.48	2.31	1.53	2.44	1.58	1.23	1.51	1.74	1.63	1.40	1.26

Table A.2. Reactor inlet data for 58 days* (cont.).

No of Day	49	50	51	52	53	54	55	56	57	58
9600TIC006	162.99	154.77	162.95	162.93	162.98	162.98	162.98	162.81	163.00	162.98
9600PI056	33.70	33.78	33.30	33.38	33.28	33.21	33.51	33.41	33.39	32.83
H ₂	4.28	4.98	4.49	3.56	3.76	4.02	4.30	4.19	4.37	4.57
CH ₄	0.14	0.14	0.15	0.09	0.09	0.09	0.11	0.10	0.12	0.12
C ₂ H ₆	0.18	0.15	0.16	0.13	0.08	0.11	0.13	0.13	0.15	0.13
C ₃ H ₈	0.11	0.11	0.08	0.08	0.04	0.07	0.09	0.09	0.09	0.08
C ₄ H ₁₀ (iso)	0.08	0.02	0.06	0.05	0.21	0.06	0.06	0.08	0.15	0.05
C ₄ H ₁₀	1.26	0.48	0.74	1.03	1.90	1.04	0.92	1.24	2.08	0.79
C ₅ H ₁₂ (iso)	4.08	3.42	3.01	3.01	3.20	3.22	4.38	4.36	4.01	3.87
C ₅ H ₁₂	4.56	3.53	3.05	3.64	3.54	3.32	4.60	4.65	4.38	4.25
C ₅ H ₁₀	0.00	0.00	0.00	0.00	0.00	0.00	0.00	0.00	0.36	0.00
C ₆ H ₁₄ (iso)	0.11	0.14	0.07	0.10	0.05	0.07	0.12	0.08	0.07	0.08
C ₆ H ₁₄ (iso)	1.68	1.62	1.33	1.48	1.19	1.28	1.46	1.42	1.02	1.39
C ₆ H ₁₄ (iso)	6.29	6.23	5.13	5.48	4.67	5.05	5.72	5.44	4.82	5.39
C ₆ H ₁₄ (iso)	4.23	4.43	3.51	3.68	3.30	3.51	4.18	4.02	3.63	4.08
C ₆ H ₁₄ (iso)	4.71	5.12	3.87	4.29	3.81	3.83	4.90	4.72	4.54	5.06
MCP	2.01	2.72	1.96	2.07	2.32	2.29	2.50	3.02	3.52	3.21
C ₆ H ₆	0.43	0.39	0.32	0.20	0.36	0.24	0.37	0.35	0.49	0.00
CH	0.98	1.45	0.89	1.09	1.30	1.21	1.16	1.30	1.74	1.56
C ₇ H ₁₆	1.29	1.84	1.68	0.85	0.70	0.99	1.14	1.00	1.16	1.54

Table A.3. Plant data for reactor and reactor outlet for 58 days*.

No of Days	1	2	3	4	5	6	7	8	9	10	11	12
9600TI013	184.06	186.17	187.06	186.31	182.45	189.55	192.36	189.71	191.31	189.12	191.36	189.56
9600TI014	184.37	186.43	187.14	186.34	182.54	189.70	192.69	189.85	191.44	189.27	191.70	189.74
9600TI015	185.49	187.56	187.92	186.97	182.85	190.22	193.50	190.37	192.09	189.70	192.67	190.36
9600TI016	184.35	186.86	187.33	186.51	182.67	189.93	193.01	190.07	191.75	189.45	192.10	189.96
9600TI017	185.28	187.76	188.15	187.22	183.42	190.66	193.68	190.68	192.26	189.99	192.59	190.47
9600TI018	186.23	188.73	189.02	187.96	184.46	191.50	194.52	191.44	192.99	190.76	193.64	191.51
9600PI058	33.19	33.19	33.19	33.19	33.19	33.19	33.19	33.19	33.19	33.19	33.19	33.19
H ₂	0.00	0.00	0.00	0.00	0.00	0.00	0.00	0.00	0.00	0.00	0.00	0.00
CH ₄	0.00	0.00	0.00	0.00	0.00	0.00	0.00	0.00	0.00	0.00	0.00	0.00
C ₂ H ₆	0.00	0.00	0.00	0.00	0.00	0.00	0.01	0.00	0.00	0.00	0.00	0.00
C ₃ H ₈	0.14	0.02	0.14	0.10	0.15	0.14	0.07	0.10	0.16	0.28	0.11	0.10
C ₄ H ₁₀ (iso)	0.30	0.12	0.30	0.29	0.39	0.34	0.29	0.33	0.33	0.46	0.34	0.22
C ₄ H ₁₀	0.80	0.54	1.19	1.28	1.63	1.42	0.87	1.12	1.06	1.18	1.18	1.10
C ₅ H ₁₂ (iso)	3.17	3.09	3.72	3.69	3.75	3.56	3.28	3.48	3.77	3.86	3.52	3.55
C ₅ H ₁₂	2.51	2.73	3.35	3.38	3.45	3.28	2.75	3.07	3.36	3.33	3.05	3.14
C ₅ H ₁₀	0.23	0.00	0.00	0.00	0.00	0.00	0.00	0.00	0.00	0.00	0.00	0.00
C ₆ H ₁₄ (iso)	0.50	0.53	0.54	0.64	0.73	0.63	0.53	0.59	0.66	0.66	0.64	0.62
C ₆ H ₁₄ (iso)	1.08	1.43	1.49	1.59	1.79	1.61	1.62	1.62	1.77	1.74	1.57	1.60
C ₆ H ₁₄ (iso)	3.93	4.57	4.80	5.19	5.80	5.22	5.37	5.23	5.80	5.71	5.02	5.16
C ₆ H ₁₄ (iso)	2.50	2.96	3.11	3.35	3.70	3.36	3.44	3.35	3.70	3.65	3.17	3.25
C ₆ H ₁₄ (iso)	2.72	3.43	3.82	4.01	4.18	4.06	3.98	3.94	4.27	4.21	3.50	3.51
MCP	2.08	2.62	2.63	2.39	2.15	2.30	2.54	2.64	2.19	2.21	1.55	1.42
C ₆ H ₆	0.00	0.00	0.00	0.00	0.00	0.00	0.00	0.00	0.00	0.00	0.00	0.00
CH	0.00	1.76	1.74	1.60	0.00	1.50	1.57	1.68	1.39	1.41	1.01	0.94
C ₇ H ₁₆	1.97	2.01	2.12	2.00	1.98	2.00	2.88	2.43	1.97	1.99	1.28	1.20

Table A.3. Plant data for reactor and reactor outlet for 58 days* (cont.).

No of Days	13	14	15	16	17	18	19	20	21	22	23	24
9600TI013	186.88	188.28	192.48	192.57	190.30	189.12	163.21	165.10	162.82	167.10	167.19	168.17
9600TI014	187.33	188.68	192.63	192.73	190.50	189.41	163.67	165.95	163.42	167.80	167.87	169.63
9600TI015	188.23	189.68	193.60	193.66	191.43	190.25	163.95	166.22	163.72	168.24	168.43	170.12
9600TI016	187.69	189.05	193.00	193.06	190.92	189.73	163.65	165.85	163.42	167.76	167.97	169.62
9600TI017	188.25	189.62	193.38	193.40	191.29	190.28	164.11	166.36	163.92	168.25	168.50	170.11
9600TI018	189.55	191.37	194.12	194.16	192.26	191.31	165.28	167.40	164.77	169.21	169.36	170.87
9600PI058	33.19	33.19	33.19	33.19	33.19	33.19	33.19	33.12	33.19	33.12	33.12	33.08
H ₂	0.00	0.00	0.00	0.00	0.00	0.00	0.00	0.00	0.00	0.00	0.00	0.00
CH ₄	0.00	0.00	0.00	0.00	0.00	0.00	0.00	0.00	0.00	0.00	0.00	0.00
C ₂ H ₆	0.00	0.00	0.00	0.00	0.00	0.00	0.00	0.09	0.00	0.00	0.00	0.07
C ₃ H ₈	0.09	0.15	0.08	0.12	0.08	0.06	0.11	0.18	0.11	0.16	0.09	0.11
C ₄ H ₁₀ (iso)	0.22	0.24	0.23	0.32	0.26	0.16	0.19	0.29	0.33	0.28	0.17	0.32
C ₄ H ₁₀	0.77	0.55	1.23	1.27	0.99	0.78	1.33	1.80	1.80	1.79	0.88	1.73
C ₅ H ₁₂ (iso)	2.88	3.04	3.56	3.51	3.08	3.28	3.99	4.32	3.79	4.15	3.80	3.52
C ₅ H ₁₂	2.57	3.08	3.17	3.06	2.55	3.15	4.05	3.98	3.55	4.02	3.65	3.58
C ₅ H ₁₀	0.00	0.00	0.00	0.00	0.00	0.00	0.00	2.54	0.00	2.51	0.00	0.00
C ₆ H ₁₄ (iso)	0.61	0.63	0.62	0.63	0.57	0.60	0.59	0.58	0.57	0.59	0.55	0.49
C ₆ H ₁₄ (iso)	1.45	1.37	1.71	1.73	1.43	1.47	1.68	0.00	1.80	0.00	1.62	1.70
C ₆ H ₁₄ (iso)	4.63	4.45	5.33	5.38	4.69	4.88	5.68	5.80	5.95	5.78	5.45	5.79
C ₆ H ₁₄ (iso)	2.91	2.79	3.34	3.37	2.96	3.12	3.61	3.69	3.76	3.65	3.57	3.81
C ₆ H ₁₄ (iso)	3.16	3.13	3.64	3.59	3.25	4.01	3.98	3.96	3.99	4.09	4.36	4.38
MCP	1.26	0.90	1.74	1.79	1.57	1.29	1.92	1.97	2.09	1.92	2.79	2.75
C ₆ H ₆	0.00	0.00	0.00	0.00	0.00	0.00	0.00	0.00	0.00	0.00	0.00	0.00
CH	0.78	0.47	1.13	1.17	1.05	0.80	1.25	1.26	1.55	1.28	2.09	2.02
C ₇ H ₁₆	1.21	1.00	1.28	1.34	1.25	0.28	0.59	0.69	0.78	0.74	0.94	1.24

Table A.3. Plant data for reactor and reactor outlet for 58 days* (cont.).

No of Days	25	26	27	28	29	30	31	32	33	34	35	36
9600TI013	165.26	171.65	169.62	171.14	172.13	169.41	171.19	171.57	170.10	172.46	172.00	172.62
9600TI014	166.64	172.42	170.16	172.09	172.85	170.09	171.85	172.22	171.16	173.54	172.64	173.60
9600TI015	167.05	172.75	170.44	172.53	173.20	170.44	172.12	172.58	171.73	174.01	172.99	174.01
9600TI016	166.58	172.34	170.07	172.26	172.77	170.25	171.74	172.09	171.22	173.56	172.47	173.33
9600TI017	167.13	172.92	170.71	172.92	173.30	170.87	172.27	172.71	171.96	174.15	173.06	173.86
9600TI018	167.98	173.81	171.45	173.94	174.20	171.76	173.19	173.38	172.46	174.83	173.68	174.35
9600PI058	33.21	33.16	33.22	33.18	33.16	33.19	33.18	33.26	33.32	33.18	33.28	33.28
H ₂	0.00	0.00	0.00	0.00	0.00	0.00	0.00	0.00	0.00	0.00	0.00	0.00
CH ₄	0.00	0.00	0.00	0.00	0.00	0.00	0.00	0.00	0.00	0.00	0.00	0.00
C ₂ H ₆	0.00	0.00	0.00	0.00	0.00	0.06	0.20	0.00	0.00	0.00	0.00	0.00
C ₃ H ₈	0.22	0.07	0.09	0.09	0.07	0.11	0.27	0.20	0.09	0.20	0.20	0.21
C ₄ H ₁₀ (iso)	0.39	0.19	0.19	0.18	0.18	0.23	0.29	0.28	0.22	0.28	0.31	0.23
C ₄ H ₁₀	1.93	1.02	1.21	1.05	1.15	1.73	1.69	1.33	1.20	1.39	1.05	1.01
C ₅ H ₁₂ (iso)	3.91	3.38	3.51	3.66	3.30	3.54	4.08	3.63	3.35	4.17	3.69	4.21
C ₅ H ₁₂	4.09	3.68	3.64	3.89	3.61	3.57	4.52	3.88	2.92	3.86	3.35	4.34
C ₅ H ₁₀	0.00	0.00	0.00	0.00	0.00	0.00	0.00	0.00	0.00	0.00	0.00	0.00
C ₆ H ₁₄ (iso)	0.47	0.64	0.56	0.62	0.64	0.69	0.59	0.64	0.25	0.56	0.57	0.51
C ₆ H ₁₄ (iso)	1.70	1.96	1.85	1.94	1.97	1.89	1.77	1.88	1.13	1.76	1.76	1.77
C ₆ H ₁₄ (iso)	5.70	6.53	6.07	6.52	6.58	6.53	6.03	6.39	3.91	5.96	5.96	6.03
C ₆ H ₁₄ (iso)	3.71	4.14	3.92	4.18	4.18	4.19	3.88	4.12	2.69	3.85	3.88	3.92
C ₆ H ₁₄ (iso)	4.22	4.65	4.51	4.72	4.69	4.74	4.56	4.81	3.78	4.15	4.34	4.50
MCP	2.61	2.22	2.91	2.13	2.11	1.98	1.86	1.99	5.58	2.26	2.70	2.51
C ₆ H ₆	0.00	0.00	0.00	0.00	0.00	0.00	0.00	0.00	0.00	0.00	0.00	0.00
CH	1.63	1.62	2.05	1.52	1.55	1.42	1.17	1.45	3.77	1.34	1.86	1.47
C ₇ H ₁₆	1.53	1.22	1.12	1.10	1.41	0.90	1.11	1.08	2.88	1.94	1.92	1.27

Table A.3. Plant data for reactor and reactor outlet for 58 days* (cont.).

No of Days	37	38	39	40	41	42	43	44	45	46	47	48
9600TI013	172.69	170.91	171.05	175.37	178.15	178.46	176.07	174.55	179.52	176.93	177.13	176.72
9600TI014	173.92	171.67	172.25	175.98	179.15	179.12	176.39	174.96	180.38	177.75	177.78	177.61
9600TI015	174.39	172.34	172.69	176.31	179.75	179.62	176.70	175.31	181.24	178.31	178.27	177.95
9600TI016	173.90	171.84	172.24	175.81	179.15	179.10	176.39	174.98	180.41	177.76	177.80	177.60
9600TI017	174.46	172.49	172.90	176.34	179.81	179.59	176.86	175.52	180.89	178.24	178.22	178.03
9600TI018	175.04	173.25	173.68	176.77	180.50	180.14	177.53	176.55	181.60	178.93	178.94	178.65
9600PI058	33.27	33.03	33.22	33.28	33.28	33.23	33.25	33.34	33.34	33.31	33.26	33.38
H ₂	0.00	0.00	0.00	0.00	0.00	0.00	0.00	0.00	0.00	0.00	0.00	0.00
CH ₄	0.00	0.00	0.00	0.00	0.00	0.00	0.00	0.00	0.00	0.00	0.00	0.00
C ₂ H ₆	0.00	0.00	0.00	0.00	0.21	0.00	0.00	0.00	0.08	0.00	0.00	0.00
C ₃ H ₈	0.10	0.11	0.11	0.14	0.24	0.30	0.34	0.27	0.14	0.18	0.15	0.00
C ₄ H ₁₀ (iso)	0.17	0.19	0.16	0.27	0.31	0.34	0.44	0.31	0.21	0.23	0.25	0.10
C ₄ H ₁₀	1.03	0.83	0.92	1.18	1.23	1.77	1.91	1.03	0.98	0.72	0.79	0.65
C ₅ H ₁₂ (iso)	3.79	3.27	3.62	4.39	3.93	3.95	3.92	3.93	3.30	3.63	3.53	3.74
C ₅ H ₁₂	3.70	2.81	3.32	3.83	3.97	4.05	4.19	4.27	3.50	3.48	3.41	3.75
C ₅ H ₁₀	0.00	0.00	0.00	0.00	0.00	0.00	0.00	0.00	0.00	0.00	0.00	0.91
C ₆ H ₁₄ (iso)	0.51	0.42	0.56	0.60	0.34	0.49	0.55	0.63	0.50	0.54	0.53	0.00
C ₆ H ₁₄ (iso)	1.87	1.57	1.69	1.86	1.37	1.75	1.79	1.89	1.83	1.96	1.90	2.10
C ₆ H ₁₄ (iso)	6.42	5.38	5.91	6.36	4.70	5.98	6.12	6.42	6.14	6.55	6.50	7.27
C ₆ H ₁₄ (iso)	4.17	3.49	4.00	4.06	3.12	3.84	3.94	4.12	3.97	4.14	4.16	4.72
C ₆ H ₁₄ (iso)	4.71	3.75	4.70	4.18	4.25	4.39	4.38	4.70	4.72	4.44	4.58	5.20
MCP	2.38	2.47	2.63	2.27	4.22	2.42	2.11	1.85	2.77	2.37	2.33	2.21
C ₆ H ₆	0.00	0.00	0.00	0.00	0.00	0.00	0.00	0.00	0.00	0.00	0.00	0.00
CH	1.42	1.69	1.68	1.34	2.39	1.39	1.23	1.13	1.86	1.60	1.57	1.54
C ₇ H ₁₆	1.35	1.48	2.17	1.53	2.08	1.44	1.13	1.44	1.77	1.84	1.70	1.21

Table A.3. Plant data for reactor and reactor outlet for 58 days* (cont.).

No of Days	49	50	51	52	53	54	55	56	57	58
9600TI013	177.09	166.85	173.42	173.37	175.81	176.07	176.27	175.34	179.08	177.49
9600TI014	177.94	168.14	173.85	173.65	176.27	176.73	176.75	175.88	179.79	178.03
9600TI015	178.51	168.53	174.68	174.27	177.34	177.93	177.32	176.52	180.66	178.74
9600TI016	177.98	167.98	174.21	173.89	176.75	177.29	176.88	176.15	179.98	178.11
9600TI017	178.42	168.30	174.62	174.27	177.12	177.69	177.33	176.60	180.41	178.59
9600TI018	179.07	168.75	175.53	175.12	177.88	178.56	178.02	177.37	180.91	179.17
9600PI058	33.31	33.40	33.08	33.17	33.09	33.09	33.33	33.35	33.28	33.35
H ₂	0.00	0.00	0.00	0.00	0.00	0.00	0.00	0.00	0.00	0.00
CH ₄	0.00	0.00	0.00	0.00	0.00	0.00	0.00	0.00	0.00	0.00
C ₂ H ₆	0.00	0.00	0.00	0.00	0.00	0.00	0.00	0.00	0.00	0.00
C ₃ H ₈	0.21	0.06	0.44	0.51	0.20	0.35	0.31	0.31	0.19	0.29
C ₄ H ₁₀ (iso)	0.24	0.43	0.36	0.39	0.33	0.41	0.38	0.38	0.21	0.40
C ₄ H ₁₀	1.07	1.02	0.79	0.97	1.42	1.15	1.06	1.06	1.15	1.54
C ₅ H ₁₂ (iso)	4.37	4.71	3.42	3.70	3.39	3.54	4.43	4.43	4.64	4.38
C ₅ H ₁₂	4.03	2.96	3.00	3.24	3.07	3.24	3.86	3.86	4.14	3.93
C ₅ H ₁₀	0.00	0.00	0.00	0.00	0.00	0.00	0.00	0.00	0.00	0.00
C ₆ H ₁₄ (iso)	0.54	2.47	0.36	0.45	0.42	0.48	0.52	0.52	0.42	0.40
C ₆ H ₁₄ (iso)	1.91	2.29	1.44	1.55	1.45	1.54	1.77	1.77	1.70	1.60
C ₆ H ₁₄ (iso)	6.46	7.02	4.97	5.28	4.96	5.19	6.09	6.09	5.72	5.44
C ₆ H ₁₄ (iso)	4.09	4.38	3.18	3.35	3.17	3.29	3.93	3.93	3.72	3.54
C ₆ H ₁₄ (iso)	4.36	3.91	3.39	3.56	3.52	3.56	4.32	4.32	4.27	4.19
MCP	2.02	1.30	1.90	1.94	2.26	1.93	2.51	2.51	2.92	3.15
C ₆ H ₆	0.00	0.00	0.00	0.00	0.00	0.00	0.00	0.00	0.00	0.00
CH	1.38	0.98	1.34	1.31	1.57	1.31	1.65	1.65	1.83	2.04
C ₇ H ₁₆	1.29	0.68	1.61	1.20	0.84	0.69	1.08	1.08	1.05	1.18

*Because of the confidentiality agreement, real plant data are multiplied by a factor.

Table A.4. Heat of formation, specific heat and physical properties data of components.

	ΔH_{form}	C_{p-A}	C_{p-B}	C_{p-C}	C_{p-D}	ω	T_c	P_c	T_B	MW
H ₂	0.00	27.14	9.27E-03	-1.38E-05	7.65E-09	-2.16E-01	33.20	13.00	-252.80	2.02
CH ₄	-74.86	19.25	5.21E-02	1.20E-05	-1.13E-08	1.10E-02	190.60	46.00	-161.50	16.04
C ₂ H ₆	-84.74	5.41	1.78E-01	-6.94E-05	8.71E-09	9.90E-02	305.40	48.80	-88.60	30.07
C ₃ H ₈	-103.92	-4.22	3.06E-01	-1.59E-04	3.21E-08	1.53E-01	369.80	42.50	-42.04	44.10
C ₄ H ₁₀ (iso)	-134.61	-1.39	3.85E-01	-1.85E-04	2.90E-08	1.83E-01	408.10	36.50	-11.72	58.12
C ₄ H ₁₀	-126.23	9.49	3.31E-01	-1.11E-04	-2.82E-09	1.99E-01	425.20	38.00	-0.50	58.12
C ₅ H ₁₂ (iso)	-160.33	-13.06	5.31E-01	-3.02E-04	6.68E-08	2.27E-01	460.40	32.90	27.84	72.15
C ₅ H ₁₂	-146.54	-3.63	4.87E-01	-2.58E-04	5.30E-08	2.51E-01	469.60	33.70	36.07	72.15
C ₅ H ₁₀	-77.29	-53.63	5.43E-01	-3.03E-04	6.49E-08	1.96E-01	511.60	45.10	49.25	70.13
C ₆ H ₁₄ (iso)	-185.68	-14.61	6.15E-01	-3.38E-04	6.82E-08	2.32E-01	488.70	30.80	49.73	86.18
C ₆ H ₁₄ (iso)	-177.90	-16.63	6.29E-01	-3.48E-04	6.85E-08	2.47E-01	499.90	31.30	57.98	86.18
C ₆ H ₁₄ (iso)	-174.42	-10.57	6.18E-01	-3.57E-04	-8.08E-08	2.78E-01	497.50	30.10	60.26	86.18
C ₆ H ₁₄ (iso)	-171.74	-2.39	5.69E-01	-2.87E-04	5.03E-08	2.70E-01	504.40	31.20	63.27	86.18
C ₆ H ₁₄ (iso)	-167.30	-4.41	5.82E-01	-3.12E-04	6.49E-08	2.99E-01	507.40	29.70	68.73	86.18
MCP	-105.93	-50.11	6.38E-01	-3.64E-04	8.01E-08	2.31E-01	532.70	37.90	71.81	84.16
C ₆ H ₆	82.98	-33.92	4.74E-01	-3.02E-04	7.13E-08	2.10E-01	562.10	48.90	80.09	78.11
CH	-123.22	-54.54	6.11E-01	-2.52E-04	1.32E-08	2.10E-01	553.40	40.70	80.72	84.16
C ₇ H ₁₆	-187.90	-5.15	6.76E-01	-3.65E-04	7.66E-08	3.49E-01	540.20	27.40	98.43	100.20

Table A.5. Reaction coefficients for 48 reactions (cont.).

	25	26	27	28	29	30	31	32	33	34	35	36	37	38	39	40	41	42	43	44	45	46	47	48
H ₂	-1	-1	-1	-1	-1	-1	-1	-1	-1	-1	-1	-1	-1	-1	-1	-1	-1	-1	-1	-1	-1	-1	-3	-3
CH ₄	1	0	1	0	0	1	1	0	0	1	1	0	1	0	1	0	1	0	0	0	0	0	0	0
C ₂ H ₆	0	1	0	1	0	0	0	1	0	0	0	1	0	0	0	1	0	0	0	0	0	0	0	0
C ₃ H ₈	0	1	0	0	2	0	0	0	2	0	0	0	0	2	0	0	0	0	0	0	0	0	0	0
C ₄ H ₁₀ (iso)	-1	0	0	0	0	0	0	1	0	0	0	0	0	0	0	1	0	0	0	0	0	0	0	0
C ₄ H ₁₀	0	0	0	1	0	0	0	0	0	0	0	1	0	0	0	0	0	0	0	0	0	0	0	0
C ₅ H ₁₂ (iso)	-1	-1	0	0	0	0	1	0	0	0	1	0	1	0	1	0	0	0	0	0	0	0	0	0
C ₅ H ₁₂	0	0	1	0	0	1	0	0	0	1	0	0	0	0	0	0	0	0	0	0	0	0	0	0
C ₅ H ₁₀	0	0	0	0	0	0	0	0	0	0	0	0	0	0	0	0	0	0	0	0	0	0	0	0
C ₆ H ₁₄ (iso)	0	0	0	0	0	0	0	0	0	0	0	0	0	0	-1	-1	0	0	0	0	1	0	0	0
C ₆ H ₁₄ (iso)	0	0	0	0	0	0	0	0	0	0	0	0	-1	-1	0	0	0	0	0	0	1	0	0	0
C ₆ H ₁₄ (iso)	0	0	0	0	0	-1	-1	-1	-1	0	0	0	0	0	0	0	0	0	1	0	0	0	0	0
C ₆ H ₁₄ (iso)	0	0	0	0	0	0	0	0	0	-1	-1	-1	0	0	0	0	0	0	0	1	0	0	0	0
C ₆ H ₁₄ (iso)	0	0	-1	-1	-1	0	0	0	0	0	0	0	0	0	0	0	1	1	0	0	0	0	0	0
MCP	0	0	0	0	0	0	0	0	0	0	0	0	0	0	0	0	0	0	-1	-1	-1	-1	1	1
C ₆ H ₆	0	0	0	0	0	0	0	0	0	0	0	0	0	0	0	0	0	0	0	0	0	0	-1	-1
CH	0	0	0	0	0	0	0	0	0	0	0	0	0	0	0	0	0	-1	0	0	0	0	0	0
C ₇ H ₁₆	0	0	0	0	0	0	0	0	0	0	0	0	0	0	0	0	-1	0	0	0	0	0	0	0

Table A.6. Estimated reaction parameters for isomerization reactions.

	$\ln k_0$ [-]	E_A [kJ/kmol]		$\ln k_0$ [-]	E_A [kJ/kmol]
Rxn 1	16.1496	81.0060	Rxn 25	25.1465	154.4652
Rxn 2	20.5494	67.6533	Rxn 26	29.0069	166.3054
Rxn 3	16.2507	83.5263	Rxn 27	16.0208	105.3756
Rxn 4	15.8793	82.0896	Rxn 28	19.4194	117.7717
Rxn 5	13.7411	78.4040	Rxn 29	19.5169	129.5021
Rxn 6	13.5646	76.7062	Rxn 30	21.1701	120.2515
Rxn 7	13.0195	77.5134	Rxn 31	21.0437	104.4294
Rxn 8	15.8885	71.4880	Rxn 32	16.8383	107.9669
Rxn 9	20.2066	73.2745	Rxn 33	14.3147	115.7203
Rxn 10	19.4558	77.0709	Rxn 34	17.6441	117.0292
Rxn 11	15.3641	72.9108	Rxn 35	19.2751	97.4337
Rxn 12	15.3751	72.4638	Rxn 36	16.1180	99.3300
Rxn 13	18.1251	64.8896	Rxn 37	15.3872	118.4098
Rxn 14	14.5013	97.8393	Rxn 38	11.8855	126.9409
Rxn 15	21.1923	62.3139	Rxn 39	16.6469	100.3874
Rxn 16	14.2308	76.4486	Rxn 40	17.9202	116.0310
Rxn 17	28.2231	144.3900	Rxn 41	13.0442	97.0347
Rxn 18	30.8761	182.4449	Rxn 42	31.7578	146.4064
Rxn 19	8.1096	87.1553	Rxn 43	25.5510	95.3259
Rxn 20	9.5353	87.3016	Rxn 44	24.5316	130.1248
Rxn 21	6.9296	89.1670	Rxn 45	23.4518	126.8108
Rxn 22	24.8342	172.7512	Rxn 46	21.6394	74.6141
Rxn 23	15.1282	132.5029	Rxn 47	14.9016	72.8719
Rxn 24	22.7139	191.4423	Rxn 48	14.4014	74.6444

Table A.7. Initial and final reaction parameter values.

No of Rxn	Ln k_0 (init)	E_A (init)	Ln k_0	E_A
1	25.366	83.693	16.150	81.006
2	25.366	83.693	20.549	67.653
3	25.356	83.655	16.251	83.526
4	25.356	83.662	15.879	82.090
5	23.221	75.312	13.741	78.404
6	23.221	75.320	13.565	76.706
7	23.221	75.312	13.020	77.513
8	23.221	75.312	15.888	71.488
9	28.984	75.315	20.207	73.275
10	28.984	75.312	19.456	77.071
11	23.794	75.312	15.364	72.911
12	23.794	75.320	15.375	72.464
13	26.121	75.295	18.125	64.890
14	26.121	75.312	14.501	97.839
15	27.220	75.310	21.192	62.314
16	27.220	75.312	14.231	76.449
17	37.082	146.434	28.223	144.390
18	37.082	146.430	30.876	182.445
19	17.585	83.693	8.110	87.155
20	17.585	83.693	9.535	87.302
21	17.585	83.693	6.930	89.167
22	33.227	167.386	24.834	172.751
23	26.130	104.345	15.128	132.503
24	33.227	167.386	22.714	191.442

Table A.7. Initial and final reaction parameter values (cont.).

25	33.227	167.386	25.147	154.465
26	33.227	167.386	29.007	166.305
27	26.130	104.345	16.021	105.376
28	26.130	104.345	19.419	117.772
29	26.130	104.345	19.517	129.502
30	27.853	104.599	21.170	120.252
31	27.853	104.599	21.044	104.429
32	27.853	104.599	16.838	107.967
33	27.853	104.599	14.315	115.720
34	27.853	104.599	17.644	117.029
35	27.853	104.599	19.275	97.434
36	27.853	104.599	16.118	99.330
37	27.853	104.599	15.387	118.410
38	27.853	104.599	11.885	126.941
39	27.853	104.599	16.647	100.387
40	27.853	104.599	17.920	116.031
41	23.773	83.693	13.044	97.035
42	37.082	146.434	31.758	146.406
43	32.545	125.521	25.551	95.326
44	32.545	125.521	24.532	130.125
45	32.545	125.521	23.452	126.811
46	32.545	125.521	21.639	74.614
47	23.371	66.932	14.902	72.872
48	23.371	66.932	14.401	74.644

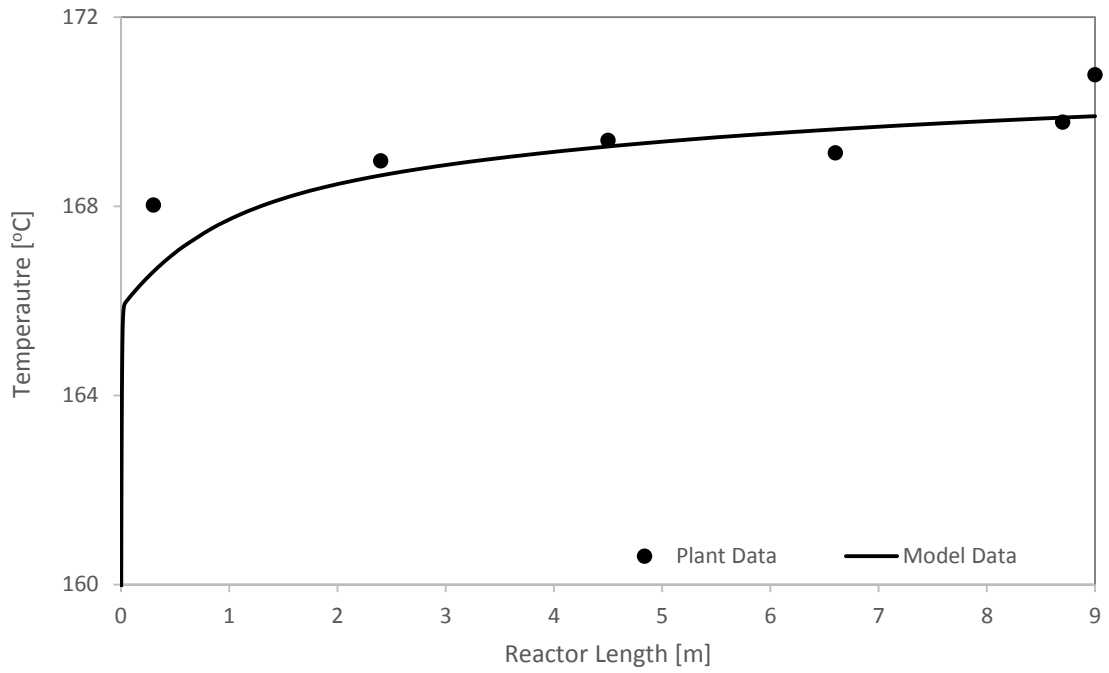


Figure A.1. Reactor simulation temperature profile for 28. Day.

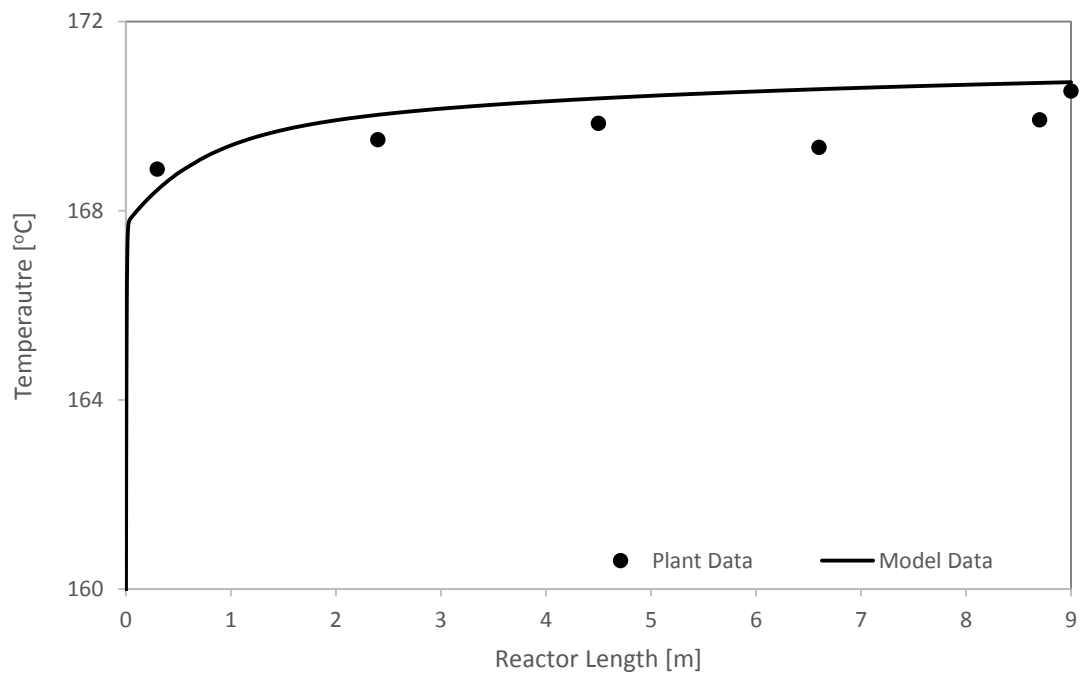


Figure A.2. Reactor simulation temperature profile for 35. Day.

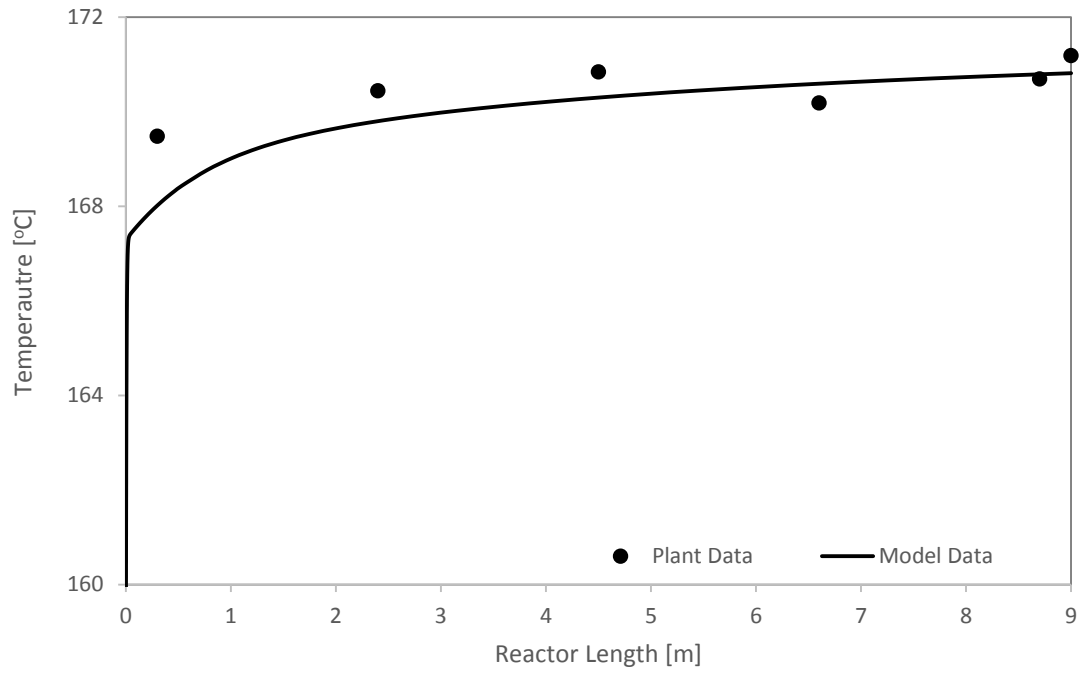


Figure A.3. Reactor simulation temperature profile for 36. Day.

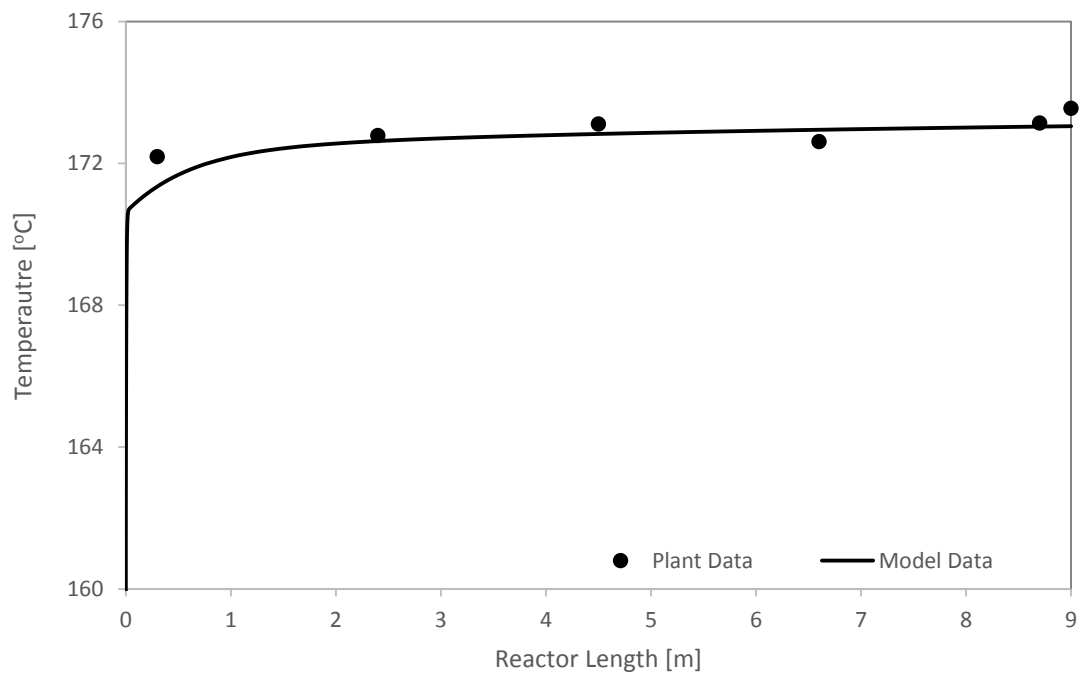


Figure A.4. Reactor simulation temperature profile for 40. Day.

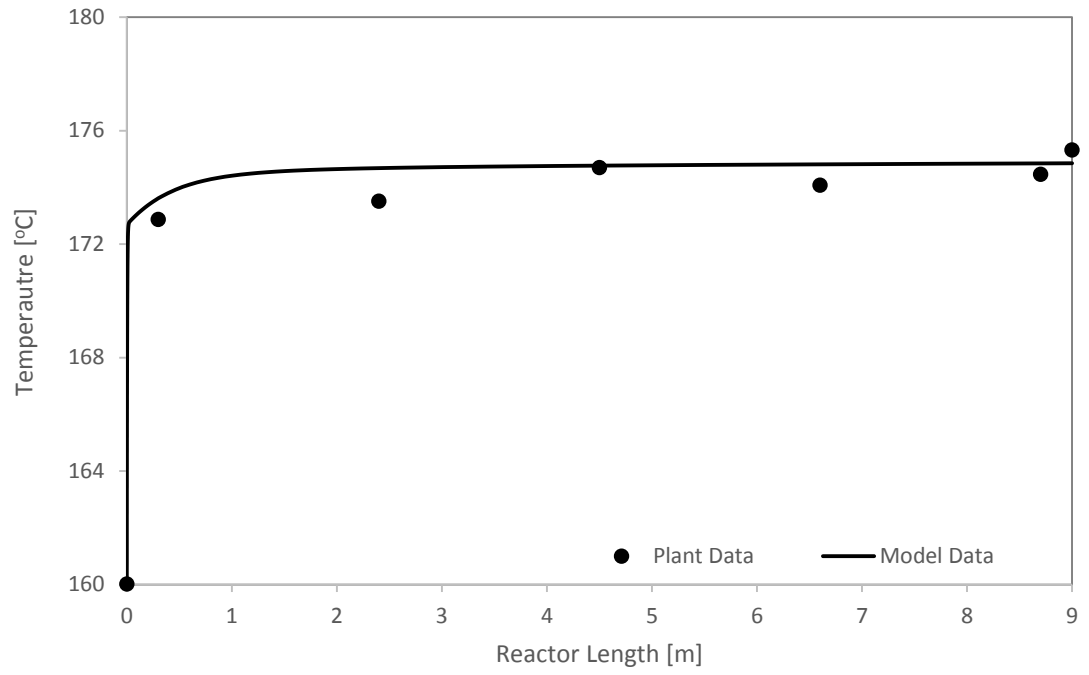


Figure A.5. Reactor simulation temperature profile for 54. Day.

APPENDIX B. DETAILED MODEL FLOW CHARTS

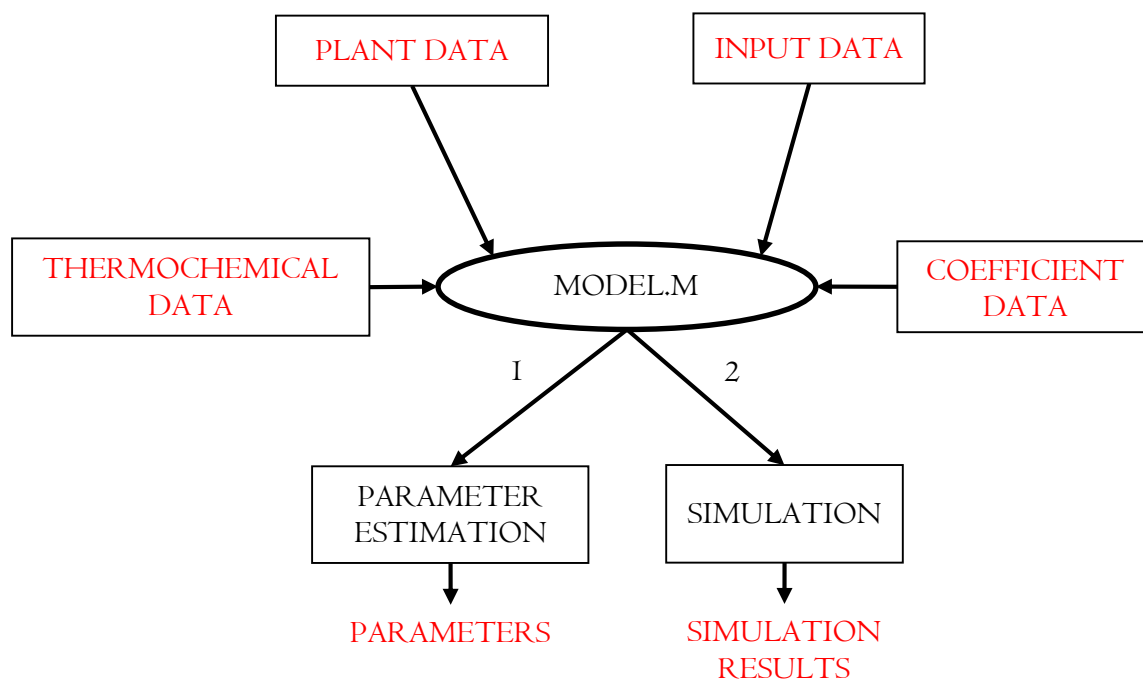


Figure B.1. Flow chart of main file.

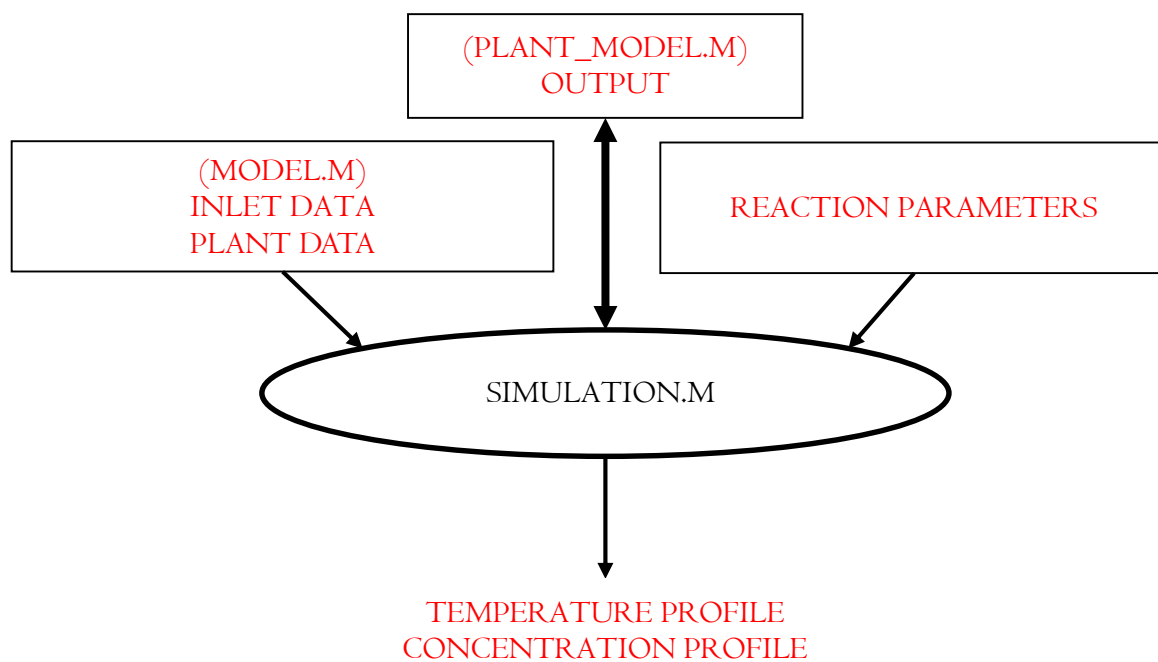


Figure B.2. Flow chart of simulation file.

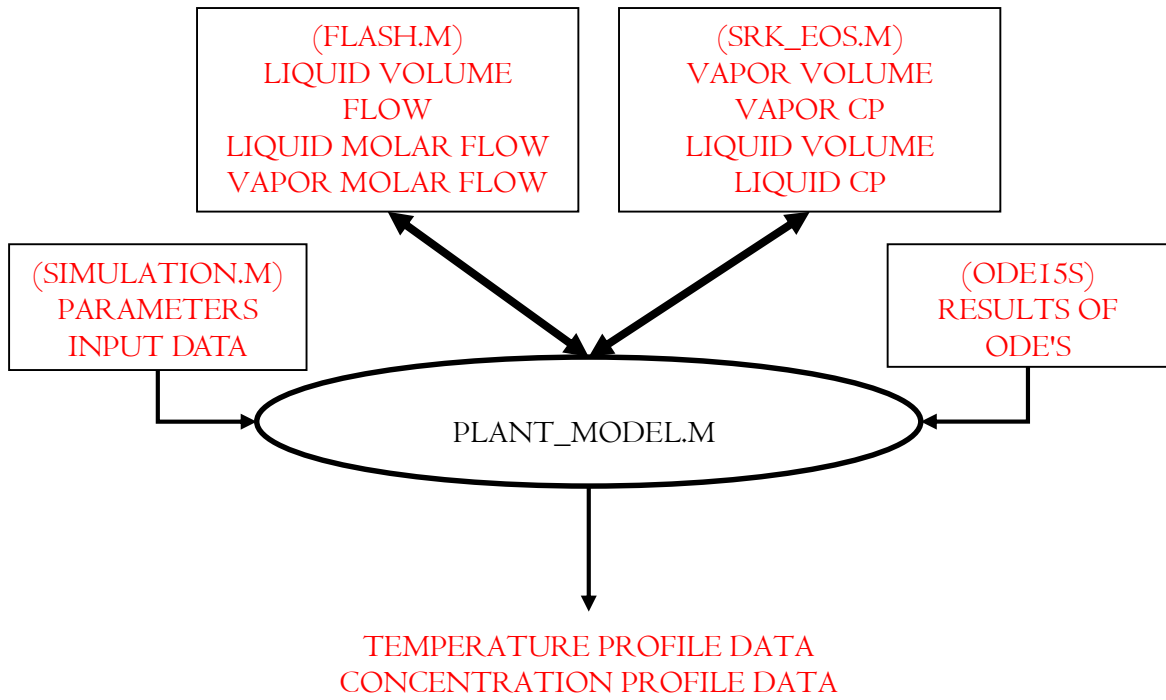


Figure B.3. Flow chart of plant model file.

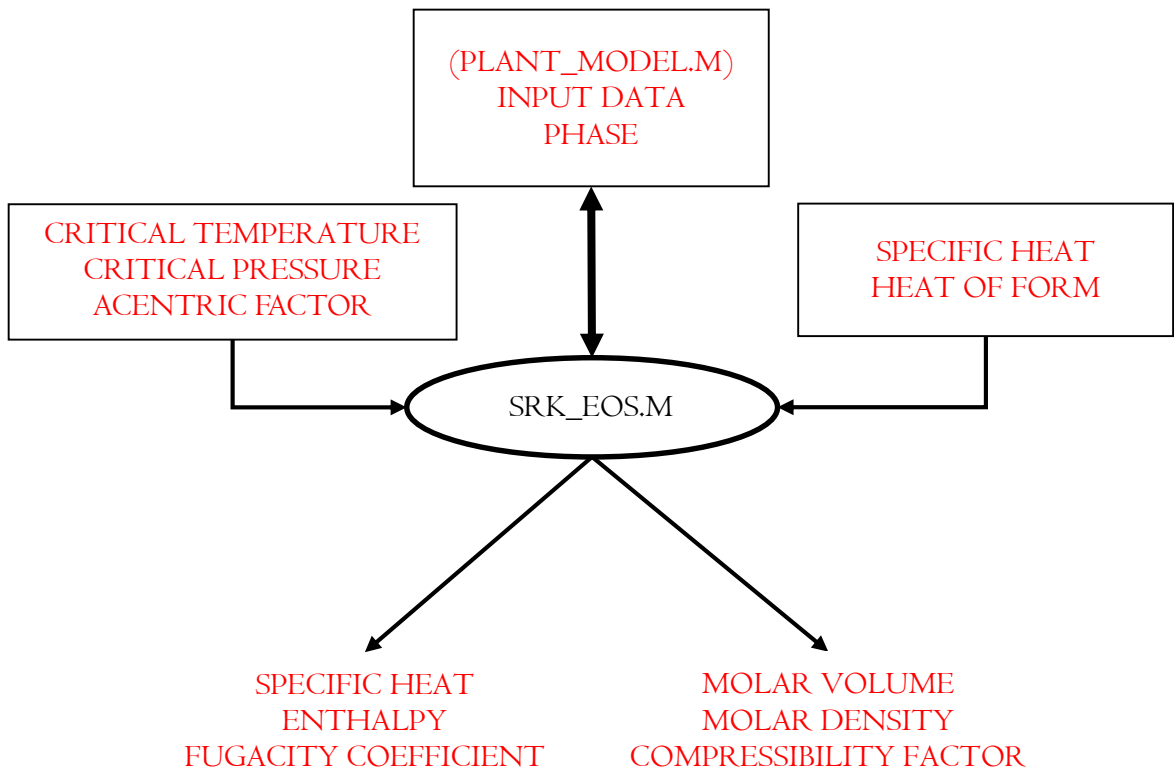


Figure B.4. Flow chart of SRK EOS calculation file.

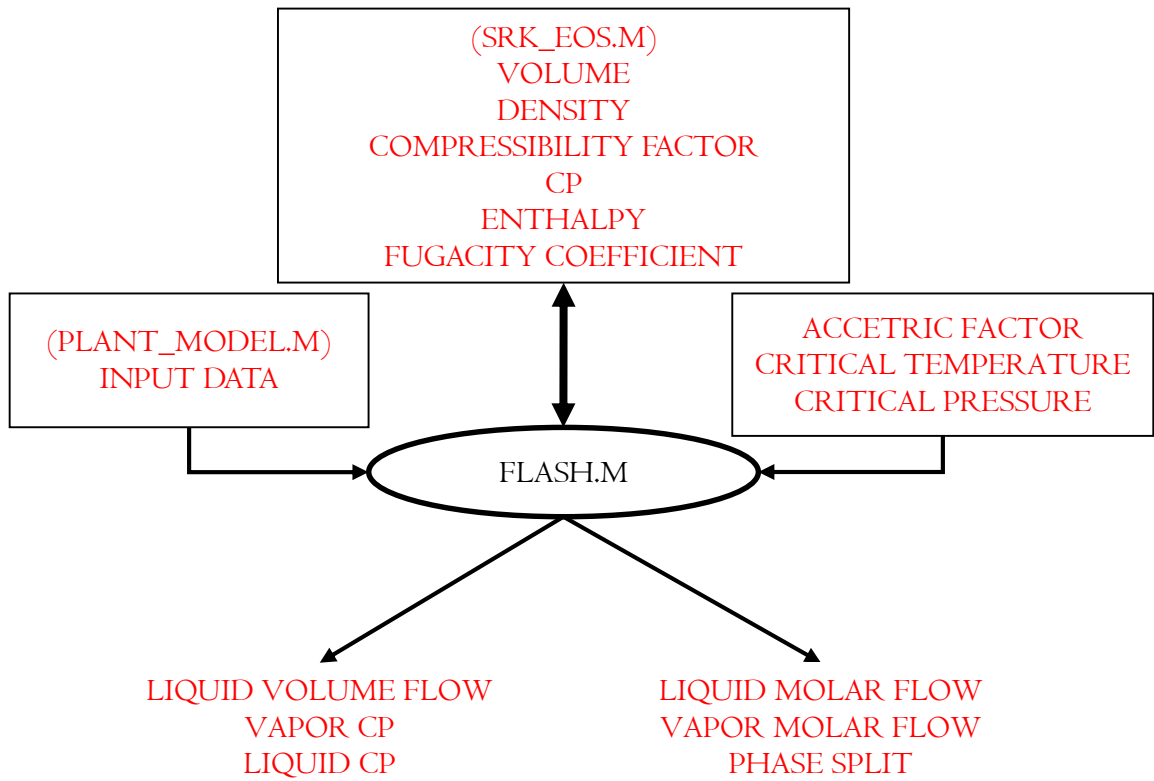


Figure B.5. Flow chart of flash calculation file.

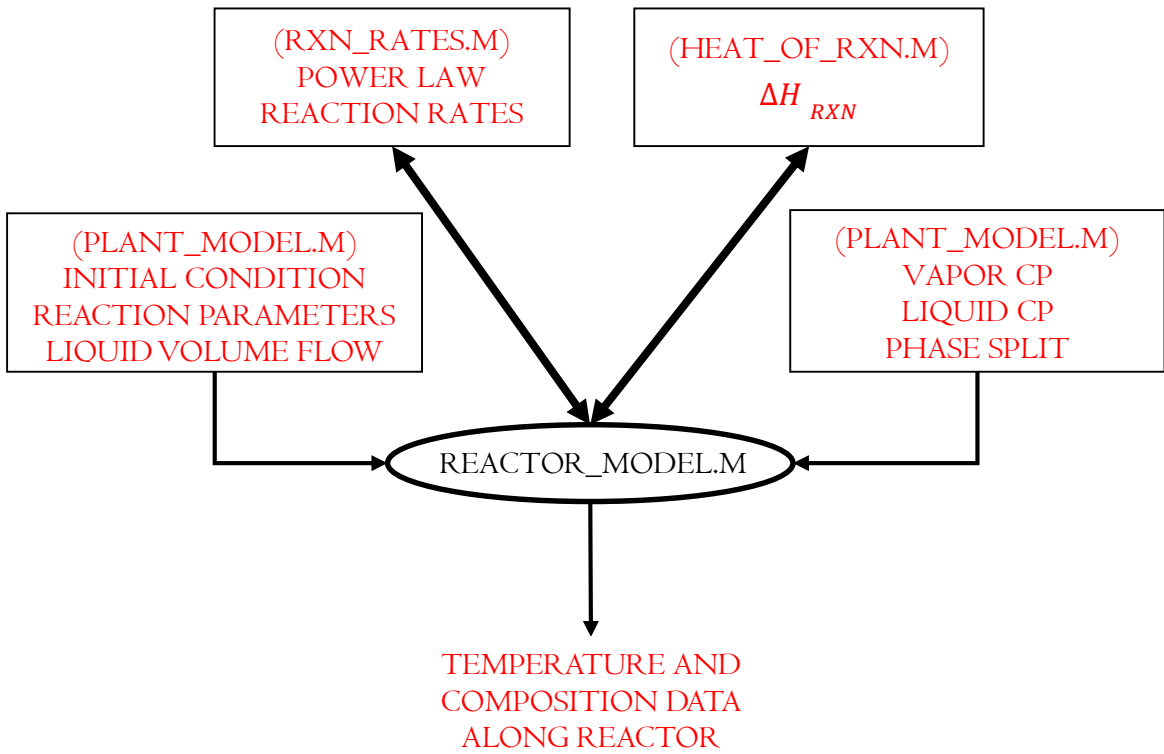


Figure B.6. Flow chart of reactor model file.

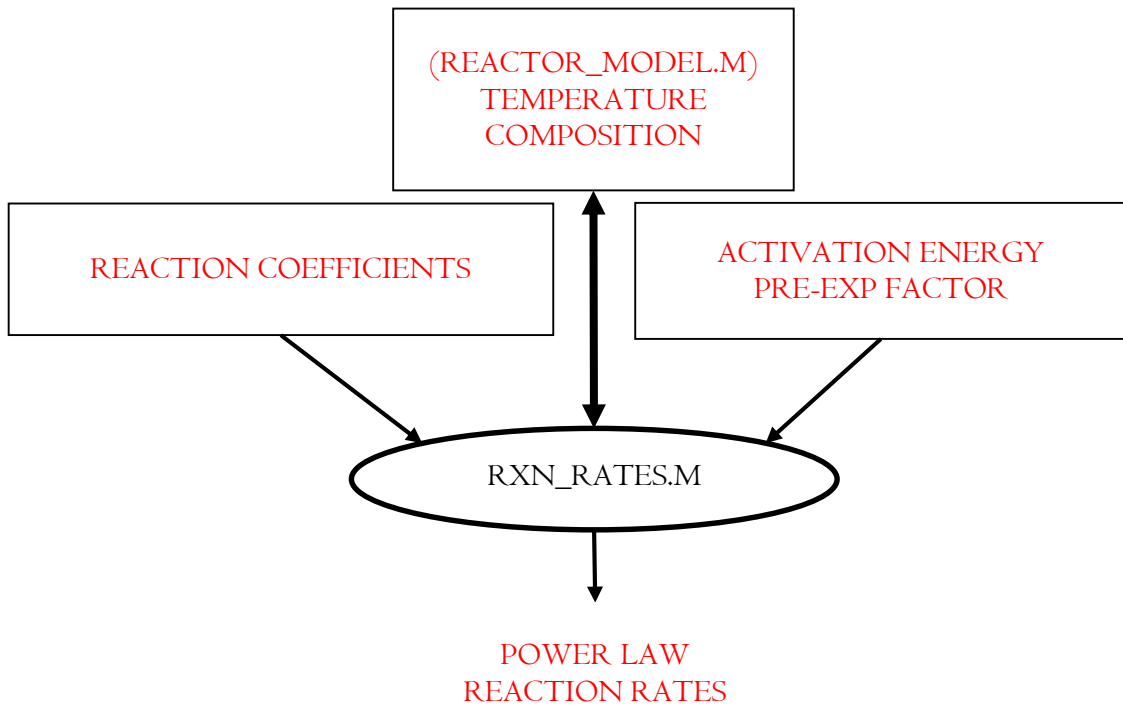


Figure B.7. Flow chart of reaction rates calculation file.

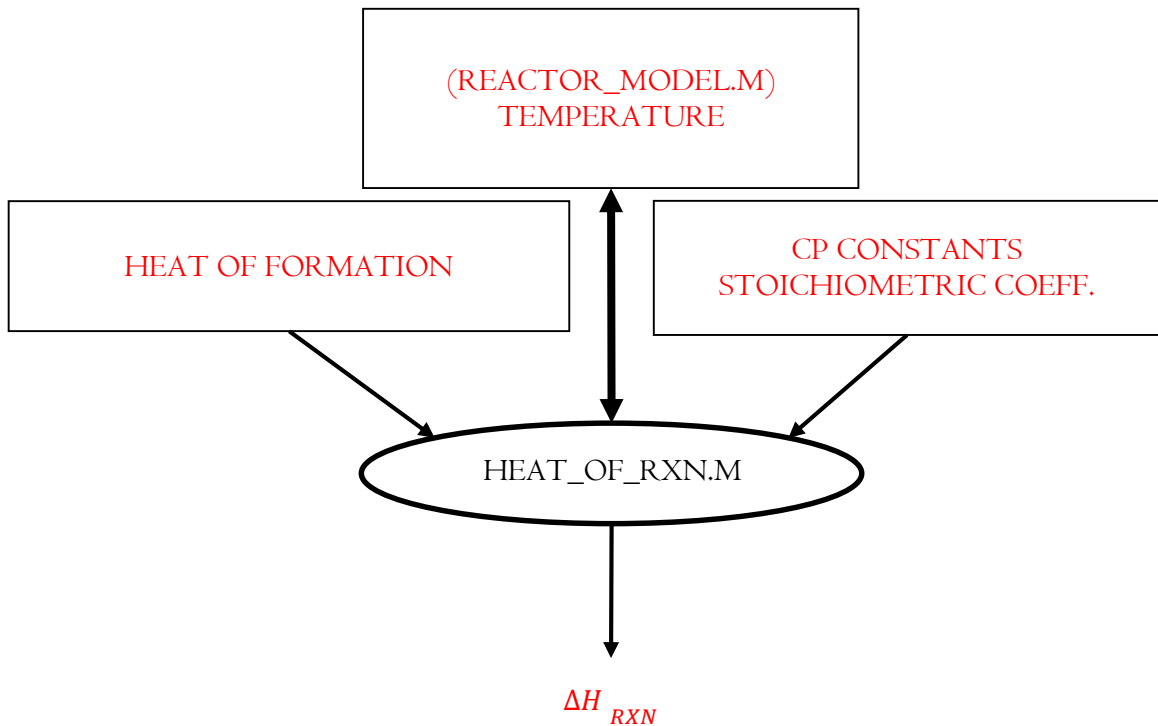


Figure B.8. Flow chart of heat of reaction calculation file.

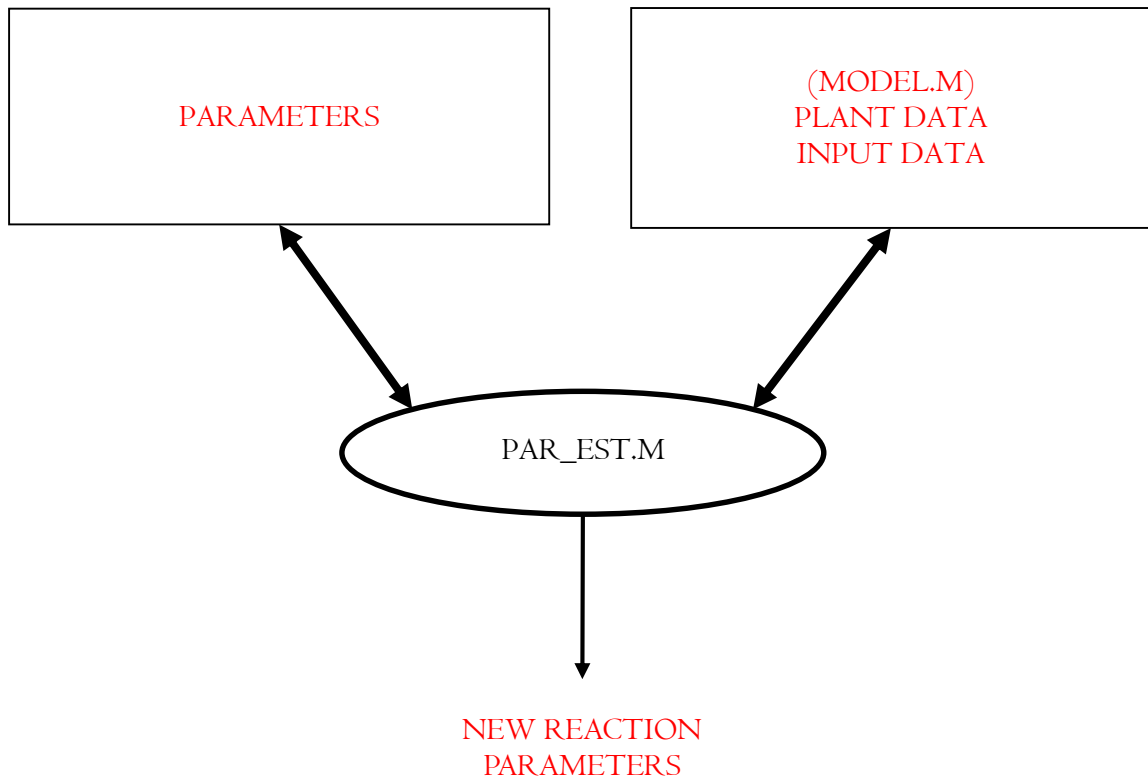


Figure B.9. Flow chart of parameter estimation file.

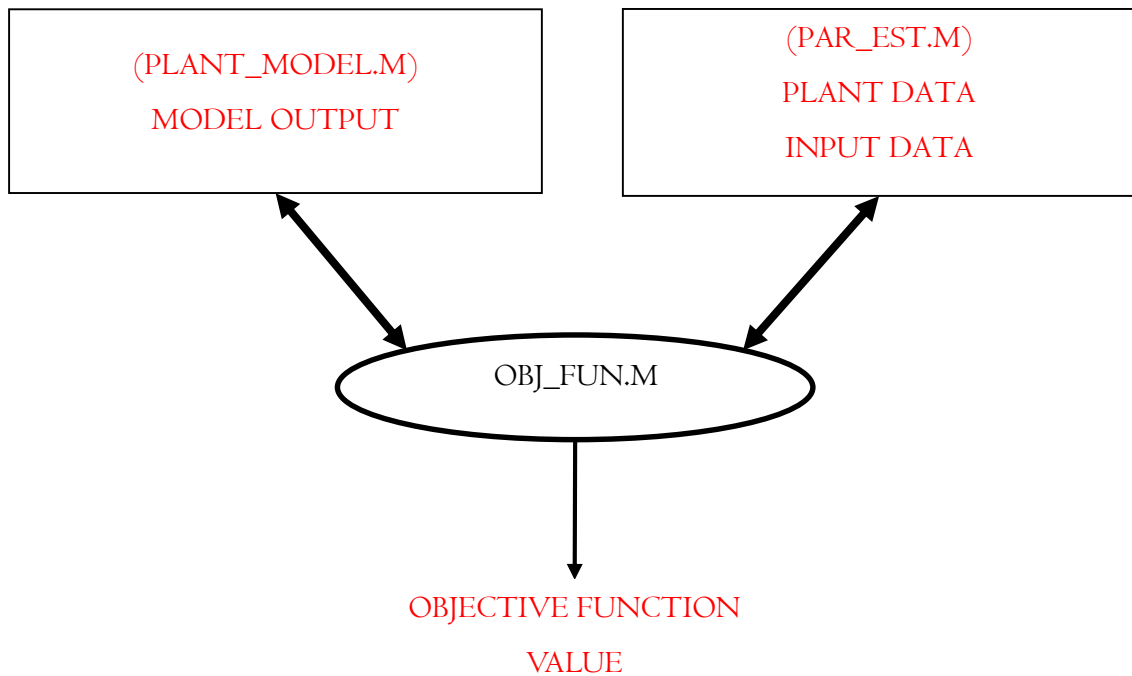


Figure B.10. Flow chart of objective function calculation file.

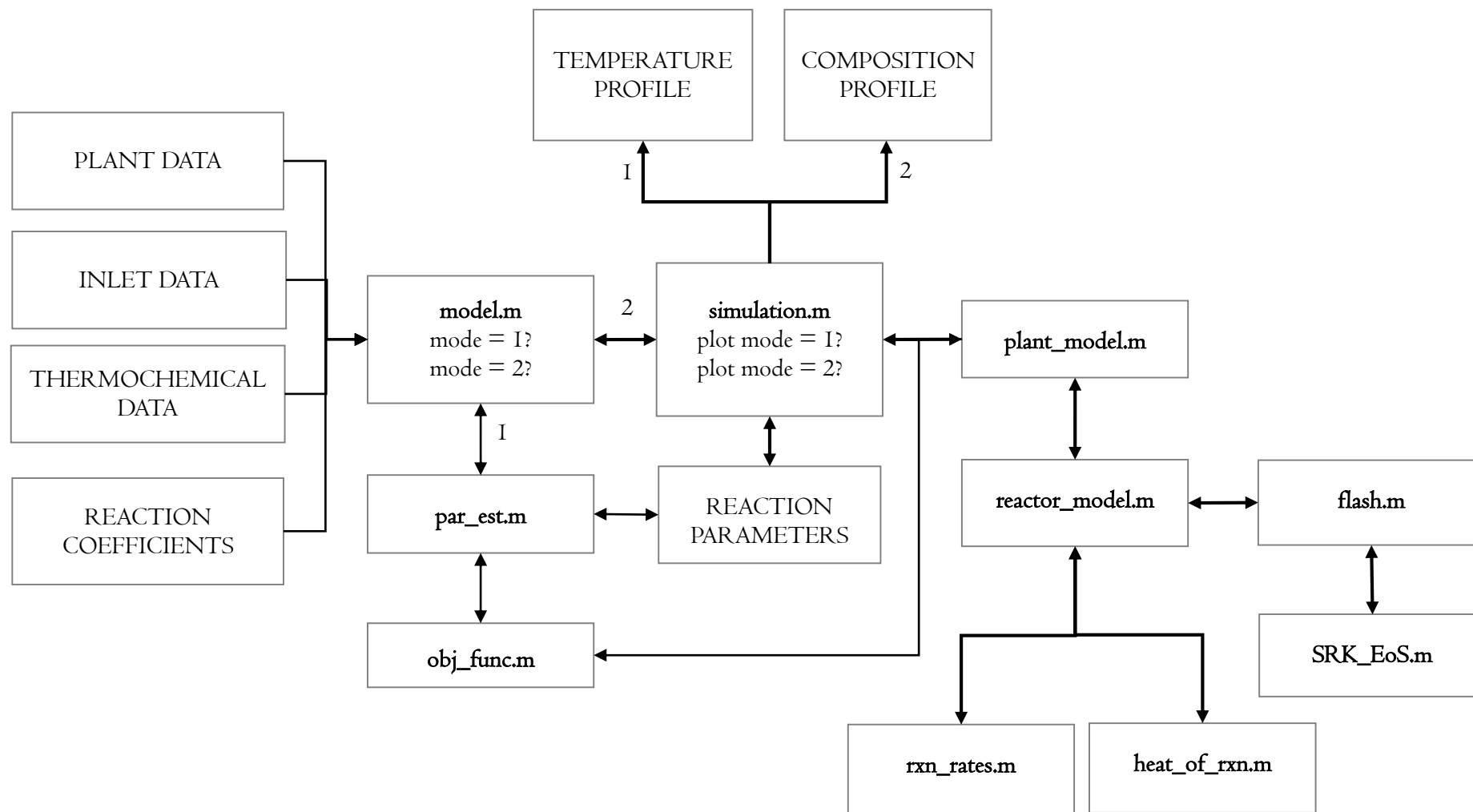


Figure B.11. Whole code flow chart .

REFERENCES

1. Løften, T., *Catalytic Isomerization of Light Alkanes*, Ph.D. Thesis, Norwegian University of Science and Technology, 2004.
2. *UOP Training Document*, Universal Oil Products Press, 2010
3. Hancsók, J., S. Magyar, A. Holló, *Importance of Isoparaffins in the Crude Oil Refining Industry*, University of Pannonia, Pannonia, 2010
4. Hart, H., R. D. Schuetz, *A Short Course in Organic Chemistry*, 2nd Edition, Houghton Mifflin, Boston, 1959.
5. Yasakova, E. A., A. V. Sitdikova, "Tendency of Isomerization Process Development in Russia and Foreign Countries", *Oil and Gas Business*, Vol. 15, pp. 1200-1217, 2010.
6. Ward, J. W., "Hydrocracking Processes and Catalysts", *Fuel Processing Technology*, Vol. 35, pp. 55–85, 1993.
7. Vazquez, I. M., A. Escardino, A. Corma, "Activity and Selectivity of Nickel-molybdenum/HY Ultrastable Zeolites for Hydroisomerization and Hydrocracking of Alkanes", *Industrial Chemical Engineering Research*, Vol. 26, pp. 1495-1500, 1987.
8. Fúnez, A., D. A. Lucas, P. Sánchez, M. J. Ramos, J. L. Valverde, "Hydroisomerization in Liquid Phase of a Refinery Naphtha Stream Over Pt–Ni/H-beta Zeolite Catalysts", *Chemical Engineering Journal*, Vol. 136, pp. 267–275, 2008.
9. Kozhevnikov, I. V., "Catalysis by Heteropoly Acids and Multicomponent Polyoxometalates in Liquid-phase Reactions", *Chemical Reviews*, Vol. 98, pp. 171-198, 1998.
10. Kozhevnikov, I.V., "Sustainable Heterogeneous Acid Catalysis by Heteropolyacids", *Journal of Molecular Catalysis A: Chemical*, Vol. 262, pp. 86-92, 2007.
11. Galadima, A., J. A. Anderson, R. P. K. Wells, "Solid Acid Catalysts in Heterogeneous N-Alkane Hydroisomerisation for Increasing Octane Number of Gasoline", *Science World Journal*, Vol. 4, pp. 15-22, 2009.

12. Matsuda, T., H. Shiro, H. Sakagami, N. Takahashi, "Isomerisation of Heptanes on Molybdenum Oxides Treated with Hydrogen", *Catalysis Letters*, Vol. 47, pp. 99-103, 1997.
13. Matsuda, T., H. Sakagami, N. Takashi, "Isomerisation of Heptanes on Molybdenum Oxide Catalysts with a Small Amount of Nickel", *Journal of Chemical Society*, Vol. 93, pp. 2225-2229, 1997.
14. Wehrer, P., S. Libs, L. Hilaire, "Isomerization of Alkanes and Alkenes on Molybdenum Oxides", *Applied Catalysis A: General*, Vol. 238, pp. 69-84, 2003.
15. Deak, V.G., R. R. Rosin, D. K. Sullivan, "Tutorial: Light Naphtha Isomerization", *American Institute of Chemical Engineers Journal*, Vol. 25, pp. 250-259, 2008.
16. Valavarasu, G., B. Sairam, "Light Naphtha Isomerization Process: A Review", *Petroleum Science and Technology*, Vol. 31, pp. 580-595, 2013.
17. Paula, S., D. Fernando, J. R. Maria, R. Rubi, J. Vicente, L. V. Jose, "Hydroisomerization of C6-C8 n-alkanes, Cyclohexane and Benzene over Palladium and Platinum Beta Catalysts Agglomerated with Betonite", *Applied Catalysis A: General*, Vol. 314, pp. 248-255, 2006.
18. Ono, Y., "A Survey of Mechanism in Catalytic Isomerisation of Alkanes", *Catalysis Today*, Vol. 81, pp. 3-16, 2003.
19. Vaudagna, S.R., R. A. Comelli, N. S. Figoli, "Influence of the Tungsten Oxide Precursor on WO_x - ZrO_2 and Pt/ WO_x - ZrO_2 Properties", *Applied Catalysis A: General*, Vol. 164, pp. 265-280, 1997.
20. Ahmad, R., J. Melsheimer, F. C. Jentoft, R. Schlögl, "Isomerisation of n-butane and n-pentane in the Presence of Sulphated Zirconia: Formation of Surface Deposits Investigated by In situ UV-vis Diffuse Reflectance Spectroscopy", *Journal of Catalysis*, Vol. 218, pp. 365-374, 2003.
21. Rawlings, J. B., J. G. Ekerdt, *Chemical Reactor Analysis and Design Fundamentals*, 2nd Edition, Nob Hill Publishing, Madison, USA, 2012.
22. Gauw, F. J. M. M., *Kinetic Studies of Alkane Hydroisomerization over Solid Acid Catalysts*, Ph.D. Thesis, Eindhoven University of Technology, 2002.

23. Batalha, N., F. Lemos, T.U. Lisbon, L. Pinard, A.L. Valant, J.L. Lemberon, Y. Pouilloux, “New Insights Into the Hydroisomerisation Reaction Mechanism”, In: DECHEMA – The Society for Chemical Engineering and Biotechnology, *International Congress on Catalysis*, Munich, 1-6 July 2012, Wiley-VCH Verlag GmbH & Co. KGaA, 2012.
24. Benitez , V. M., J. M. Grau, J. C. Yori, C. L. Pieck, C. R. Vera, “Hydroisomerization of Benzene-Containing Paraffinic Feedstocks over Pt/WO₃-ZrO₂ Catalysts”, *Energy and Fuels*, Vol. 20, pp. 1791-1798, 2006.
25. Runstraat, A. V., J. A. Kamp, P. J. Stobbelaar, J. V. Grondelle, S. Krijnen, R. A. V. Santen, “Kinetics of Hydro-isomerization of n-Hexane over Platinum Containing Zeolites”, *Journal of Catalysis*, Vol. 171, pp. 77-84, 1997.
26. Ribeiro, F., C. Marcilly, M. Guisnet, “Hydroisomerization of n-hexane on platinum zeolites: I. Kinetic study of the reaction on platinum/Y-zeolite catalysts: Influence of the platinum content”, *Journal of Catalysis*, Vol. 78, pp. 267-274, 1982.
27. Steijns, M., G. F. Froment, “Hydroisomerization and Hydrocracking. 3. Kinetic Analysis of Rate Data for n-decane and n-dodecane”, *Industrial and Engineering Chemistry Product Research and Development*, Vol. 20, pp. 660-668, 1981.
28. Holló, A., J. Hancsó, D. Kalló, “Kinetics of Hydroisomerization of C₅–C₇ Alkanes and Their Mixtures over Platinum Containing Mordenite”, *Applied Catalysis A: General*, Vol. 229, pp. 93-102, 2002.
29. Beltramini, J. N., T. J. Wessel, R. Datta, “Kinetics of Deactivation of Bifunctional Pt/Al₂O₃-Cl Catalysts by Coking”, *American Institute of Chemical Engineers Journal*, Vol. 37, pp. 845-854, 1991.
30. Graeme, S., M. Van der Laan, “Butane and Light Naphtha Isomerization”, *Petroleum Technology Quarterly*, Vol. 8, pp. 47-49, 2003.
31. Mohamed, A. H. A. K., M. Kamel, “Hydroisomerization of N-Alkane Over Zeolite Supported Catalyst”, *Journal of Engineering*, Vol. 15, 2009.

32. Joint Stock Company Scientific Industrial Enterprise Neftehim, *Pentane-hexane Isomerization Process and Catalysts*, 2014, <http://nefthim.com/node/185>, Accessed on 23.11.2014.
33. Raseev, S., *Thermal and Catalytic Processes in Petroleum Refining*, Marcel Dekker, New York, USA, 2003.
34. Ullmann, F., *Ullmann's Encyclopedia of Industrial Chemistry*, 7th Edition, John & Wiley Sons, New York, USA, 2014.
35. Gates, B. C., *Catalytic Chemistry*, John Wiley & Sons, New York, 1992.
36. Iordanidis, A. A., *Mathematical Modeling of Catalytic Fixed Bed Reactors*, Ph.D. Thesis, University of Twente, 2002.
37. Gear, C. W., *Numerical Initial Value Problems in Ordinary Differential Equations*, Prentice-Hall, New Jersey, USA, 1971.
38. Schiesser, W. E., *The Numerical Method of Lines: Integration of Partial Differential Equations*, Academic Press, Massachusetts, USA, 1991.
39. Villadsen, J. V., W. E. Stewart, "Solution of Boundary-value problems by orthogonal Collocation", *Chemical Engineering Science*, Vol. 22, pp. 1483-1501, 1967.
40. Khadilkar, M. R., *Performance Studies of Trickle Bed Reactors*, Ph.D. Thesis, Washington University, 1998.
41. Fogler, H. S., *Elements of Chemical Reaction Engineering*, 4th edition, Prentice Hall, New Jersey, USA, 2006.
42. Jarullah, T. A., I. M. Mujtaba, A. S. Wood, "Whole Crude Oil Hydrotreating from Small-Scale Laboratory Pilot Plant to Large-Scale trickle-Bed Reactor: Analysis of Operational Issues through Modeling", *Energy and Fuels*, Vol. 26, pp. 629-641, 2012.
43. Akgerman, A., G. M. Collins, B. D. Hook, "Effect of Feed Volatility on Conversion in Trickle Bed Reactors", *Industrial and Engineering Chemistry Fundamentals*, Vol. 24, pp. 398-401, 1985.

44. Meyers, R. A., *Handbook of Petroleum Refining Processes*, 2nd edition, McGraw-Hill, New York, USA 1997.
45. Skogestad, S., *Chemical and Energy Process Engineering*, 2nd edition, CRC Press, New York, USA 2008.
46. Ham, Y. M., C. Chun, S. G. Lee, "Some Higher Order Modifications of Newton's Method for Solving Nonlinear Equations", *Journal of Computational and Applied Mathematics*, Vol. 222, pp. 477-486, 2008.
47. Naji, H. S., "Conventional and Rapid Flash Calculations for the Soave-Redlich-Kwong and Peng-Robinson Equations of State", *Emirates Journal for Engineering Research*, Vol. 13, pp. 81-91, 2008.
48. Sandler, S. I., *Chemical, Biochemical, and Engineering Thermodynamics*, 4th edition, John Wiley, New York, USA, 2006.
49. Chen, J., N. Wang, F. Mederos, J. Ancheyta, "Vapor-Liquid Equilibrium Study in Trickle Bed Reactors", *Industrial Chemical Engineering Research*, Vol. 48, pp. 1096-1106, 2009.
50. Chekantsev, N.V., M. S. Gyngazova, E. D. Ivanchina, "Mathematical Modelling of Light Naptha (C₅,C₆) Isomerization Process", *Chemical Engineering Journal*, Vol. 238, pp. 120-128, 2014.
51. Englezos, P., N. Kalogerakis, *Applied Parameter Estimation for Chemical Engineers*, Marcel Dekker, New York, USA, 2001.